eman ta zabal zazu

Universidad del País Vasco

Euskal Herriko Unibertsitatea

Regulation of IRF7 by m6A-mediated mechanisms: a link between viral infections and celiac disease

Doctoral Thesis

Maialen Sebastian de la Cruz

Leioa, 2023

Supervised by:

Ainara Castellanos Rubio

Jose Ramon Bilbao Catalá

This work was funded by a predoctoral fellowship from the University of the Basque Country (UPV/EHU) to Maialen Sebastian de la Cruz (PIF18/119).

Lehenik eta behin eskerrak eman nahi dizkiet Ainara eta Buliri, nire zuzendariei, laborategira iritsi nintzenetik eta urte hauetan guztietan lagundu eta irakatsi didazuen guztiagatik.

Nire laborategiko lankideei ere elkarrekin pasatako denbora eskertu nahi nieke. Izortze, Ane, Itziar, Henar, Jon, Leire eta Luisma, mila esker dudak argitzen laguntzeagatik, ideiak konpartitzeagatik eta emaitzen araberako umore aldaketetan lagun izateagatik. Sobre todo quiero agradecerle a Henar su apoyo y su paciencia para escuchar todas mis idas y venidas, que no han sido pocas.

Me gustaría agradecer a Marta por ser luz en los días más oscuros, por comprenderme, por creer en mí en los momentos en que ni yo lo hacía, y por hacerme ver que todo suma y que cada persona tiene su tempo. Y gracias a todas aquellas personas que habéis sido parte de este proceso, porque de una manera o de otra, vosotros también me habéis ayudado a llegar hasta aquí. Muchisímas gracias!

I'd like to thank Thomas, Alyssa, Rodri**…** and all the people that were part of my life during the last year, you helped me grow as a scientist and as a person in many different ways and thanks to you I reached my goal. It's been a bumpy ride but I finally made it. Thank you!

Nire esker onak ere nire lagunentzat. Maddalen, Maider, Maddi, Irati, Ana eta Lara, eskerrik asko behar izan dudanetan zulotik ateratzen laguntzeagatik: egindako bidaiak, edozein aurrerapauso ospatzeko edandako zerbezak, barrenak hustutzeko emandako paseoak… mila, mila esker! Eta Mikel, zuri ere eskerrik asko, pixukiderik ezin hobea izateagatik eta Bilbon bizitako azken bi urteak denetan onenak bihurtzeagatik.

Azkenik nire eskerrik beroenak nire familiari. Aita, muchísimas gracias por enseñarme tanto, por procurar que no me faltase de nada, por estar siempre ahí en caso de necesitar ayuda. Ama, zuri dena daukat eskertzeko, mila esker emandako aholku guztiengatik, beti entzuteko eta laguntzeko prest egoteagatik, zure maitasunarekin ni zaintzeagatik, txarrenari ere alde ona bilatzen irakasteagatik, eta egunik okerrenetan ere aurrera egiteko indarra dudala ikusarazteagatik. Aita y ama, gracias por ayudarme a ser la persona que soy, por vuestro apoyo incondicional y por vuestra confianza, este doctorado también es vuestro. Jon, eskerrik asko, anai-arreben arteko maitasunak izandako liskar guztiek baino indar handiagoa duelako eta beti hori demostratu didazulako. Abuelo, gracias por todo el cariño que me diste. Abuela, gracias por tu fortaleza, por ser tan valiente y luchadora. Eres un ejemplo a seguir. Y muchas gracias también a todos mis tíos y primos por apoyarme y por mostrar interés por mi trabajo y mis avances.

Eta nola ez, Unai. Eskerrik asko hilabete zail hauetan izan dezun pazientziagatik, egunik tristeenak ere alaitzen saiatzeagatik, ulertezina ere ulertzeko ahalegina egiteagatik, baina batez ere bizitako momentu on eta ez hain onetan beti hor egoteagatik. "*Eta zure eskutik bidean aurrera egin…*" eskerrik asko, egoera zailen aurrean askatu ez, baizik eta indar gehiagorekin heltzeagatik. Bihotz bihotzez, mila esker!

CONTENTS

ABBREVIATIONS

ac4C	N4-acetylcytidine
AFT2	Activating transcription factor 2
ALKBH5	AlkB homolog 5, RNA demethylase
Anti-EMA	Anti endomysium antibodies
Anti-TGA	Anti transglutaminase antibodies
CDS	Coding sequence
CeD	Celiac disease
cGAS	cyclic GMP-AMP synthase
CXCL10/16	C-X-C Motif Chemokine Ligand 10/16
DAMP	Damage-associated molecular pattern
dsRNA	Double strand RNA
eIF4F	Eukaryotic initiation factor 4F
eIF4G2	Eukaryotic translation initiation factor 4 gamma 2
EV71	Enterovirus 71
FOXO3	Forkhead box O3
FTO	FTO alpha-ketoglutarate dependent dioxygenase
GFD	Gluten free diet
GWAS	Genome wide association studies
HCV	Hepatitis C virus
HDAC3	Histone deacetylase 3
HLA	Human leukocyte antigen
hnRNPD	Heterogeneous nuclear ribonucleoprotein D
IEL	Intra epithlelial lymphocyte
IFITM1	interferon induced transmembrane protein 1
IFN	Interferon

IFNB1	Interferon beta 1
IFNR	Interferon receptor
IFN-I	Type I IFN
IL15/18	Interleukine 15/18
IKK	Inhibitor of NF-κB kinase
IRF	Inrterferon regulator factor
ISG	Interferon stimulated gene
ISG15	Interferon stimulated gene 15
ISGF3	Interferon stimulated gene factor 3
IPS1	Interferon beta promoter stimulator protein 1
ISRE	Interferon-sensitive response element
JAK	Janus kinase
lnc13	Long non-coding 13
lncRNA	Long non-coding RNA
LPS	Lipopolysaccharides
m1A	N1-methyladenosine
m3C	3-methylcytidine
m5C	5-methylcytidine
m6A	N6-methyladenosine
m6Am	N6,2′-O-dimethyladenosine
m7G	7-methylguanosine
MAVS	Mitochondrial antiviral signaling protein
MDA5	Melanoma differentiation-associated protein 5
meRIP	m6A RNA immunoprecipitation
mRNA	Messenger RNA

METTL3 Methyltransferase 3, N6-adenosine-methyltransferase complex catalytic subunit

METTL14 methyltransferase 14, N6-adenosine-methyltransferase subunit

MIC-A MHC class I chain-related gene A

MUT Mutated

MYD88 MYD88 innate immune signal transduction adaptor

NAP1 Nucleosome assembly protein 1

NCOR2 Nuclear receptor corepressor 2

NFkB Nuclear factor kappa-light-chain-enhancer of activated B cells

NFX1 Nuclear transcription factor, x-box binding 1

NK Natural killer

NKG2D Natural killer group 2D

NT Non-treated

OASL1 2'-5'-oligoadenylate synthetase like 1

PABP1 Poly(A) binding protein 1

PAMP Pathogen-associated molecular patterns

PCR Polymerase chain reaction

PIC Polyinosinic:polycytidylic acid

PRR Pattern-recognition receptors

RBM15 RNA binding motif protein 15

REPIC RNA Epitranscriptome Collection

RIG-I Retinoic acid-inducible gene I

RIP RNA immunoprecipitation

RLR RIG-I like receptor

RPMI Roswell Park Memorial Institute medium

rRNA Ribosomal RNA

RT-qPCR Real-time quantitative reverse transcription polymerase chain reaction

SAMHD1 SAM and HD domain containing deoxynucleoside triphosphate triphosphohydrolase 1

SNP Single nucleotide polimorphism

SOCS Suppressor of cytokine signaling

SRAMP Sequence-based RNA adenosine methylation site predictor

SRSF3 Serine and arginine rich splicing factor 3

ssDNA Single strand DNA

ssRNA Single strand RNA

STAT Signal transducer and activator of transcription

STING Stimulator of interferon response cGAMP interactor 1

TBK1 TANK-binding kinase 1

TG2 Transglutaminase 2

TLR Toll like receptor

TRAF6 TNF receptor associated factor 6

TRIF TIR-domain-containing adapter-inducing interferon-β

tRNA Transfer RNA

UTR Untranslated Region

VIRMA Vir like m6A methyltransferase associated

WB Western Blot

WT Wild type

WTAP WT1 associated protein

XPO1 Exportin 1

YTHD YT521-B homology domain

YTHDC1-2 YTH Domain Containing 1-2

YTHDF1-3 YTH N6-Methyladenosine RNA Binding Protein 1-3

ZC3H13 Zinc finger CCCH-type containing 13

ψ Pseudouridina

PROJECT JUSTIFICATION AND SCOPE

Celiac disease (CeD) is a chronic inflammatory disease developed by an inadequate immune response to dietary gluten in individuals with genetic susceptibility. In CeD patients, the interaction of genetic and environmental factors leads to the loss of tolerance to gluten and the development of an intestinal damage. This lesion leds to highly variable symptoms that are very different among individuals, which often makes an early diagnosis of the disease difficult, especially in adults where typical gastrointestinal symptoms are less frequent.

CeD is a complex disorder that develops in subjects with genetic susceptibility. However, the gluten-induced immune response derived by the genetic susceptibility explains less than 50% of the heritability, suggesting that apart from gluten there might be additional environmental factors contributing to the onset of the immune response. On this basis, viral infections have been proposed as candidate triggering agents in CeD. To date, a strict attachment to a life-long gluten free diet (GFD) is the only way to overcome intestinal damage and reduce symptomatology. However, a tight GFD is difficult to comply with, it negatively affects the quality of life of CeD patients, and it does not relieve symptomatology in a percentage of cases, manifesting the necessity of developing novel treatments.

Therefore, it becomes essential to define which genes, pathways and regulatory mechanisms are involved in disease pathogenesis. These studies will contribute to the understanding of the pathogenic mechanisms underlying CeD development and will provide new insights into the relationship between viral infections and CeD. Additionally, the identification of master regulators of antiviral pathways will help identify novel targets for intervention. Thus, works like the present thesis open the door to the development of new alternative therapies or prevention approaches. Moreover, the new findings presented here postulate new points of view in the understanding of the mechanisms

behind immune system activation that could also be extrapolated to other complex and autoimmune diseases.

In order to dissect the implication of viral infections in the development of CeD, the current project has focused on the search of functional determinants related to the innate immune response against RNA virus infections using genetic approaches and functional *in vitro* validation of those candidates. More specifically, in the present doctoral thesis we have analyzed a new layer of gene regulation of IRF7 after the combination of viral infection and gluten consumption, and we have scrutinized the involvement of m6A RNA methylation in the regulation of this antiviral transcript and its downstream activity in the IFN-I pathway.

INTRODUCTION

1. Celiac disease

Celiac disease (CeD) is a chronic inflammatory disease developed by an inadequate immune response to dietary gluten, a mixture of proteins present in cereals such as wheat, barley, or rye (B Meresse et al., 2009). This immune disorder develops in genetically predisposed individuals and affects a 1-3% of the population worldwide, with increasing incidence in the last decades (Lerner, 2014; Lerner & Matthias, 2015).

Symptoms are highly variable, including typical gastrointestinal symptoms such as chronic diarrhea, weight loss, and/or abdominal pain; atypic extraintestinal symptoms such as fatigue, low bone density, and/or anemia; and those grouped as neurogluten symptoms such as migraines, epilepsy and/or cerebellar ataxia, among others (Feighery, 1999; Lionetti et al., 2015; Rodrigo, 2016). These clinical presentations, however, are very different among individuals, which often makes an early diagnosis of the disease difficult, especially in adults where gastrointestinal symptoms are less frequent (Cicarelli et al., 2003; Green, 2005; Green et al., 2001; Lionetti et al., 2015).

In CeD patients, the interaction of genetic and environmental factors leads to the loss of tolerance to gluten and the development of an intestinal damage. This lesion is characterized by an increase in intraepithelial lymphocytes in the epithelium and lamina propria, loss of villi or villous atrophy, crypt hyperplasia, enterocyte apoptosis and mucosal remodeling (Caio et al., 2019; Dieli-Crimi et al., 2015; S. M. Kim & Jabri, 2015). These intestinal damage signs, together with the presence of anti-transglutaminase (anti-TGA) and anti-endomysium (anti-EMA) autoantibodies are considered the main signs required for CeD diagnosis (Husby et al., 2012).

To date, a strict attachment to a life-long gluten free diet (GFD) is the only way to overcome intestinal damage and reduce symptomatology (Murray et al., 2004). However, a tight GFD is difficult to comply mostly due to the reduced variety of products and their high cost. As such, the quality of life of CeD patients is negatively affected (Samasca et

al., 2014). Besides, there is a small subgroup of CeD patients that suffers non-responsive or refractory CeD. Even on a tight adherence to a GFD, these patients do not respond to the treatment and present persistent or recurrent symptoms and inflammation and injury of the intestine (Rubio-Tapia & Murray, 2010). Hence, the development of new alternative therapies or prevention approaches would be of great benefit for CeD patients in general, and refractory CeD patients in particular.

1.1. Immune response in CeD

Gluten consumption induces the activation of the innate and adaptative immune responses, and both of them are involved in the pathophysiology of CeD. The contribution of the adaptive immune system is well stablished and was described long ago. On the contrary, the contribution of the innate immunity is not deeply understood, and even though several studies have helped us gain a large amount of knowledge about this proccess (Abadie & Jabri, 2014; Kim & Jabri, 2015; Schulzke et al., 1998), the puzzle is not yet complete.

1.1.1. Adaptive immunity in CeD

Gluten is composed of gliadins and glutenins, proteins rich in glutamines and prolines. These proteins, especially gliadin, are resistant to proteases and other gastrointestinal enzymes and therefore they do not degrade completely, generating toxic and immunogenic peptides (Ciccocioppo et al., 2005; Silano et al., 2009). These immunogenic peptides can cross the epithelial barrier of the intestine and pass into the lamina propria, where they are deamidated by tissue transglutaminase. This enzyme converts glutamine residues into negatively charged glutamate residues, increasing their immunogenicity (Briani et al., 2008; Molberg O et al., 1998). Antigen-presenting cells in the lamina propria are able to recognize this deamidated gliadin peptides through HLA-DQ2 and/or HLA-DQ8 molecules and present them to T lymphocytes. As a result, T cells acquire Th1 and Th17 phenotypes and secrete proinflammatory cytokines, generating an inflammatory

environment in the intestine (B Meresse et al., 2009; Briani et al., 2008; Castellanos-Rubio et al., 2009) (Figure 1).

Additionally, B cells are also activated and produce anti-gliadin antibodies, and anti-EMA and anti-TGA autoantibodies. Thus, this attack in the intestine against own tissues and endogenous TG2 proteins initiates the autoimmune response that finally leads to the characteristic tissue damage of CeD (B Meresse et al., 2009; Lejeune et al., 2021).

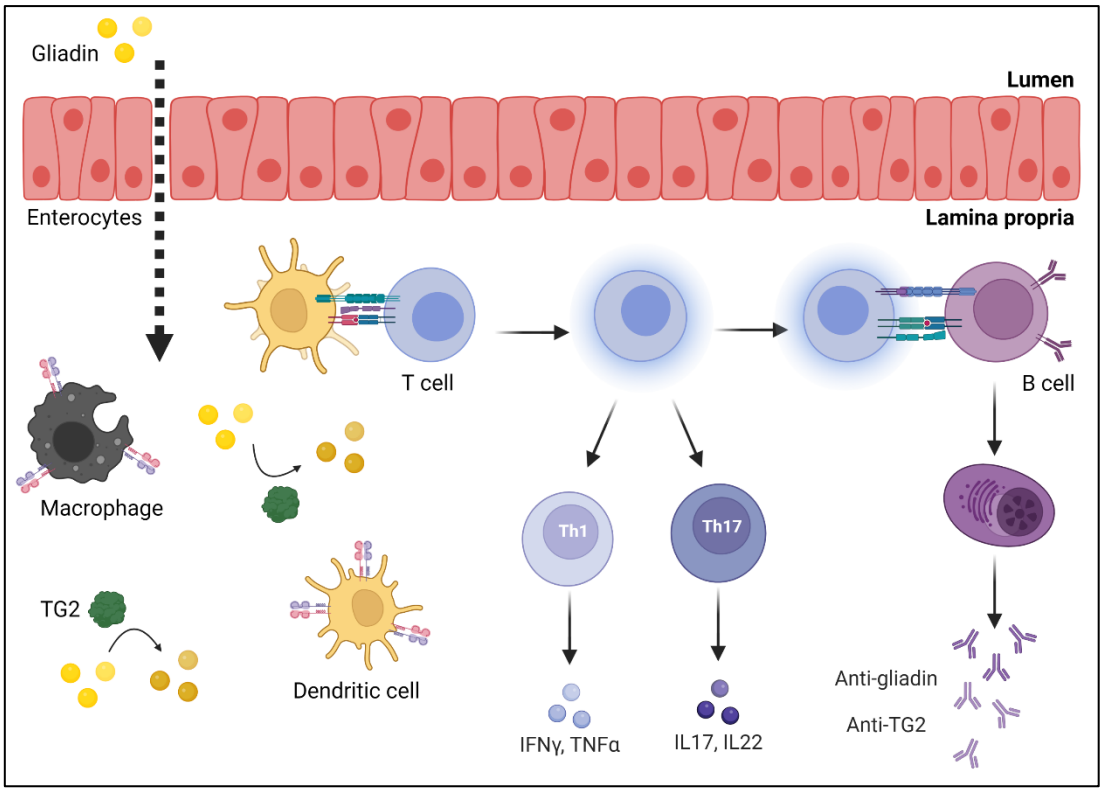

Figure 1. Schematic image of adaptive immune response in CeD. Gliadin peptides cross the epithelial layer from lumen to lamina propria, and there they are deamidated by TG2 enzyme. HLA-DQ2 or -DQ8 present on the surface of APCs, such as macrophages and dendritic cells, recognize deamitaded gliadin peptides and present them to T cells. Hence, T cells are activated and adopt Th1 and Th17 phenotypes, leading to proinflammatory cytokine production. B cells are also activated, provoking their shift to anti-gliadin and anti-TG2 autoantibodies producing plasmacytoid cells. Image created with BioRender.

1.1.2. Innate immunity in CeD

The epithelial barrier is a very important element of the immune system, since it is the first defense line against pathogens entering our organism. Intestinal epithelial cells form a wall that divides the intestinal lumen on the one side and the lamina propria on the other side. These cells are connected by tight junctions or *zonula occludens*, making the

barrier an almost impermeable structure, which allows to regulate the transit of molecules from one side to the other. In CeD this permeability is altered (Jauregi-Miguel et al., 2019; Schulzke et al., 1998), facilitating the passage of toxic gliadin peptides to the lamina propria. These gliadin peptides induce enterocyte apoptosis and increase the expression of *IL15* and *IL8* (Abadie et al., 2020; Goel et al., 2019). On the one hand, IL15 promotes the proliferation and activation of IELs, and induces the production of NKG2D, a molecule that activates NK cells (Abadie & Jabri, 2014; B Meresse et al., 2009). On the other hand, IL8 attracts and activates neutrophils to inflammation sites (Barone et al., 2014; Jelínková et al., 2004) (Figure 2).

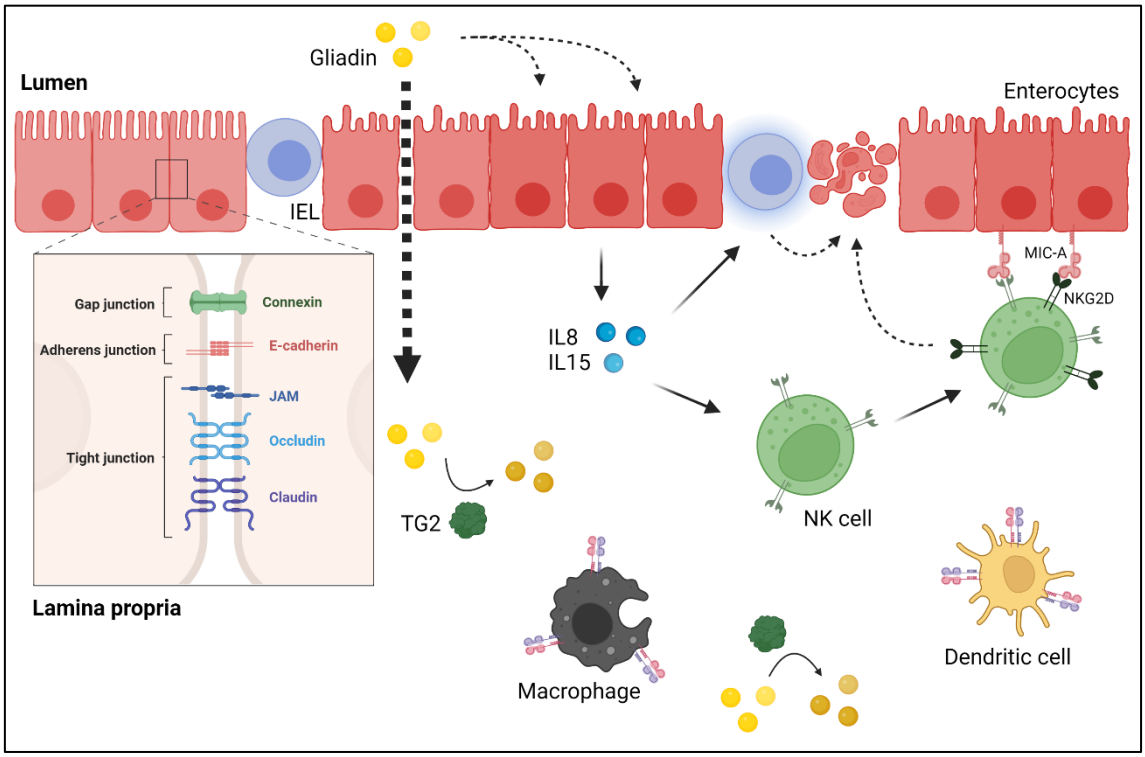

Figure 2. Schematic image of a the innate immune response in CeD. Enterocytes form the epithelial barrier by connecting to each other by Gap, Adherense and Tight Juncions. However, these junctions are impaired in CeD, increasing permeability between lumen and lamina propria, what lead to and easier crossing of gliadin peptides. These gliadin peptides, apart from activating the adaptive immune response via APCs, they also provoke the induction of proinflammatory cytokines production such as IL8 and IL15, and MIC-A molecules expression on the surface of stressed enterocytes. These cytokines induce the activation of innate immune cells such as IELs and NK cells. Thus, activated NK cells present NKG2D receptors on their surface, which recognize and interact with MIC-A molecules and provoke immune cells to shift to cytotoxic phenotype, inducing enterocyte apoptosis. Image created qwith BioRender.

Furthermore, under situations of stress and/or infection, overexpression of the MIC-A molecule occurs on the surface of enterocytes. This cell surface antigen interacts with the activating receptor NKG2D, causing IELs to adopt a cytotoxic profile, promoting the apoptosis of intestinal cells (Allegretti et al., 2013; Hü et al., 2004).

1.2. Genetic factors involved in CeD development

As previously stated, CeD is a complex disorder that develops in subjects with genetic susceptibility. The major contributors to the genetic susceptibility are the HLA class II DQ2 and DQ8 receptors, encoded by genes located in the HLA region on chromosome 6. The HLA-DQ2 and HLA-DQ8 heterodimers are necessary for the development of the disease pathology, since they can recognize and present gliadin peptides to CD4+ T lymphocytes, thus initiating the immune response (Ciccocioppo et al., 2005; Sciurti et al., 2018). HLA-DQ2 heterodimers are encoded by the *DQA1*05* and *DQB1*02* alleles and are identified in almost 90% of celiac patients. Almost all remaining patients (5-10%) express HLA-DQ8 heterodimers, which are normally encoded by *DQB1*03:02* and *DQA1*03* (Cecilio & Bonatto, 2015; Megiorni & Pizzuti, 2012). However, expressing these molecules is not enough to develop the disease, as shown by the fact that 30% of the non-celiac population carries these alleles (Caio et al., 2019). The contribution of the HLA region to disease heritability is thought to be approximately 40% (Megiorni & Pizzuti, 2012). Thus, the HLA genes are necessary, but not sufficient to develop CeD.

The introduction of high-throughput genotyping platforms and increased information on genomic variation have made it possible to perform Genome Wide Association Studies (GWAS). The aim of these type of studies is to analyze the whole genome of people with a variety of disorders and identify the most frequent alleles present in each of the disease analyzed, revealing the connection or association between SNPs and pathologies (Nica & Dermitzakis, 2013; Visscher et al., 2012).

Since the first CeD GWAS was performed 15 years ago (van Heel et al., 2007), much progress has been made in understanding the genetic contribution of CeD. Nowadays, a total of 57 associated non-HLA regions have been identified and associated with CeD susceptibility (Dubois et al., 2010; Trynka et al., 2011). Some of those regions have been functionally validated. In addition, several mechanisms dependent on associated SNPs have also been described and their contribution to the characteristic inflammation of CeD has been explained (Castellanos-Rubio et al., 2016; Jauregi-Miguel et al., 2019; Olazagoitia-Garmendia et al., 2021).

Among the CeD-associated SNPs that have been functionally characterized, one is located in the exon of *lnc13*, a long noncoding RNA (lncRNA) involved in CeD pathogenesis. This SNP affects the interaction of *lnc13* and hnRNPD, consequently affecting *lnc13* mediated gene repression of certain inflammatory genes (Castellanos-Rubio et al., 2016).

XPO1 is a protein involved in the regulation of the NFkB pathway and it harbors another CeD-associated SNP on its 5'UTR. The presence of the risk allele results in higher m6A methylation in the 5'UTR of *XPO1* RNA, increasing XPO1 protein amounts and subsequently leading to downstream NFkB activation and inflammation (Olazagoitia-Garmendia et al., 2021).

1.3. Environmental factors potentially involved in CeD development

Gluten is the main triggering environmental agent in CeD, and its role in the development of the disease has been deeply studied. However, there probably are additional environmental agents apart from gluten that may also contribute to the onset of the immune response.

The gastrointestinal tract harbors the largest microbial population in the human body (X. Zhang et al., 2020). Gut microbiota plays an important function in digestion and in the

modulation of the host immune response, so that changes in its composition could alter the intestinal barrier and lead to an increased epithelial permeability (Lerner et al., 2017). Indeed, many studies have reported differences in the composition and diversity of the gut microbiome (including virome) in patients with autoimmune disorders when compared to healthy individuals (Pecora et al., 2020; Spencer et al., 2022; X. Zhang et al., 2020), suggesting an implication of the microbiota in the development of these pathologies. However, this research field is in its infancy in CeD and little is known about the effect of the microbiota on its pathogenesis (Leonard et al., 2021).

Recently, the discovery of the association of Epstein Barr virus with the development of multiple sclerosis (Bjornevik et al., 2022) has highlighted the importance viral infections may have in the onset of autoimmunity. Regarding CeD pathogenesis, infections by rotavirus and reovirus are the main candidates as potential viral contributing factors. Several studies have shown association between these *Reoviridae* dsRNA viral infections and CeD, but none of them has been validated yet (Bouziat et al., 2017; Lars C Stene et al., 2006).

2. Viral infections

As stated before, viral infections have been proposed as triggering agents for some autoimmune pathologies including CeD.

Viruses are complex units of "life", as they are not able to complete their life cycle without infecting a host cell. They need the host cell machinery to replicate and be able to infect other cells. During evolution, organisms and viruses have co-evolved and and as a result of this interplay, a wide variety of virus and different antiviral defense mechanisms have been developed (Kaján et al., 2020).

In mammals, virus can infect many different types of cells, including epithelial cells, T cells or other immune cells, as well as neurons or other central nervous system cells. However, the main entrance of virus into the host organism are the respiratory airways and the gastrointestinal track (Liang & Bushman, 2021; Spencer et al., 2022). The latter harbors the largest viral population in the human body, and this huge reservoir of virus is commonly known as the gut virome (Cao et al., 2022). The Global Virome Database indicates that 97.7% of the human gut virome are phages (virus that infect bacteria), 2.1% are eukaryotic viruses (plant and mammalian viruses), and 0.1% are archaeal viruses (Gregory et al., 2020).

Eukaryotic DNA viruses are mostly latent and dormant in steady state. Meanwhile, eukaryotic RNA viruses are rare in a healthy scenario (Liang & Bushman, 2021). The eukaryotic viruses that are involved in enteric infections are known as enteric viruses. Generally, the RNA virome in the human gut has been significantly less studied than the DNA virome. This is because RNA viruses appear to be less stable in biological samples compared to DNA viruses, making their identification by metagenomic sequencing difficult (Krishnamurthy et al., 2016).

Pathogenic RNA viruses may appear in the gut when the human host is under infection, provoking diarrheal diseases (Julio-Pieper et al., 2021). The most frequently detected

eukaryotic viruses in acute gastroenteritis are *Reoviridae* (rotavirus) and *Picornaviridae* (enterovirus, echovirus etc.) (Finkbeiner et al., 2008; Wilhelmi et al., 2003). Indeed, rotavirus was reported as the leading cause of death among diarrheal patients below 5 years old (Fulci et al., 2021). Furthermore, some enteric viral infections have been linked to autoimmune disease onset. For example, enteroviruses are considered the main viral candidates for causing type 1 diabetes in humans, being Coxsackie B virus the most prevalent enterovirus in pre-diabetic and diabetic patients (Filippi & Von Herrath, 2008; Hyöty & Taylor, 2002) .

2.1. Viral infections and CeD

In the context of CeD, several cohort studies of more than 6000 children aged 1-4 years carrying risk HLA, reported that gastrointestinal infections are associated with the risk of developing CeD autoimmunity in the following 3 months post infection (Kemppainen et al., 2017; Lindfors et al., 2020). Moreover, one of these studies also revealed that children vaccinated against rotavirus showed reduced risk of CeD autoimmunity, in comparison to non-vaccinated children, suggesting that at least part of the gastrointestinal infections associated with CeD may be caused by rotavirus (Kemppainen et al., 2017). Additionally, rotavirus has been suggested as a trigger for celiac disease, since early onset of CeD autoimmunity in children is correlated with serologic evidence of repeated rotavirus infections (Lars C Stene et al., 2006).

Mammalian orthoreovirus T1L, another enteric dsRNA virus of the *Reoviridae* family, has also been proposed as the viral triggering agent in CeD (Bouziat et al., 2017). Bouziat *et al* reported that celiac patients tend to have higher anti-reovirus antibody titters than non-celiac controls. Reovirus infection breaks oral tolerance to gluten and induces TG2 activation. Moreover, it provokes a shift from the peripheral regulatory T cell to a Th1 type immunity to dietary antigen, through a mechanism that is dependent on IRF1 and

IFN-I. Another study by Brigleb *et al* revealed that this inflammatory shift observed upon reovirus infection is induced by activated NK cells (Brigleb et al., 2022).

2.2. Antiviral immunity

The antiviral innate immunity is the first line of host defense against virus infections. In mammalian cells, viral infections induce the expression of interferons (IFNs) in the host. IFN production leads to the activation of the antiviral response by induction of interferon-stimulated genes (ISGs) in order to inhibit viral replication (Schmid et al., 2010; Schoggins & Rice, 2011). ISGs encode for proteins known for their direct antiviral activities, that although present at basal levels, are upregulated upon virus infection (Schoggins & Rice, 2011). These ISGs are regulated by the IRF and STAT families of transcription factors, both in a JAK-STAT-dependent or-independent manner (Chiang & Liu, 2019; Schmid et al., 2010).

2.2.1. *Type I IFN signaling pathway and IFN production*

IFNs were discovered in the 1950s and are classified in three families: Type I, II and III IFNs. Among them, type I IFNs are the main IFN family and consist of several *IFNa* genes and a unique *IFNb* gene. Still, all of them bind a ubiquitously expressed, heterodimeric transmembrane IFN receptor (IFNR) complex to exert their antiviral functions (Negishi et al., 2018). Thus, IFNs play a pivotal role in the innate immune response against viral infections. However, their aberrant activation may contribute to the development of autoimmune disease, such as systemic lupus erythematosus (Banchereau & Pascual, 2006). Therefore, IFN production should be tightly regulated.

Upon viral infections, IFNs are produced after a series of signal transduction steps through the IFN-I pathway (Figure 3). The signaling cascade initiates with the recognition of pathogen-associated molecular patterns (PAMPs) through cytoplasmic and endosomal pattern-recognition receptors (PRRs) or by cytokine-receptor binding (Medzhitov & Janeway, 2000). PRRs, including membrane receptors known as toll like

receptors (TLRs) and cytosolic RIG-I like receptors (RLRs), are key factors of the innate immune response, as they lead to the activation of transcription factors of the interferon regulatory factors (IRF) family.

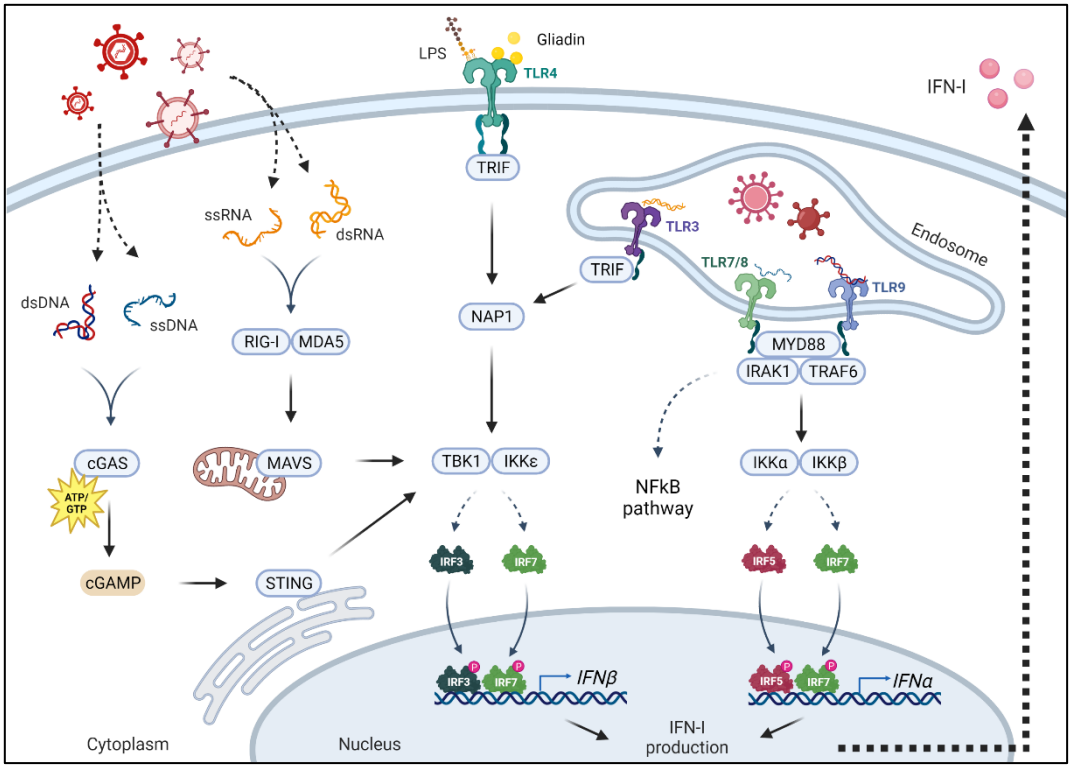

Figure 3. Schematic image of IFN-I pathway. Virus can infect cells by introducing only their nucleic acids or by entering the whole virus through endosomes. Therefore, viral infections induce IFN-I production via different signaling pathways. On the one hand, cytoplasmic DNA or RNA derived from viral particles induce IFN-I production through cGAS-STING and RIG-I/MDA5-MAVS, respectively, converging in TBK1/IKKe. dsRNAs are also recognized by endosomal TLR3 receptor and activate TBK1/IKKe through TRIF-NAP1. TLR4 ligands LPS and gliadin activate TRIF-NAP1 pathway too. TBK1/IKKe phosphorylate IRF3/7 and promote their translocation to the nucleus, inducing mainly *INFB1* expression. On the other hand, endosomal TLR7/8 and TLR9 reconginze ssDNA and non-methylated dsDNA, respectively, and activate IKKa/b. NFkB pathway is also induced through Myd88-TRAF6. IKKa/b phosphorylate IRF5/7 and promote their translocation to the nucleus, inducing mainly *INFA* genes expression. Image created with BioRender.

The mammalian IRF family consists of nine members named IRF1-9 (Mancino & Natoli, 2016; Paun & Pitha, 2007). Among these nine IRFs, IRF3 and IRF7 are the main transcription factors involved in the induction of IFN genes during viral infection. IRF1 and IRF5 are also implicated in the antiviral response, even though to a lesser extent (Negishi et al., 2006; Takaoka et al., 2005). The IRF family of proteins plays critical and diverse roles that connect the sensing of microbial signatures to the expression of IFNs and pro-inflammatory cytokines (Ikushima et al., 2013).

TLR signaling is considered one of the most relevant IRF activating pathways (Medzhitov, 2001; Uematsu & Akira, 2007). The regulation mediated by TLR signaling is driven through two different pathways: one dependent on the adapter protein MyD88, and the other related to the adapter protein TRIF. Both pathways activate many transcription factors, including IRFs (Kawai & Akira, 2006a; Negishi et al., 2018; Uematsu & Akira, 2007). Once activated, IRFs can bind to specific sequences of DNA (also known as ISREs) and promote the transcription of IFN-I and proinflammatory cytokine genes (Aria Csumita et al., 2019; Tanaka et al., 1993).

TLR3 is located mainly within the membrane of endosomes and phagosomes. TLR3 recognizes viral dsRNA and the synthetic dsRNA analog poly(I:C) (Alexopoulou et al., 2001; Matsumoto & Seya, 2008). On the contrary, TLR4 is a cell surface receptor that recognizes LPS from gram-negative bacteria and a variety of other PAMPs or DAMPs (Y.-C. Lu et al., 2008; Negishi et al., 2012). TLR4 also recognizes gliadin peptides from gluten (Palová -Jelínková et al., 2013). Both TLR3 and TLR4 use the TRIF adaptor protein to recruit downstream NAP1 and TBK1 and activate IRF3 and IRF7 by phosphorylation (Kawai & Akira, 2005; Matsumoto & Seya, 2008; Perry et al., 2004). Together with TLR3, TLR7/8 and TLR9 are the best characterized PRRs for the recognition of viral PAMPs located in the endosomal compartments. TLR7/8 and TLR9 recognize viral ssRNA and unmethylated CpG DNA motifs, respectively (Chan et al., 2015; de Oliveira Mann & Hornung, 2021; Kawai & Akira, 2006b). These TLRs recruit MyD88 to induce IKKa- or IKKb-dependent phosphorylation and activation of IRF7 or IRF5 (Balkhi et al., 2010; Bergstrøm et al., 2015). IRF7 also interacts with TRAF6 for IRF7 self-activation (Honda K et al., 2005; Kawai et al., 2004).

On the other hand, several RNA viruses directly enter the cytoplasm where they are detected by RLR family members RIG-I and MDA5 (Kato et al., 2006; Yoneyama et al., 2005). Ligand recognition (mainly dsRNA) results in the recruitment of RIG-I and MDA5

to the mitochondria, followed by interaction with MAVS (also known as IPS1) (Kawai & Akira, 2006a; H. Kumar et al., 2006; Q. Sun et al., 2006). This interaction leads to signal transduction to activate TBK1 and IKK-e, and phosphorylate IRF3 and IRF7 (Fitzgerald et al., 2003; Sharma et al., 2003). Similar to RLR-mediated IFN-I expression, IRF3 and IRF7 also contribute to the IFN-I induction after cytosolic DNA sensing and endosomal DNA/RNA recognition. Upon viral DNA binding, cGAS catalyzes the production of cGAMP from ATP and GTP, a second messenger that binds and activates STING (Cai et al., 2014; L. Sun et al., 2013; J. Wu et al., 2013). STING functions as an adaptor protein that promotes TBK1-dependent IRF3 and IRF7 phosphorylation (Ishikawa et al., 2009; Zhong et al., 2008).

Virus infections induce specific IRF3 phosphorylation that leads to its dimerization with itself or with IRF7 subsequently forming a complex containing CBP/p300 and other coactivators (Honda & Taniguchi, 2006; Yoneyama et al., 1998). Following translocation into the nucleus, they bind to ISRE sequences on promoters of IFN-I and stimulate their transcription (Honda & Taniguchi, 2006). This way, the production of large amounts of interferon is enhanced and a proper antiviral response is induced.

2.2.2. JAK-STAT signaling pathway and ISGs production

Almost all cell types respond to IFN-I for effective antiviral immunity (Müller et al., 1994; Platanias, 2005). When IFNs bind to their receptors, IFNR and JAK dimerization or oligomerization occur, allowing the transphosphorylation of JAK on tyrosine residues. Thus, the transduction of IFNR-associated JAK-STAT pathway signaling starts, which ends up with the induction of ISG transcription. After IFN binding to its receptor and JAK phosphorylation, activated JAKs induce tyrosine phosphorylation of IFNR cytoplasmic tails, providing the binding sites for STAT proteins. The STAT molecules are then recruited to the JAKs and phosphorylated at a tyrosine residue. The phosphorylation of STAT1 and STAT2 leads to the formation of the STAT1/STAT2 heterodimer that

interacts with IRF9 to form the ISGF3 complex. Then it translocates into the nucleus to trigger the expression of ISGs by binding to ISRE sequences on their promoter region (Chiang & Liu, 2019; Ivashkiv & Donlin, 2014; Negishi et al., 2018; Pestka et al., 2004; Schmid et al., 2010; Taniguchi & Takaoka, 2001) (Figure 4).

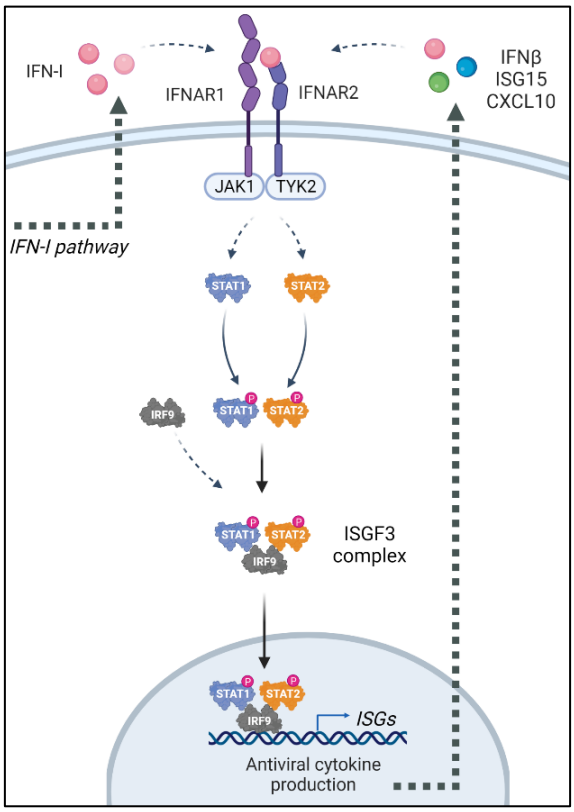

Figure 4. Schematic image of JAK-STAT signalling pathway. IFN-I bind to IFNR and activate JAK-TYK2 kinanes, which phosphorylate STAT1/2, promoting their dimerization. IRF9 binds and interacts with STAT1/2 and hence ISGF3 complex is formed. ISGF3 complex translocate to the nucleus and induce ISGs expression. Thus, antiviral cytokines such as IFNb, ISG15 and CXCL10 among others, are produced. IFNb can then bind to IFNR and create a positive regulatory feedback. Image created with BioRender.

The antiviral functions of several ISGs have been well characterized. For example, IFIT1-3, viperin, and Mx1 can all inhibit virus replication (Schoggins & Rice, 2011). JAK2, STAT1, STAT2, and IRF9 belong to another subset of ISGs that amplify JAK-STAT signaling to reinforce IFN responses (Ivashkiv & Donlin, 2014). Moreover, ISGs such as RIG-I, cGAS, IRF5, and IRF7 can further prime cells for increased detection of viral PAMPs and upregulated IFN expression (Schneider et al., 2014). Interestingly, the expression of subsets of ISGs can also be induced directly by IRFs in a pathway that is independent of JAK-STAT signaling (Wu & Chen, 2014). For example, IRF3 causes the expression of

ISG15 and *SAMHD1* as the first responders in antiviral immunity (Maelfait et al., 2016; Morales & Lenschow, 2013). IRF7 can also regulate ISG expression in the absence of IFN signaling (Daffis et al., 2008; Schoggins & Rice, 2011).

2.2.3. IRF7

The IRF family has coevolved with the NFkB family (Hiscott, 2007; Nehyba et al., 2009). As a result, they share some evolutionary characteristics: both families are activated by signaling pathways from the same PRRs and by the same IKKs; they cooperate extensively in the regulation of target cytokines such as IFNb, and together they represent the major players in innate immune responses (Honda & Taniguchi, 2006; Iwanaszko & Kimmel, 2015; Tamura et al., 2008).

The IRF family members share significant homology within the conserved N-terminal DBD, which consists of a signature tryptophan pentad that is essential for DNA binding genes (Aria Csumita et al., 2019; Tanaka et al., 1993; Veals et al., 1992). The C-termini of IRFs are different and confer on each member distinct functions. In general, they contain an IRF-association domain, a nuclear export sequence, an autoinhibitory domain, and a signal-responding domain (W. Chen & Royer, 2010). This signal-responding domain has key serine residues subjected to phosphorylation upon infection by pathogens (Ikushima et al., 2013; Ning et al., 2011).

Among the IRF proteins, IRF3 and IRF7 are the main IRF family members involved in antiviral response to dsRNA virus, such as rotavirus and reovirus. IRF3 is a constitutively expressed but tightly regulated transcription factor in the cytoplasm. It is usually present in an inactive form due to its auto-inhibitory mechanisms (Qin et al., 2003; Yanai et al., 2018). The activation process of IRF7 is similar to that of IRF3. However, in contrast to IRF3, IRF7 is expressed at low levels in basal conditions but it is strongly induced by IFN-I mediated responses in an autocrine feedback loop after virus infection. (Kawai et al., 2004; Litvak et al., 2012; Ning et al., 2011)

Unlike IRF3, which acts and is produced immediately upon viral infections, IRF7 is induced during later stages of infection (W. Wu et al., 2020). At the early stage of virus infection, the low level of endogenous IRF7 in the cell is phosphorylated and activated by IFN-I signaling pathway (Honda K et al., 2005; Honda & Taniguchi, 2006). Upon activation, IRF7 forms a transcriptional enhanceosome complex together with IRF3, NFkB, c-Jun, AFT2 and p300/CREB-binding protein on the promoter region of the *IFNB1* gene (Wathelet et al., 1998), leading to enhanced IFNb production and consequently to the activation of the JAK-STAT signaling pathway. *IRF7* is a ISG itself, hence, the ISGF3 complex binds to the ISRE on the *IRF7* promoter and induces synthesis of more IRF7. Later, the newly synthesized IRF7 is activated and induces more IFNs so that increasing amounts of IRF7 and IFNs are produced (Marie et al., 1998; Ning et al., 2011; Sato et al., 1998). Thus, a positive regulatory loop that is the major source of IRF7 in the cell is generated.

IRF7 is considered the master regulator of IFN-I response since it plays the critical role of maintaining this pathway activated in late stage of viral infections (Honda K et al., 2005). As a result, the proper regulation of IRF7 is crucial for a correct immune response, and constant upregulation may lead to augmented immune responses also in basal conditions, that in turn can end up in the development of autoimmunity. IRF5 is to date the most studied IRF in terms of autoimmune pathology and many polymorphisms have been associated, particularly with systemic lupus erythematosus in different populations (Banchereau & Pascual, 2006), nevertheless, their functionality has not been addressed. On the other hand, little is known about IRF7 implication in autoimmunity.

IRF7 regulation at the protein level has been deeply studied. It is well-known that it is activated by phosphorylation by TBK1, IKKe and IKKa (Hemmi et al., 2004; Iwamura et al., 2001; Sharma et al., 2003), among others. However, IRF7 undergoes other post-translational modifications too. These modifications include ubiquitination, sumoylation,

and acetylation. Ubiquitination affects both degradation (Higgs et al., 2010) and activation (Ling et al., 2019; Ning et al., 2008), depending on the ubiquitination type. Sumoylation (Kubota et al., 2008) and acetylation (Caillaud et al., 2002) impair IRF7 transcriptional activity and DNA binding capacity, respectively.

Although many post-translational modifications affecting IRF7 have been identified and their effect on IRF7 protein levels is well characterized, only two mechanisms controlling protein synthesis have been described. On the one hand, *IRF7* mRNA translation is repressed by the translational repressors 4E-BP1/2 as they inhibit the formation of the eIF4F complex (Colina et al., 2008). On the other hand, OASL1 inhibits the translation of *IRF7* mRNA by binding to the 5′UTR of *IRF7* and probably impeding the scanning of the 43S preinitiation complex (M. S. Lee et al., 2013).

Lastly, little is known about *IRF7* regulation at the transcriptional level. The human *IRF7* gene is located on chromosome 11p15.5 and encodes four isoforms or natural splicing variants (L. Zhang & Pagano, 2002). The *IRF7* promoter contains a putative CpG island flanking the TATA box. The CpG island is endogenously methylated in human fibroblasts. Methylation of the *IRF7* promoter results in *IRF7* gene silencing in these cells, even in the presence of IFN (R. Lu et al., 2000). Another epigenetic regulatory mechanism for *IRF7* silencing has also been described. FOXO3 transcription factor interacts with NCOR2 and HDAC3 and recruits them to the *IRF7* promoter in order to keep a closed chromatin structure due to histone deacetylation (Litvak et al., 2012).

Epitranscriptomics, and more specifically, m6A machinery has also been reported to be implicated in *IRF7* regulation, even although in an m6A-independent fashion. m6A reader YTHDF3 interacts with PABP1 and eIF4G2, to promote FOXO3 protein synthesis by binding to the translation initiation region of *FOXO3* mRNA (Y. Zhang et al., 2019). Thus, indirectly YTHDF3 affects *IRF7* expression. However, the direct effect that m6A RNA methylation may have on IRF7 has not been revealed yet.

3. Epitranscriptomics

Epitranscriptomics is the field of epigenetics studying post-transcriptional alterations that occur in the transcriptome. To date, more than 150 chemical modification molecules have been identified in RNA (S. Kumar & Mohapatra, 2021; Mathlin et al., 2020). Most of them take place mainly in small non-coding RNAs such as tRNAs and rRNAs (Machnicka et al., 2013; Schwartz, 2016). Yet, epitranscriptomic marks including m6A (Dominissini et al., 2012), m1A (Dominissini et al., 2016), inosine (Slotkin & Nishikura, 2013), m7G (Furuichi & Sekiya, 2015), m3C (Luang Xu et al., 2017), m5C (Hussain et al., 2013), ac4C (Arango et al., 2018) and pseudouridine (Simen Zhao & He, 2015) have also been detected in mRNA and lncRNA molecules (Figure 5). Among these, m6A is the most prevalent post-transcriptional modification in mRNAs of several eukaryotic species including yeast, plants, flies, and mammals (Desrosiers et al., 1974; Schwartz, 2016; Yue et al., 2015). It has been deeply studied during the last decade and its involvement in health and disease has been described.

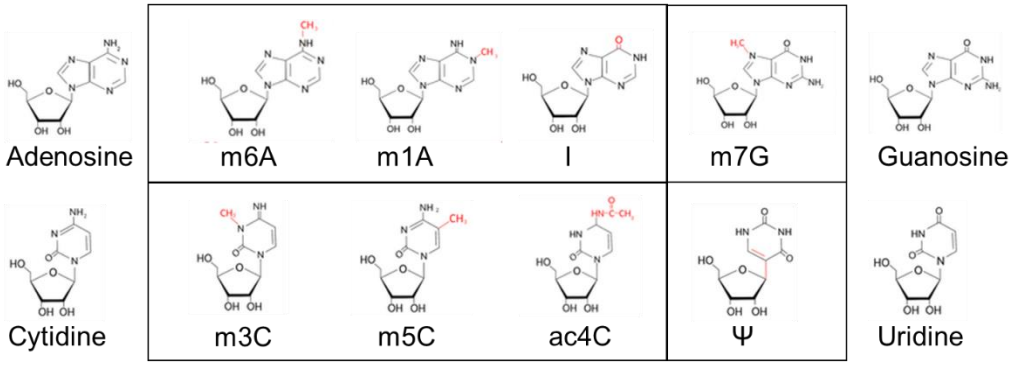

Figure 5. Chemical formulas for the main types of epitranscriptomic marks on mRNA and lncRNA molecules. Chemical changes are highlighted in red and unmodified RNA bases are shown beside. Image modified from (Mathlin et al., 2020).

3.1. N^6-methyladenosine (m6A)

The m6A modification consists of an extra methyl group on the adenosine (A) nucleotide within the consensus RNA motif of DRACH (when D = A, G or U; R = A or G, and H = A, U, or C) (Dominissini et al., 2012; Linder et al., 2015). It was first discovered in the 1970s (Desrosiers et al., 1974), but its function and implication in cell processes was not deciphered until 10 years ago, when high resolution sequencing, mapping and quantification techniques were developed. So far, more than 10.000 m6A motifs have been validated in over 25% of human transcripts and it has been found to be enriched in long exons, near stop codons and 3'UTRs (Meyer et al., 2012) (Figure 6).

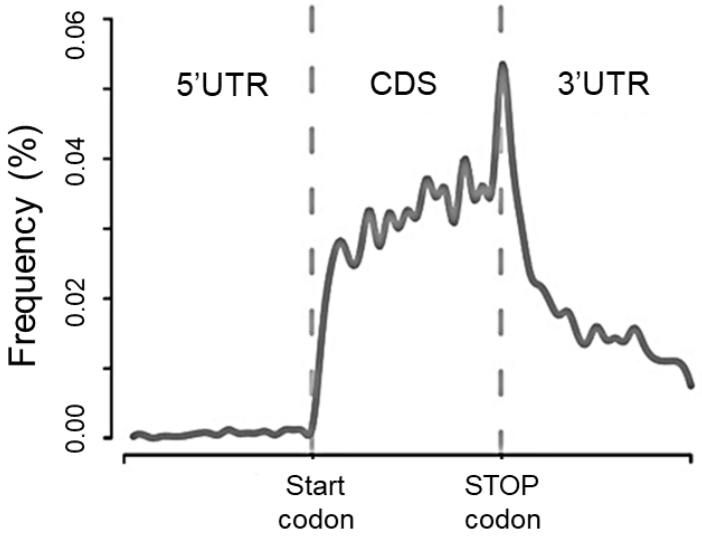

Figure 6. Frequency of m6A motifs and their distribution along mRNA molelules. Image modified from (Z. Zhang et al., 2019).

Numerous studies have analyzed the effects of this modification on mRNA metabolism. Nowadays, it is known that m6A can alter RNA folding, structure (N. Liu et al., 2017) and stability (Huang et al., 2018; C. Tang et al., 2017; X. Wang et al., 2014), affect mRNA maturation by modulating splicing and inducing alternative polyadenylation (C. Tang et al., 2017; Xiao et al., 2016), and enhance nuclear processing and export of mRNAs (Lesbirel & Wilson, 2019; Roundtree et al., 2017). Besides, m6A also takes part in translation and mRNA decay

processes (A. Li et al., 2017; Mao et al., 2019; Meyer et al., 2015; Shi et al., 2017; X. Wang et al., 2015; Y. Yang et al., 2017).

Apart from being a key factor in mRNA metabolism, m6A modification plays an important role in different processes that take place in the cells, including cell differentiation and reprogramming, cell cycle regulation, and maintenance of the circadian rhythm (Fustin et al., 2013; Geula et al., 2015; H. Luo et al., 2021). Moreover, m6A is also implicated in stress responses, immune response modulation and autoimmunity (Bechara & Gaffen, 2021; Lou et al., 2021; J. Luo et al., 2021; Shulman & Stern-Ginossar, 2020; L. Tang et al., 2021).

3.2. m6A machinery

m6A is a dynamic, non-permanent modification that is regulated by the so-called m6A machinery (Figure 7).

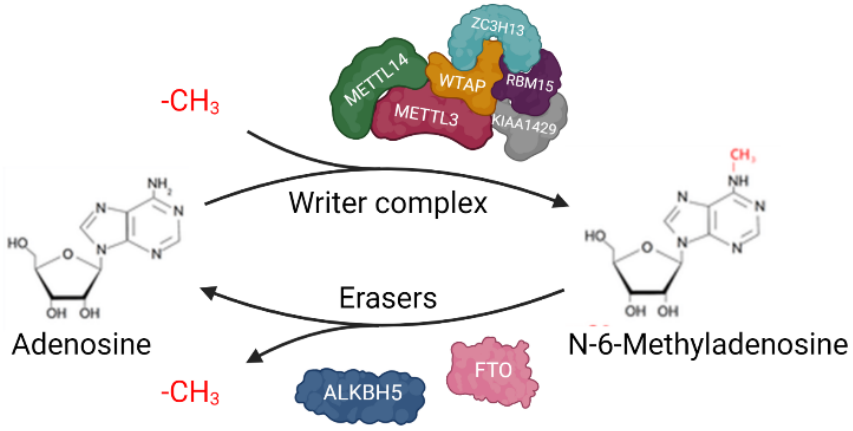

Figure 7. m6A modification is generated by adding a methyl group to adenosine nucleotide by the m6A wrtiter complex. Erasers remove it causing m6A to be a dynamic RNA methylation. Image created with BioRender.

This machinery is composed of methyltransferases or *writers*, demethylases or *erasers* and RNA binding proteins that recognize m6A marks or *readers*; proteins involved in encoding or *writing*, removing or *erasing* and decoding or *reading* the methyl group, respectively (Maity & Das, 2016; Y. Yang et al., 2018) (Figure 8).

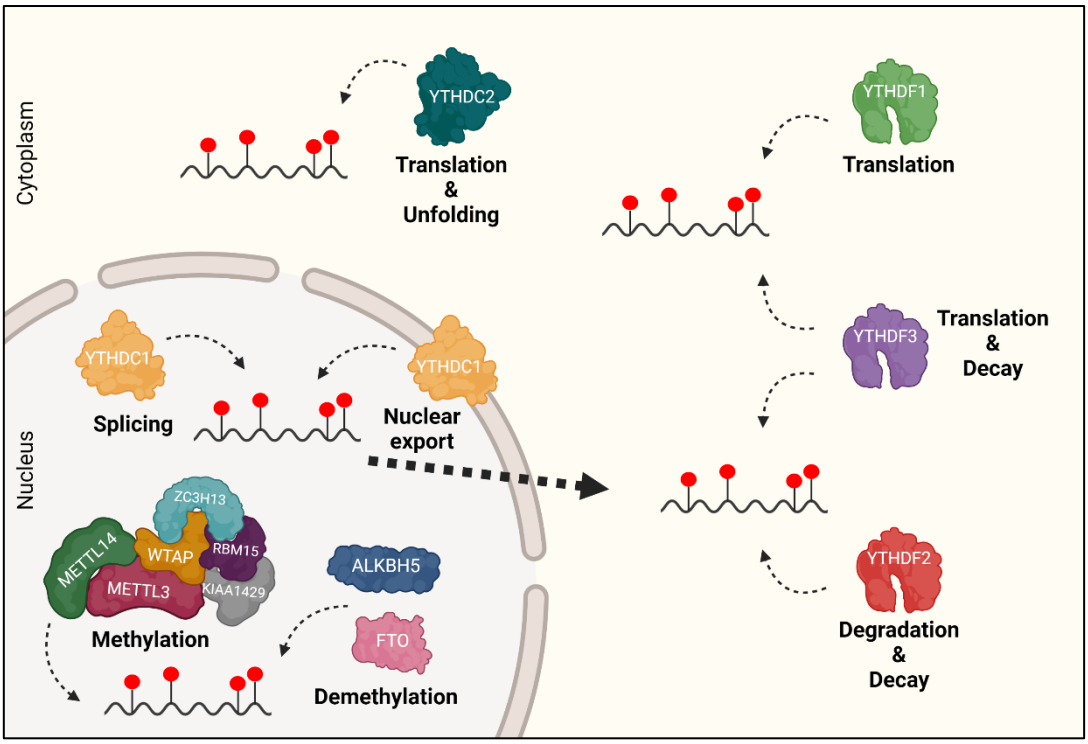

Figure 8. Schematic image of m6A machinery proteins and their main location within the cell. Their functions are indicated below each protein or group of proteins. Image created with BioRender.

3.2.1. m6A writers

The family of proteins that add a methyl group to adenosine ribonucleotides are designated as m6A writers. m6A is deposited onto RNA molecules by a methyltransferase complex formed by METTL3, METTL14, WTAP, KIAA1429, RBM15 and ZC3H13.

METTL3 is the catalytic subunit of the m6A writer complex, and it is located into nuclear speckles (X. Wang et al., 2017). METTL3 exerts its function mainly in the nucleus where methyltransferase activity has been found to be higher (Harper et al., 1990). However, METTL3 can also translocate to the cytoplasm and take part in translation in a methyltransferase-independent manner (Lin et al., 2016). METTL3 depleted mice die at early embryonic stage, indicating its importance in embryonic development and early stages of life. Indeed, its role in embryonic development modulation, cell reprogramming, and spermatogenesis has been described (T. Chen et al., 2015; Geula et al., 2015; Xu et al.,

2017). METTL3 also regulates T cell homeostasis and endothelial-to-hematopoietic transition (H. B. Li et al., 2017; C. Zhang et al., 2017).

METTL3 forms a stable heterodimer with METTL14, another component of the m6A methyltransferase complex. METTL14 acts as scaffold that binds to RNA molecules, allosterically activating and enhancing METTL3 catalytic activity (P. Wang et al., 2016). Thus, even if METTL14 does not catalyze the methyl group transfer directly, it is as crucial as METTL3 in RNA methylation by m6A deposition. This is corroborated since METTL14 depletion blocks embryonic stem cell self-renewal, and differentiation and embryonic developmental defects and impaired gametogenesis occur, as when METTL3 is missing (Y. Wang et al., 2014).

WTAP interacts with METTL3 an METTL14 and together form the core methyltransferase catalytic complex (Kobayashi et al., 2018; Ping et al., 2014). WTAP lacks methyltransferase activity, but it is necessary for m6A methyltransferase complex location in nuclear speckles (Ping et al., 2014).

KIAA1429 (also known as VIRMA) and RBM15 (and/or its paralogue RBM15B) interact with the METTL3/METTL14/WTAP complex and recruit and guide it to specific locations within mRNA or lncRNAs sequences, suggesting that they are required to ensure the specificity of m6A deposition (Patil et al., 2016; Schwartz et al., 2014; Yue et al., 2018). On the other hand, ZC3H13 has been found to act as an adaptor between WTAP and RBM15 in mice and flies (Knuckles et al., 2018).

3.2.2. m6A erasers

m6A erasers are proteins that have demethylase activity and remove the methyl group from m6A marks in RNA molecules. Their discovery marked a difference in the epitranscriptomics field as it revealed for the first-time evidence of reversible post-transcriptional modifications in mRNAs. As of now, only two m6A demethylases are known: FTO and ALKBH5 (Jia et al., 2011; G. Zheng et al., 2013).

FTO demethylates internal m6A modifications, and its inhibition has been shown to lead to augmented total m6A levels in mRNAs (Su et al., 2018). Apart from m6A marks, FTO can also act on different substrates, such as m6Am, and hence it is not an m6A-specific demethylase (Zou et al., 2016). FTO takes part in alternative splicing and alternative polyadenylation of pre-mRNA molecules (Bartosovic et al., 2017; Zhao et al., 2014).

The demethylase activity of ALKBH5 is similar to that of FTO. However, ALKBH5 seems to act on m6A marks in a sequence-dependent manner, since it shows preference for m6A within its consensus sequence rather than other methylated nucleotides in single-stranded RNA (Zou et al., 2016). ALKBH5 is expressed in most tissues with a particularly high expression in testis. Indeed, it affects spermatogenesis and fertility in mice (C. Tang et al., 2017; G. Zheng et al., 2013). In addition, ALKBH5 plays an important role in the immune response to viral infections (Y. Liu et al., 2019; Q. Zheng et al., 2017).

3.2.3. m6A readers

m6A readers are a group of RNA binding proteins that recognize m6A methylation marks in RNA molecules and bind them to exert their function on RNA molecule processing. Members of the YTH protein family, including YTHDF1-3 and YTHDC1-2, are the most studied m6A readers and their molecular functions have already been described (Zhen et al., 2020) (Figure 9).

YTHDF1 is located in the cytoplasm, and it interacts with the translation initiation machinery to enchance translation efficiency of m6A-modified mRNA molecules (Olazagoitia-Garmendia et al., 2021; X. Wang et al., 2015; Zong et al., 2021). The YTHDF1 RNA binding pattern is concurrent with m6A sites distribution on mRNA molecules, confirming its sequence-specificity for RNA binding (X. Wang et al., 2015).

YTHDF2 is also located in the cytoplasm. However, it co-localizes with both deadenylation and decapping enzyme complexes into P-bodies to induce mRNA decay

(X. Wang et al., 2014). YTHDF2 recruits the CCR4-NOT deadenylase complex and thus accelerates the degradation of m6A-containting mRNAs and lncRNAs (Du et al., 2016).

YTHDF3 plays a double role in RNA processing. On the one hand, it has been shown to interact with YTHDF1 to induce protein synthesis (A. Li et al., 2017). On the other hand, it also interacts with YTHDF2, and thus, takes part in mRNA decay and degradation (Shi et al., 2017).

YTHDC1 is the only YTH family member that is localized in the nucleus (B. Zhang et al., 2010). At least two different roles have been described for YTHDC1, depending on its binding partner. YTHDC1 recruits splicing factors such as SR proteins and blocks splicing processes, therefore promoting exon inclusion of target mRNA and lncRNAs (Xiao et al., 2016). Conversely, YTHDC1 also interacts with NXF1 and with SRSF3 and induces the nuclear export of target mRNAs and lncRNAs by promoting translocation of m6A-modified mRNA molecules out of the nucleus (Roundtree et al., 2017).

YTHDC2 is the largest member of the YTH protein family, with a molecular weight of 160 kDa, since apart from YTH and RNA-binding domains, YTHDC2 also contains two helicase domains. Indeed, YTHDC2 is the only YTH family member with helicase activity (Hsu et al., 2017; Wojtas et al., 2017). Due to this unique characteristic, YTHDC2 is able to modify RNA secondary structure in an m6A-dependent manner (Tanabe et al., 2016; Wojtas et al., 2017). m6A modifications provoke ribosome pausing in methylated A nucleotides, slowing down translation and decreasing its efficiency (Choi et al., 2016; Mao et al., 2019). However, even if translation efficiency has been reported to be less efficient from m6A containing mRNA transcripts, abrogating m6A from m6A-containing mRNA molecules impairs their translation (Mao et al., 2019). This is in part because of the YTHDC2 helicase activity, since YTHDC2 recognizes m6A marks, unfolds mRNA secondary structure, and enhances overall translation of the target methylated mRNA

transcripts. Thus, YTHDC2 is indirectly involved in m6A-containing mRNA translation (Mao et al., 2019).

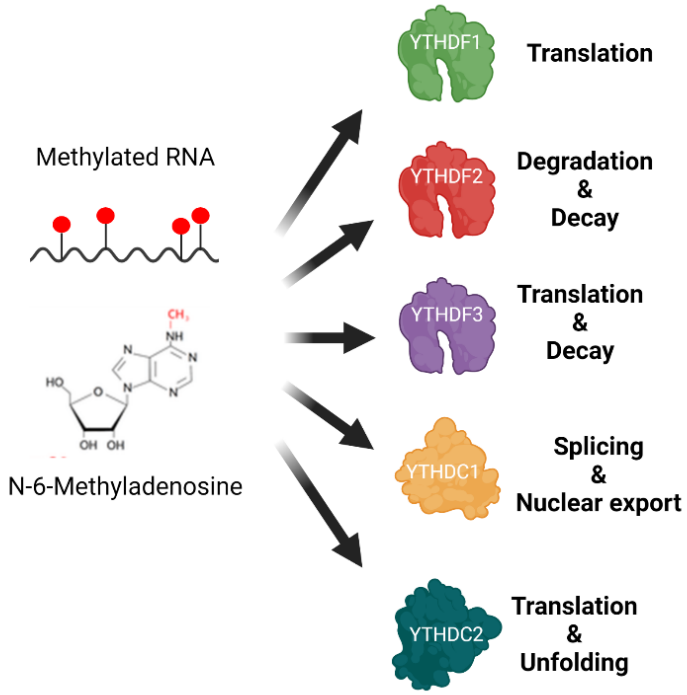

Figure 9. Readers recognize the m6A marks on RNA molecules and affect their metabolism by influencing their ~~next steps and pointing their~~ path. Image created with BioRender.

3.3. m6A in viral infections

Similarly to mRNA and lncRNA molecules, viral RNA molecules also present m6A modifications (Brocard et al., 2017; Gokhale et al., 2016; Kennedy et al., 2017; Tsai & Cullen, 2020). In addition, it is known that viruses can alter the expression of certain genes in infected cells for their own benefit. In this context, alterations in m6A machinery members have been observed after some viral infections, indicating m6A modification may be a key modulator of virus life cycles. For example, enterovirus 71 (EV71) and hepatitis C virus (HCV) present m6A motifs in its genome, which affect differently their life cycle. On the one hand, METTL3 and METTL14 are upregulated during EV71 infection, probably induced by EV71 itself to enhance its own replication (Hao et al., 2019). On the other hand, YTHDF readers are relocated from the cytoplasm to lipid droplets during HCV infection, where they bind to the HCV genome and prevent viral RNA packaging into new virus

particles in an m6A-dependent manner. This binding ultimately results in suppressing viral assembly and HCV particle production (Gokhale et al., 2016).

Changes in the viral epitranscriptome have been suggested to act as an immune evasion mechanism, since m6A-modified RNAs cannot activate TLRs and trigger the innate immune system, while unmodified RNAs do stimulate them (Karikó et al., 2005). Likewise, RIG-I can recognize viral RNA to activate antiviral immune response through IFN-I pathway induction, but it is not triggered by m6A-modified viral RNA, mediating viral evasion of the innate immune system (Durbin et al., 2016; M. Lu et al., 2020).

3.4. m6A in immune response

m6A modification is also involved in the regulation of immune responses, including innate immunity to viral infections and autoimmunity.

The IFN-I pathway plays a key role in antiviral response, inducing the expression of ISGs and the production of cytokines that lead to immune response activation (Negishi et al., 2018; Schoggins & Rice, 2011). Therefore, its expression must be tightly regulated. Some antiviral transcripts have been identified as m6A-modified mRNAs that are regulated by m6A-dependent mechanisms (McFadden et al., 2021; Winkler et al., 2019; Q. Zheng et al., 2017). *IFNB1* transcription is negatively regulated by m6A in a METTL3- and YTHDF2-dependent manner, as the loss of METTL3 and YTHDF2 activity increases its stability (Winkler et al., 2019). *TRAF3*, *TRAF6* and *MAVS* mRNAs also contain m6A marks in their 3'UTR. In these cases, the m6A modification is needed for a correct antiviral response, and it has been described that when they lose their m6A marks by ALKBH5 during viral infection, their export to the cytoplasm is blocked, thereby suppressing antiviral innate immunity (Q. Zheng et al., 2017). Similarly, *IFITM1* antiviral transcript translation is enhanced by the m6A methylation and by METTL3 and METTL14 (McFadden et al., 2021).

In the context of autoimmunity, m6A is implicated in T cell homeostasis by targeting the IL-7/STAT5/SOCS pathway (H. B. Li et al., 2017; J. Yang et al., 2019). The SOCS protein family is formed by inhibitory proteins involved in JAK-STAT signaling and encoded by *SOCS1-3* mRNAs. *SOCS* mRNA expression is regulated by m6A-dependent mechanisms that induce their degradation by m6A methylation, thereby activating the JAK/STAT pathway and initiating naïve T cell re-programming for proliferation and differentiation (H. B. Li et al., 2017).

Several studies have reported that m6A machinery members are altered in patients with autoimmune pathologies such as systemic lupus erythematosus and rheumatoid arthritis (Wardowska, 2021). However, little known about the functional role of the m6A modification in autoimmune disorders. In the context of CeD, the previously mentioned work by Olazagoitia-Garmendia *et al* is the only known study that reported the relation between m6A and CeD pathogenesis so far, in which a gluten-derived and m6A-dependent mechanism is described for the XPO1/NFkB/IL8 regulatory axis (Olazagoitia-Garmendia et al., 2021).

HYPOTHESIS
AND
AIMS OF THE STUDY

The hypothesis of this study is that reovirus infections contribute to the development of CeD via m6A-mediated mechanisms, and that gluten consumption can reactivate the IFN-I pathway through m6A-dependent regulation of antiviral transcripts in patients that have been previously infected by this enteric RNA virus.

The pesent work has four main objectives that aim to test this hypothesis:

1. To evaluate reovirus as a new viral triggering agent for CeD development.
    a. To develop a technique to quantify anti-reovirus antibodies in human serum.
    b. To assess the association between reovirus infections and CeD onset.

2. To determine whether the antiviral immune response is involved in CeD pathogenesis.
    a. To compare the levels of proinflammatory cytokines related to viral infections in CeD and non-CeD individuals.
    b. To identify players implicated in the regulation of innate immunity.

3. To understand the role of m6A methylation in CeD pathogenesis.
    a. To compare m6A methylation levels in CeD and non-CeD individuals.
    b. To investigate the implication m6A machinery members in CeD.

4. To generate an *in vitro* model resembling intestinal viral infections and gluten consumption.
    a. To examine the effect of those environmental factors on m6A machinery members, proinflammatory cytokines and innate immune response-related genes.
    b. To assess a possible connection between viral infections and CeD through m6A-dependent mechanisms contributing to inflammation.

MATERIALS AND METHODS

1. Materials

1.1. Human samples

Celiac disease was diagnosed according to the ESPGHAN (European Society of Pediatric Gastroenterology Hepatology and Nutrition) criteria in force at the time of recruitment, and including anti-gliadin, anti-endomysium (anti-EMA) and anti-transglutaminase (anti-TGA) antibody determinations as well as a confirmatory small bowel biopsy (Husby et al., 2012).

Serum samples from peripheral blood were collected for CeD-related antibody determinations and were stored at -80 ºC until use. Information of the human serum samples used is summarized on Table 1.

Table 1. Details about patients of used human serum samples.

Dx	**Number of samples**	**Age (Mean ± Standard deviation)**	**Sex**	**Positivity for celiac serology**
CeD	n = 44	5.5 ± 3.6	Female 59.1%	100%
			Male 40.9%	
Non-CeD (Controls)	n = 44	9.6 ± 2.7	Female 47.7%	0%
			Male 52.3%	

Biopsy specimens from the distal duodenum of each individual were obtained during routine diagnostic endoscopy, after informed consent had been obtained from their parents. None of the patients suffered from any other concomitant immunological

disease. None of the controls showed inflammation of the small intestine at the time of the biopsy. Information of the intestinal biopsy samples used is summarized on Table 2.

Table 2. Details about patients of used human intestinal biopsy samples.

Dx	**Number of samples**	**Age (Mean ± Standard deviation)**	**Sex**	**Positivity for celiac serology**	**Positivity for CeD-risk associated HLA**	**Marsh classification (0-3)**
Active CeD	n = 16	5.7 ± 4.2	Female 58.3% Male 41.7%	100%	HLA-DQ2 83.3% HLA-DQ2/DQ8 16.7%	3 – 100% ⇒ 3a – 25.0% ⇒ 3b – 33.3% ⇒ 3c – 41.7%
CeD on GFD	n = 13	2.0 ± 0.7	Female 66.7% Male 33.3%	0%	HLA-DQ2 72.7% HLA-DQ2/DQ8 27.3%	0 – 90.9% 1 – 9.1%
Non-CeD (Controls)	n = 16	8.1 ± 3.6	Female 68.8% Male 31.3%	0%	N/A	0 100%

1.2. Cell lines and treatments

Intestinal cell line HCT-15 was purchased from Sigma-Aldrich (#91030712) (Poole, UK) and cultured in RPMI (Lonza, #12-115F) supplemented with 10% FBS (Millipore, Burlington, MA, USA #S0115), 100 units/ml penicillin and 100 µg/ml streptomycin (Lonza, #17-602E).

1.2.1. PIC+PTG in vitro model

To mimic viral infections, the synthetic viral dsRNA analog PIC (InvivoGen, San Diego, CA, USA #31852-29-6) was used at a final concentration of 1.5 µg/ml and transfected using Lipofectamine-2000 (Invitrogen, #11668027).

To simulate gluten exposure, cells were stimulated with pepsin trypsin-digested gliadin (PTG) at a final concentration of 1.5 mg/ml.

1.2.1.1. Endotoxin-free PTG preparation

PTG was prepared by enzymatic digestion with pepsin and trypsin, as previously described (Mendoza-Gomez et al., 2022). Briefly, 5 g of gliadin (Sigma-Aldrich, #G3375) were mixed with 50 mg of pepsin (Sigma-Aldrich, #6887) and dissolved in 50 ml of 0.2 M HCl and incubated overnight at 37 ºC with gentle agitation. Afterwards, 50 mg of trypsin (Sigma-Aldrich, #T9201) were added to the pepsin-digested gliadin, which had been previously neutralized to pH 7.4 with 1 M NaOH, and incubated for 5-6 h at 37 ºC with agitation. Finally, the mix was boiled for 2 h to inactivate the enzymes, centrifuged at 2000 g for 10min and the solution containing PTG was purified by filtration through a 0.22 µM filter. Additionally, PTG was tested for the presence of endotoxin with the PYROGENT® Plus Single Test (Lonza, #N289-25), and total protein amounts were quantified using BCA reagent (Thermo Scientific, #23227) before first use. The PTG solution was aliquoted and stored at -80 ºC until used.

1.2.1.2. PIC+PTG *in vitro* model set-up

The PIC+PTG *in vitro* model consists of a combination of PIC treatment for 24 h and subsequent PTG stimulation for 4 h. For the development of this approach, 300,000 HCT-15 intestinal cells were seeded per well, and PIC was transfected with Lipofectamine-2000 while the cells were still in suspension. After 24 h incubation, the PIC-containing transfection medium was replaced with fresh RPMI medium, and cells were incubated overnight. The following morning PTG was added to the culture at a

concentration of 1.5 mg/ml. Lastly, after 4 h of PTG stimulation, the cells were harvested for RNA and protein analyses (Figure 10).

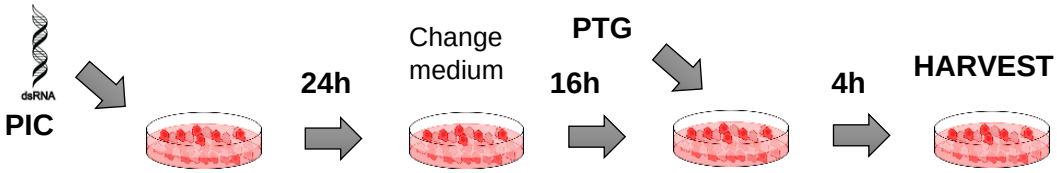

Figure 10. Schematic image of the steps followed to develope the PIC+PTG *in vitro* model.

1.2.2. Other treatments

For mRNA stability analyses, 250,000 cells/well were seeded for ovMETTL3 transfection and two different treatments were applied in independent experiments. On the one hand, HCT-15 cells were treated with actinomycin D (Sigma-Aldrich, #A9415) at a final concentration of 5 µg/ml for 2 h, 4 h and 6 h; and on the other hand, HCT-15 cells were treated with cycloheximide (Sigma-Aldrich, #01810) at a final concentration of 20 µg/ml for 3 h and 24 h.

To evaluate the effect of m6A inhibition, 250,000 cells/well were seeded and treated the following morning with 100 mM cycloleucine (Sigma Aldrich, #A48105) for 3 h.

2. Methods

2.1. Overexpression

For overexpression experiments 250,000 cells/well were seeded and 500 ng plasmid was transfected using X-TremeGENE HP DNA transfection reagent (Sigma-Aldrich, #6366546001). When double overexpression was carried out, 250 ng of each plasmid were transfected. Cells were harvested 48 h post transfection.

For METTL3 overexpression, a commercially available plasmid from Addgene (#53739) was used. For YTHDC1 overexpression a Flag-tagged YTHDC1 plasmid cloned with Gateway recombination (Graindorge et al., 2019) kindly provided by Dr Alena Shkumatava's lab at Institute Curie (Paris) was transfected. For YTHDC2 overexpression, a Flag-tagged YTHDC2 plasmid kindly provided by Prof. Chuan He's Group at Chicago University was used, in which the CDS of *YTHDC2* was cloned into the pFastBac vector (Hsu et al., 2017). For *IRF7* overexpression, a CMV driven overexpression plasmid containing the *IRF7* CDS was purchased from VectorBuilder (Neu-Isenburg, Germany).

2.1.1. Plasmid construction

The construction of MUT *IRF7* plasmid (with truncated m6A motifs) was performed in four steps (Figure 11). First, the region harboring the m6A motifs (250bp) was amplified by PCR with specific primers containing restriction sites for *Bsm*BI and *Sfi*I (Arrow 1). Afterwards, m6A motifs were removed by reamplifying the previous *Bsm*BI/*Sfi*I PCR product with specific primers to introduce a silent point mutation (A→C) of the A nucleotide in the consensus m6A motif, generating a mutated PCR product (Arrows 2 and 3). The resulting two subproducts of similar size were joined together by overlapping PCR (Arrows 4 and 5). Finally, the mutated PCR product was cloned into the *IRF7* overexpression vector using *Bsm*BI (NEB #R0580) and *Sfi*I (NEB #R0123S) restriction

enzymes (Arrow 6). The primers used for mutagenesis and cloning are listed on Table 3.

Table 3. Primers used for MUT IRF7 plasmid construction and their sequences.

NAME	**PRIMER SEQUENCE (5'→3')**
IRF7 Fw + *Sfi*I	AGGGTGGGCCCCCAGGGCCATT
IRF7 Rv + *Bsm*BI	GGGTCGTCTCTACTGCCCACCC
IRF7 Fw + *Sfi*I + 1st m6A mutation	GGTGGGCCCCCAGGGCCATTCCTGGCACACACACATGCTGGCCT
IRF7 Fw + 2nd m6A mutation	GAGAGGGCCAAGAAGGGCTT
IRF7 Rv + 2nd m6A mutation	AAGCCCTTCTTGGCCCTCTC

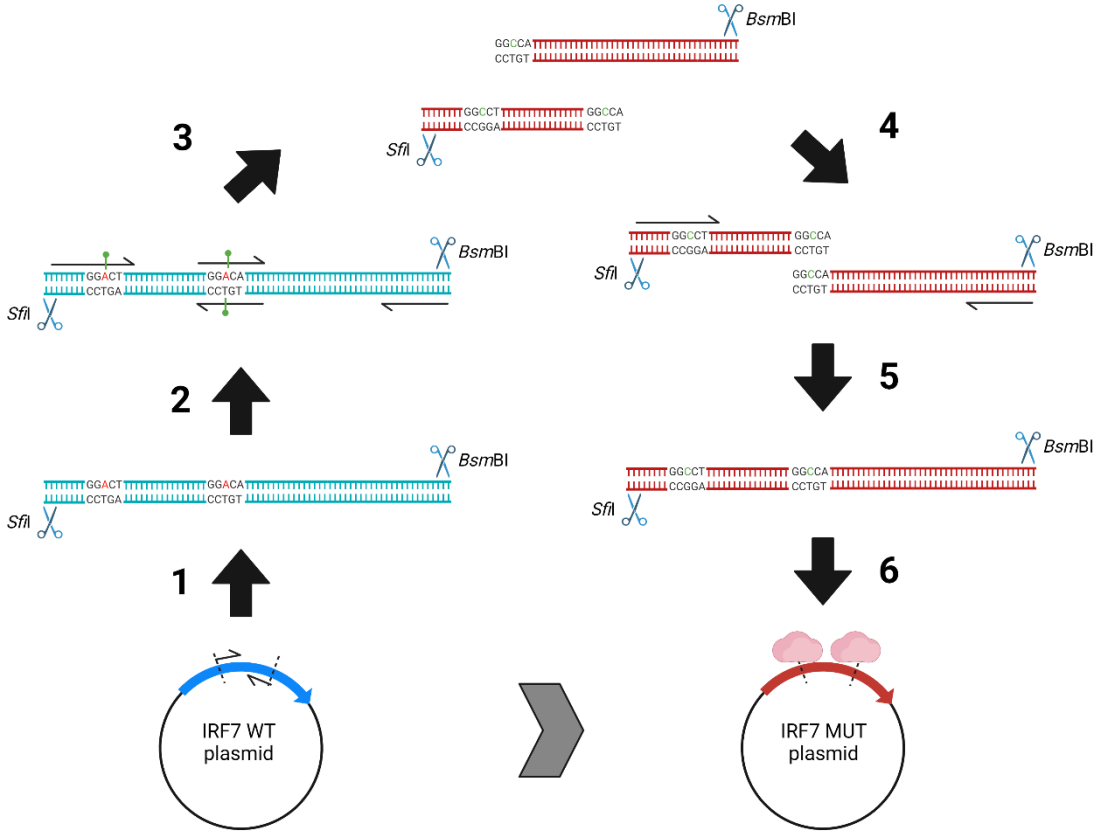

Figure 11. Schematic image of the steps followed to remove m6A motifs within the CDS of *IRF7* and generate the *IRF7* MUT plasmid. Image created with BioRender.

2.2. Silencing experiments

For silencing experiments, 150,000 cells/well were seeded and specific siRNAs against *ALKBH5* or *METTL3,* or a negative siRNA control were transfected into cells using Lipofectamine RNAiMax reagent (Thermo Fisher, #13778075). For *ALKBH5* silencing, the final concentration of siRNA used was 30 nM, and for *METTL3* silencing 60 nM. The sequences of the siRNAs used are listed on Table 4.

Table 4. siRNA sequences used for silencing experiments.

TARGET	LOCATION	PRODUCT REFERENCE
ALKBH5	Exon 4 (3'UTR)	IDT, #hs.Ri.ALKBH5.13.1
	Exon 1,2 (CDS)	IDT, #hs.Ri.ALKBH5.13.3
METTL3	Exon 11 (3'UTR)	IDT, #hs.Ri.METTL3.13.1
	Exon 5 (CDS)	IDT, #hs.Ri.METTL3.13.2
Negative control	Nowhere	IDT, #51-01-14-01

After 16 h the siRNA-containing transfection medium was replaced with fresh complete RPMI medium. Cells were harvested 48 h after medium replacement. In the PIC+PTG model, PIC treatment was started 24 h after transfecting METTL3 siRNA.

2.3. Cell fractionation

Nuclear and cytoplasmic fractions were separated by cell lysis in C1 lysis buffer (1.28 M sucrose, 40 mM Tris-HCl pH 7.5, 20 mM $MgCl_2$, 2% Triton X-100) followed by a centrifugation step. The cell pellet was resuspended in diluted C1 solution (20% C1 lysis buffer, 20% PBS), and kept on ice for 15 minutes. Lysates were centrifuged at 2500 g for 15 min at 4 ºC, and the pellet was kept as the nuclear fraction and the supernatant as the cytoplasmic fraction. RNA was extracted from both compartments, and gene expression was analyzed to assess the localization of the target RNAs. *RPLPO* was used as cytoplasmic and *lnc13* as nuclear controls, respectively.

2.4. RNA and protein extraction

For gene expression analyses, RNA was extracted from human intestinal biopsies, cells and cell fractions with the NucleoSpin RNA Kit (Macherey Nagel, #740984.50).

To assess RNA-protein interactions, immunoprecipitated RNA was purified from protein A agarose beads using the PureLink RNA extraction kit (Invitrogen, Carlsbad, USA, #12183016).

Proteins were extracted by cell lysis in RIPA buffer (150 mM NaCl, 1.0% NP-40, 0.5% Sodium Deoxycholate, 0.1% SDS, 50 mM Tris-HCl, 1 mM EDTA).

2.5. Gene expression analyses

In each reaction, 500-1000 ng of RNA were retrotranscribed using iScript cDNA Synthesis Kit (BioRad, CA, USA, #1708890). Expression levels were determined by RT-qPCR using iTaq SYBR Green Supermix (Bio-Rad, #1725124) and specific primers. *RPLPO* was used as endogenous control. Reactions were run in a BioRad CFX384 machine and melting curves were assessed to ensure the amplification of a single product. All qPCR measurements were performed in duplicate and expression levels were analyzed using the $2^{-\Delta\Delta Ct}$ method. All primers used are listed on Table 5.

Table 5. Specific primers for gene expression analysis by qPCR.

GENE	FORWARD PRIMER SEQUENCE	REVERSE PRIMER SEQUENCE
ALKBH5	CGGCGAAGGCTACACTTSCG	CCACCAGCTTTTGGATCACCA
CXCL10	GTGGCATTCAAGGAGTACCTC	TGATGGCCTTCGATTCTGGATT
HPRT	ACCAGTCAACAGGGGACATAA	CTTCGTGGGGTCCTTTTCACC
IFNB1	GCTTGGATTCCTACAAAGAAGCA	ATAGATGGTCAATGCGGCGTC
IL15	TTGGGAACCATAGATTTGTGCAG	AGAGAAAGCACTTCATTGCTGTT
IL18	TCTTCATTGACCAAGGAAATCGG	TCCGGGGTGCATTATCTCTAC
IRF1	ATGCCCATCACTCGGATGC	CCCTGCTTTGTATCGGCCTG
IRF3	AGAGGCTCGTGATGGTCAAG	AGGTCCACAGTATTCTCCAGG

IRF7	CCCACGCTATACCATCTACCT	GATGTCGTCATAGAGGCTGTTG
IRF7 (m6A motifs)	CATTCCTGGCACACACACAT	AAGCCCTTCTTGTCCCTCTC
Lnc13	AAGGATCATTGCAGGGTCTC	GTGGCCAAAAGAAGTCTGAGTC
METTL14	GAGTGTGTTTACGAAAATGGGGT	CCGTCTGTGCTACGCTTCA
METTL3	TCGAGAGCGAAATTTTTCAAC	GGAGATAGAGAGCCTTCTGAACC
RPLP0	GCAGCATCTACAACCCTGAAG	CACTGGCAACATTGCGGAC
SOCS1	AGACCCCTTCTCACCTCTTG	AGTTAAGCTGCTACAACAACCAG
STAT1	CGGCTGAATTTCGGCACCT	CAGTAACGATGAGAGGACCCT
YTHDC1	CTTCTGATGAGCAAGGGAACAA	GGCCTCACTTCGAGTGTCATAA
YTHDC2	CTCCGGAACTTTTGAGAATGCC	TTAAAGCTGGTGGAGGTTCAGG
YTHDF1	ACCTGTCCAGCTATTACCCG	TGGTGAGGTATGGAATCGGAG
YTHDF2	TGAACCTTACTTGAGTCCACAGG	AAGCCAATGGAGGGACTGTAG

2.6. Western Blot

Laemmli buffer 6X (62 mM Tris-HCl, 100 mM DTT, 10% glycerol, 2% SDS, 0.2 mg/ml bromophenol blue, 5% 2-mercaptoethanol) was added to the protein extracts and proteins were denaturized at 95°C for 10 minutes. Then, proteins were migrated on 10% or 8% SDS-PAGE gels, depending on the size of the proteins of interest. Following electrophoresis, proteins were transferred onto nitrocellulose membranes using a Transblot-Turbo Transfer System (BioRad) and blocked with 5% non-fat milk diluted in TBST (20 mM Tris, 150 mM NaCl and 0.1% Tween 20) at room temperature for 1 h. The membranes were incubated with primary antibodies at a 1:1000 dilution at 4 ºC overnight. Primary antibodies used are listed on Table 6.

Table 6. Information of the primary antibodies used for protein detection by Western Blot.

PROTEIN	SIZE (kDa)	SOURCE	PRODUCT REFERENCE
ALKBH5	50	Rabbit	Novus Biologicals, #NBP1-82188
GAPDH	37	Mouse	Santa Cruz Biotechnologies, #sc-47724
HSP90	90	Rabbit	Cell Signaling, #4874
IRF7	70	Mouse	Santa Cruz Biotechnologies, #sc-74472
METTL3	64	Rabbit	Abcam, #195352
TUBULIN	55	Mouse	Sigma-Aldrich, #T9026
YTHDC2	160	Rabbit	Proteintech, #27779-1-AP

The following morning, membranes were washed three times by agitation in TBST for 10 minutes. Afterwards, membranes were incubated with a horseradish peroxidase-conjugated anti-rabbit (Santa Cruz Biotechnologies, #sc-2357) or anti-mouse (Santa Cruz Biotechnologies, #sc-516102) secondary antibody at a 1:10000 dilution in 2.5% non-fat milk at room temperature for 1 h. Next, membranes were washed again as previously. Immunoreactive bands were revealed using the Clarity Max ECL Substrate (BioRad, #1705062) in a Bio-Rad Molecular Imager ChemiDoc XRS system (BioRad) and quantified using the ImageJ software (BioRad).

2.7. RNA immunoprecipitation

2.7.1. m6A RNA immunoprecipitation (meRIP)

RNA was fragmented with RNA fragmentation buffer (100 mM Tris, 2 mM $MgCl_2$) at 95 ºC for 3 min and placed on ice immediately after heating. Protein A Sepharose beads (GE Healthcare, Chicago, USA #17-0780-01) at 25% vol/vol were washed twice in reaction buffer (150 mM NaCl, 10 mM Tris-HCl, 0.1% NP-40) prior to the preclearing and antibody coupling steps. For preclearing , 100 µl of beads were used per sample; and for antibody coupling, 30 µl of the bead suspension were used per sample. After washes,

beads were resuspended in the same initial volume of reaction buffer. In the preclearing step, 6 µg of fragmented RNA were incubated with 100 µl of the bead suspension. For antibody coupling, 1 µg of anti-m6A antibody (Abcam, #ab151230) and control antibody (IgG, Santa Cruz Biotechnologies, Dallas, USA, #sc-2025) were coupled to 30 µl of Protein A Sepharose beads each. Both RNA-beads and beads-antibody mixes were incubated in a rotation wheel at 4 ºC for 1 h. After incubation, beads were precipitated by centrifugation at 1.500 rpm for 1 min. Beads coupled to antibodies were washed twice in reaction buffer. On the other hand, beads from the preclearing step were discarded and 10% of the supernatant (precleared RNA) was kept as input. The remaining supernatant was separated, and each part (45% of the total precleared RNA) was added to the corresponding antibody-coupled beads. The tubes were incubated in a rotating wheel at 4 ºC for 3 h. Subsequently, beads were washed twice in reaction buffer, twice in low salt buffer (50 mM NaCl, 10 mM TrisHCl and 0.1% NP-40) and twice in high salt buffer (50 mM NaCl, 10 mM TrisHCl and 0.1% NP-40). After the last wash, beads were resuspended in Lysis buffer and RNA was extracted using the PureLink RNA extraction kit (Invitrogen, Carlsbad, USA, #12183016).

2.7.2. RNA immunoprecipitation of m6A machinery proteins

Cells were lysed in RIP buffer (150 mM KCl, 25 mM Tris, 0.5 mM DTT, 0.5% NP-40) complemented with Proteinase Inhibitor (Thermo Scientific, #A32955). Lysates were kept on ice for 10 minutes and homogenized using a syringe. Meanwhile, 10 µl per sample of magnetic bead suspension (Protein G Dynabeads, Invitrogen, # 10004D) were washed twice with RIP buffer and resuspend in 10 µl. Lysates were pre-cleared with magnetic beads in a rotating wheel at 4 ºC for 1 h.

After incubation, beads were removed using a magnetic separator and the cleared supernatant was kept. This precleared lysate was separated as follows: 45% was used for immunoprecipitation of the target protein, 45% for negative immunoprecipitation control, and 10% for input. Target proteins were immunoprecipitated with 1 µg of the

antibody against the corresponding protein (ALKBH5, METTL3 or YTHDC2, mentioned on Table 6); while for negative immunoprecipitation control, 45% of the precleared lysate was incubated with 1 µg of anti-rabbit IgG antibody (Santa Cruz Biotechnologies, #sc-2025) in a rotating wheel at room temperature for 1 h. The input fraction was kept on ice or at -80 ºC until use.

During the incubation for antibody coupling, 20 µl of Dynabeads were washed as previously described. After 1 h, washed Dynabeads were added to the antibody-lysate mix and samples were kept rotating on a rotating wheel at room temperature for 30 min. Afterwards, beads coupled to antibody-protein complexes were washed twice in RIP buffer, twice in low salt buffer (50 mM NaCl, 10 mM Tris-HCl, 0.1% NP-40) and twice in high salt buffer (500 mM NaCl, 10 mM Tris-HCl, 0.1% NP-40). After the washes, 70% of the beads were resuspended in RNA extraction buffer and 30% were kept for confirmation of specific protein immunoprecipitation by Western Blot.

2.8. ELISA

2.8.1. Anti-reovirus antibody detection in serum samples

Serum reactivity against Reovirus was measured using an in-house ELISA technique based on Amy Rosenfeld's protocol (Rosenfeld et al., 2022), with several changes (Figure 12). The binding assay was performed in flat-bottomed microtiter plates (Nunc MaxiSorp ELISA plates, Thermo Fisher, #44-2404-21). Wells were coated with 10^5 PFU/well of Mammalian Orthoreovirus Type 1 Lang (reovirus) diluted in binding buffer (0.1 M bicarbonate/carbonate buffer, pH 9.6) and incubated on a rocking platform at 4 °C overnight. Binding buffer alone without viral particles was used as non-virus control. The next morning, unbound virus was discarded, and wells were washed with PBST [PBS tablets (Invitrogen, #003002) diluted in distilled water and 0.1% Tween 20], three times at room temperature (Step 1)

Wells were blocked with 50% horse serum in PBST in movement on an orbital platform at room temperature for 10 h. After blocking wells were washed five times as already described (Step 2).

Two-fold serial dilutions of the standard serum in PBST (ranging from 1:128 to 1:8192) were included in each plate for interplate normalization. The 3 serum samples from CeD patients previously used for the set-up and optimization of the technique, because they presented high reactivity against reovirus, were pooled and used as the standard sample. The test serum samples were diluted 1:1024 in PBST. A final volume of 100 µl of diluted serum was added to wells and incubated rocking at 4°C overnight. The following morning, the serum was discarded, and wells were washed 5 times with PBST on a rocking platform at room temperature for 20 min each time (Step 3).

Afterwards, a final volume of 100 µl of Peroxidase-conjugated AffiniPure Goat Anti-Human IgG (Jackson Immuno Research, #109-035-088) diluted 1:10000 in PBST was added to the wells and incubated on a rocking platform at room temperature for 90 minutes. After incubation, wells were washed again as described above (Step 4).

Substrate solution BD Pharmingen TMB Substrate Reagent Set (#555214) was used to develop the HRP-conjugated secondary antibody signal. After five-minute exposure, the reaction was quenched with 2 N H_2SO_4 and absorbance was read at 450 nm and 570 nm (Step 5).

Relative serum reactivity against reovirus was calculated by subtracting absorbance values at 570 nm to values at 450 nm and relativizing them to the absorbance values of the 1:1024 dilution of the standard sample in the same plate.

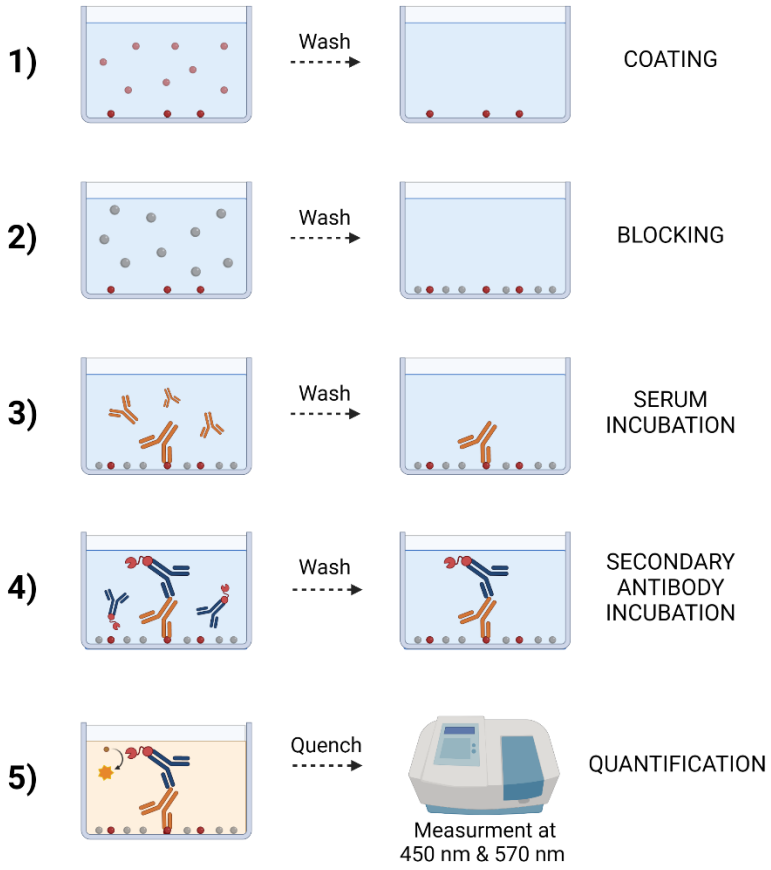

Figure 12. Schematic image of the steps followed during the ELISA-based approach to detect anti-reovirus antibodies and measure serum reactivity against reovirus. The numbers on the left indicate each step explained with details in the text. Briefly, in step 1 reovirus particles (red dots) are seeded; in step 2, wells are blocked with horse serum (represented as grey dots); in step 3, serum samples (represented as orange antibodies) are incubated with coated reovirus particles; in step 4, HRP-conjugated anti-human secondary antibody (represented as blue antibodies) is added to the wells; and in step 5, color is deveoped and measured afterwards in a spectrophotometer. Image created with BioRender.

2.8.2. CXCL10 quantification in serum samples

The concentration of CXCL10 in serum was determined using a commercially available sandwich ELISA kit (Proteintech, Germany, #KE00128) following the manufacturer's instructions. In brief, 100 µl of the standard samples provided and the test serum samples were incubated in plate wells precoated with anti-CXCL10 antibody at 37ºC for 2 h. Serum samples were diluted 1:1 in Sample Diluent PT 4-oc buffer before the assay, as recommended. Afterwards, 100 µl of CXCL10 detection antibody solution was added to each well and plates were incubated at 37 ºC for 1 h. Then, 100 µl of HRP detection

antibody solution was added and incubated at 37 ºC for 40 min. Between each step, wells were washed with wash buffer four times.

TMB substrate was used to develop HRP signal by incubating the plate at 37ºC for 15 min in the dark. Finally, stop solution was added to the wells and absorbance was measured immediately at 450 nm and 630 nm. CXCL10 concentration was calculated using the standard curve.

2.8.3. Total m6A quantification

Total m6A levels were measured using 200 ng of RNA from intestinal biopsy samples and HCT-15 cells in different conditions using a commercially available m6A ELISA kit (Epigentek, NY, USA, #P-9005-96).

First, the RNA sample of interest and both positive and negative controls were diluted in 80 µl binding solution, added to the corresponding wells and incubated for at 37 ºC for 90 min. Afterwards, diluted m6A capture antibody was added and the plate was incubated at room temperature for 1 h. Then, detection antibody was added and incubated at room temperature for 30 min. Later, wells were incubated with enhancer solution at room temperature for 30 min. Between each step, wells were washed with 150 µl wash buffer three times. After the last wash, developer solution was added, and wells were incubated at room temperature in the dark for 10 min. When samples turned blue, indicating the presence of m6A, stop solution was added and the color changed to yellow. Then, absorbance was measured at 450 nm. Total m6A percentage was calculated by subtracting absorbance values of the negative control to the values of the test samples and of the positive control, normalizing them to the RNA amount used as input, and relativizing to the positive control.

2.9. Online servers

2.9.1. SRAMP

SRAMP is an online and publicly available m6A prediction server (Zhou et al., 2016). It uses genomic or cDNA sequences as input for the prediction of m6A sites. These predictions take into account the sequence itself and the estimated secondary structure surrounding the m6A motifs. Based on those parameters it calculates a prediction score that classifies each putative m6A site into very high, high, moderate or low confidence groups for m6A methylation probability. Different tissues or cells can be chosen including liver, brain, lung (A549 cells), kidney (HEK293 cells), immune cells (CD8+ T cells) and there is also a generic (default) option. For the prediction of m6A sites within *IRF7,* both primary and mature mRNA sequences were used as input, and they were analyzed using the generic option.

2.9.2. RNAfold

The RNAfold web server is a tool to predict the secondary structure of RNA sequences based on the minimum free energy of the nucleotide combination of each sequence. It is an online tool that is publicly available at the Vienna RNA web services (Gruber et al., 2008). Single strand of RNA or DNA sequences up to 7500 nucleotides can be used as input. In the case of *IRF7*, the mature mRNA sequence was analyzed.

2.10. Statistical analyses

The data are represented as the mean ± standard deviation (SD) of at least three biological replicates or as the as the mean ± standard error of the mean (SEM) when groups are of more than six samples. Groups were compared using Student's t-test or ANOVA test. Correlation was analyzed using Pearson correlation coefficients. All statistical tests were performed using the GraphPad Prism 8 software. p values < 0.05 were considered statistically significant ,while $p < 0.1$ was found as an indicative of suggestive trend.

RESULTS

1. Reovirus infections and CeD

1.1. Development and optimization of an anti-reovirus reactivity detection technique

Viral infections have been proposed as environmental triggering factors for CeD development, and more specifically mammalian orthoreovirus (reovirus) infections have been associated with CeD susceptibility (Bouziat et al., 2017).

To confirm the association between CeD and reovirus infections, we measured anti-reovirus antibody titers in serum samples from CeD and non-CeD children. For this purpose, we developed an ELISA method to quantify immunological reactivity against reovirus particles. Reovirus infections are hardly ever diagnosed, and an accurate record of infected and non-infected patients is not usually available. To our knowledge no ELISA based approach has ever been used before for reovirus reactivity detection, so the first step to carry out the proposed measures was the optimization of the assay.

First, we tested several concentrations of serum and reovirus particles diluted in washing buffer and coating buffer, respectively. We used a total of 6 serum samples from 3 celiac and 3 non-celiac individuals, and we observed that the signal detected was viral load- and serum volume-dependent, confirming the accuracy of our system (Figure 13A). We selected the 1:1024 dilution for serum concentration since it was the only dilution in which the absorbance values of all samples were below the saturation point (Figure 13A). The 1:16 dilution was chosen as optimal viral load concentration (Figure 13B). We also evaluated the use of sera from different animal-origins for the blocking step. We found that horse serum at 50% in washing buffer was the best option. TBST and PBST were tested too, being the latter the most suitable washing buffer.

Next, in order to assess the specificity of our approach, we decided to include a blank or no virus condition for each serum sample. In addition, we also included a standard curve to correct for variability across experiments. The three samples with higher absorbance values out of the six tested so far, were selected and pooled and subsequently used to generate a standard curve. Measurement of the serum reactivity to reovirus in the standard sample using a broad range of dilutions confirmed its suitability (Figure 13C).

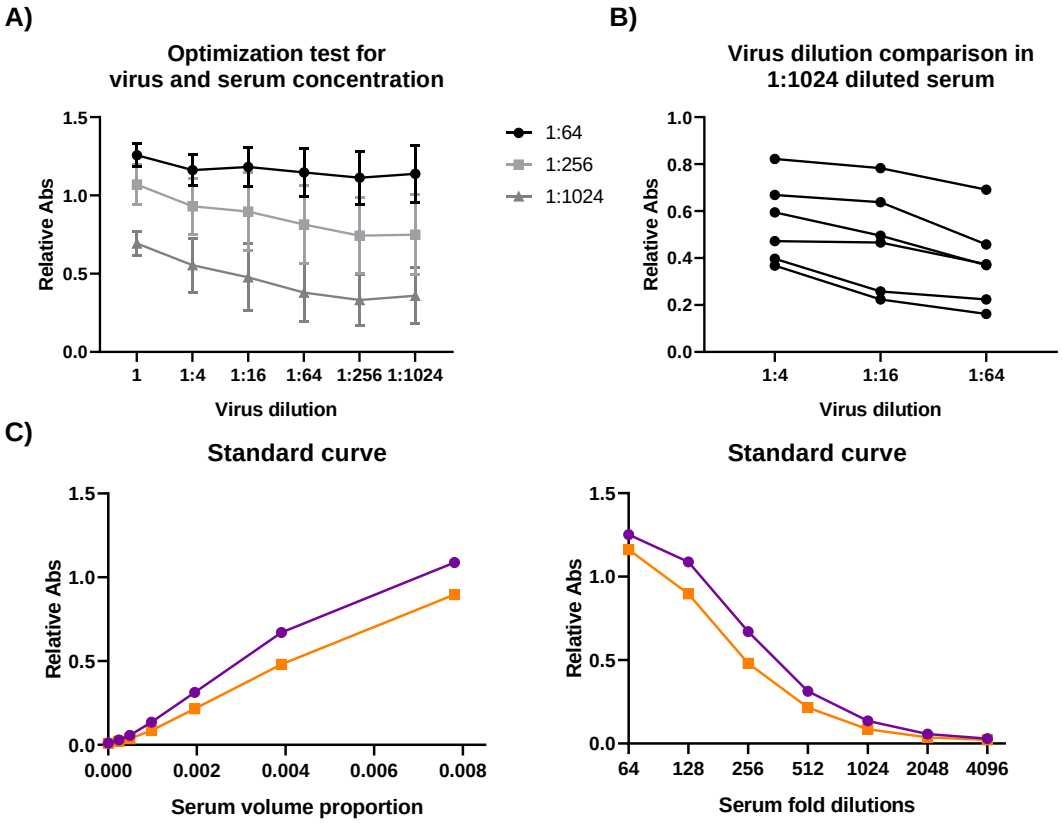

Figure 13. A) Relative absorbance quantification using different virus loads and serum dilutions. **B)** Relative absorbance quantification of individual samples at 1:1024 serum dilution and comparison between 1:4, 1:16 and 1:64 viral load dilutions. **C)** Standard curves of the pooled samples used as standard in a six serial 2-fold dilution starting at 1:128 and washing buffer as blank. In the left serum concentration values are represented as serum volume proportion, and in the right as serum fold dilution. Purpled dots and line regard to 1:16 virus dilution and the orange ones to no virus condition. Relative absorbance was calculated by subtracting absorbance values at 570nm to those at 450nm.

1.2. Serum reactivity against reovirus in CeD

Once the technique had been optimized, we evaluated the reovirus serum reactivity in 44 celiac and 44 non-celiac individuals, and we observed that CeD patients presented significantly higher serum reactivity to reovirus (Figure 14A), suggesting that they had been infected more often or their anti-reovirus immune response was stronger. In any case, these results confirm the association between reovirus infections and CeD and support the involvement of this infection in the risk to develop CeD.

As reovirus infections commonly occur in childhood (Soleimanjahi & Heydarabadi, 2022), we wanted to clarify whether age affects anti-reovirus antibody titers. We compared younger and older patients taking the overall median age of 8 years as reference. Older patients presented lower serum reactivity, but differences were not significant (Figure 14B).

Sex is a biological variable that affects our immune system, since males and females display different immune responses to pathogens, mainly due to sex hormones and genes located on the chromosome X (Klein & Flanagan, 2016; Oertelt-Prigione, 2012). Hence, we also wanted to evaluate the possible implication of sex on serum reactivity against reovirus. In general, females tend to present a stronger innate and adaptive immune response than males (Klein & Flanagan, 2016). However, we did not find any differences between male and female individuals in terms of serum reactivity to reovirus (Figure 14C).

Therefore, these data show that neither age nor sex affect to serum reactivity against reovirus. Still, differences between CeD patients and controls in each group (old and young; and male and female), remain significant, reinforcing the idea that being or not celiac is the determinant factor.

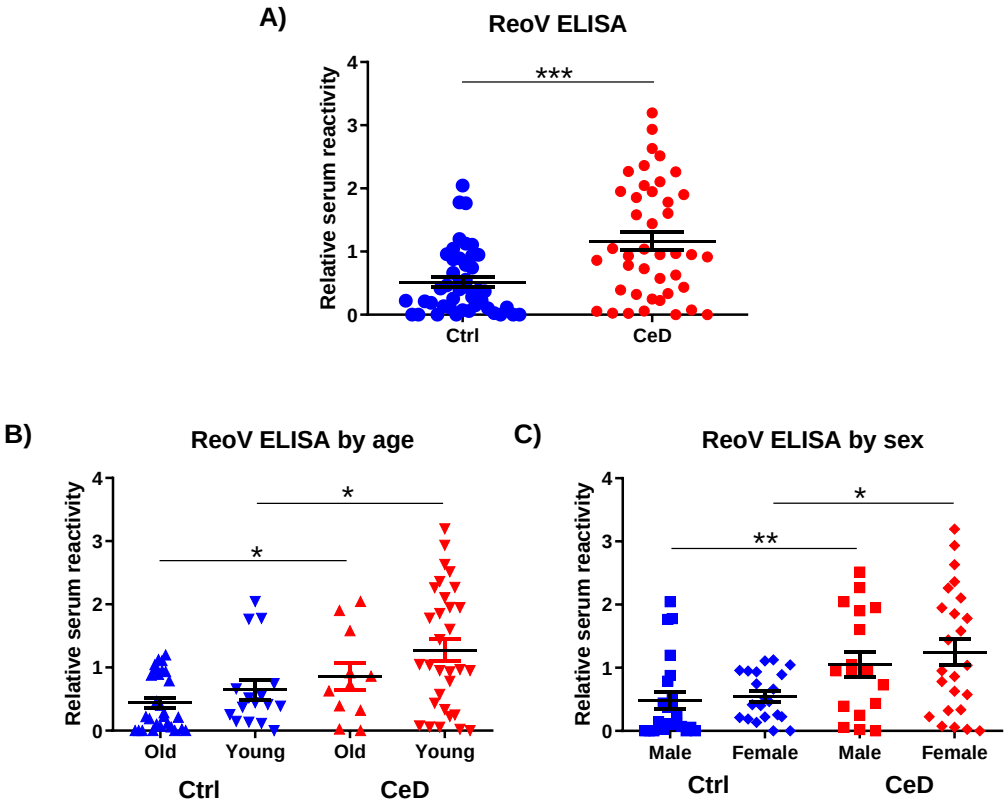

Figure 14. A) Relative serum reactivity to reovirus (ReoV) measured by ELISA in sera samples from pediatric celiac (CeD) and non-celiac (Ctrl) patients. **B)** Comparison of relative serum reactivity against reovirus stratified by age. The median age of 8 years old was consider for division of the groups. **C)** Comparison of relative serum reactivity against reovirus stratified by sex of the individuals. Reactivity was calculated by subtracting absorbance values at 570nm from absorbance values at 450nm and relativizing to reference sample of the standard curve at 1:1024 dilution. ***p<0.001;**p<0.01;*p<0.05 based on t-student analysis.

2. Antiviral immunity in CeD

Taking into account the involvement of CXCL10 in reovirus infection (Carew et al., 2017; Steele et al., 2011) and in CeD development (Haghbin et al., 2019; E. Y. Lee et al., 2009), we wanted to evaluate the connection between these two factors. Thus, we measured CXCL10 concentration by ELISA the in the same serum samples from CeD patients and controls previously used to assess anti-reovirus reactivity. In accordance with the reovirus reactivity results, CeD patients showed significantly higher CXCL10 levels than non-celiac individuals (Figure 15A). Moreover, we observed that CXCL10 levels were correlated with serum reactivity to reovirus, both in celiac and non-celiac individuals (Figure 15B). These results reveal a relation between reovirus infection, CXLC10 and CeD and suggest that reovirus infections might contribute to the increased CXCL10 levels observed in CeD patients.

Reovirus, like rotavirus, is a dsRNA virus of the *Reoviridae* family and that induces the IFN-I signaling pathway through RIG-I, MAD5 and MAVS (Sherry, 2009). Considering that CeD patients showed higher serum reactivity against reovirus, we wondered whether the antiviral immune response was also augmented in CeD patients.

IRF3 and *IRF7* genes encode for two master regulators of IFN pathway, IRF3 and IRF7, and their expression is enhanced upon RNA viral infections (Chiang & Liu, 2019; Ikushima et al., 2013; Ning et al., 2011; Santana-de Anda et al., 2011; Sin et al., 2020). In order to evaluate the immune response to RNA viral infections in the context of CeD, we quantified the expression of *IRF3* and *IRF7* in intestinal biopsy samples from active CeD patients, CeD patients on GFD and non-CeD individuals. Both *IRF3* and *IRF7* showed higher expression in CeD patients (Figure 15C, D). However, only *IRF7* expression remained upregulated in CeD patients on GFD (Figure 15D).

These results pointed to an increased immune response to viral infections that in the case of *IRF7* expression is sustained even after CeD remission when gluten has been

removed from the diet, suggesting that repeated viral infections could leave a mark in the host immune system that might enhance basal inflammation levels, compared to uninfected or less-infected individuals.

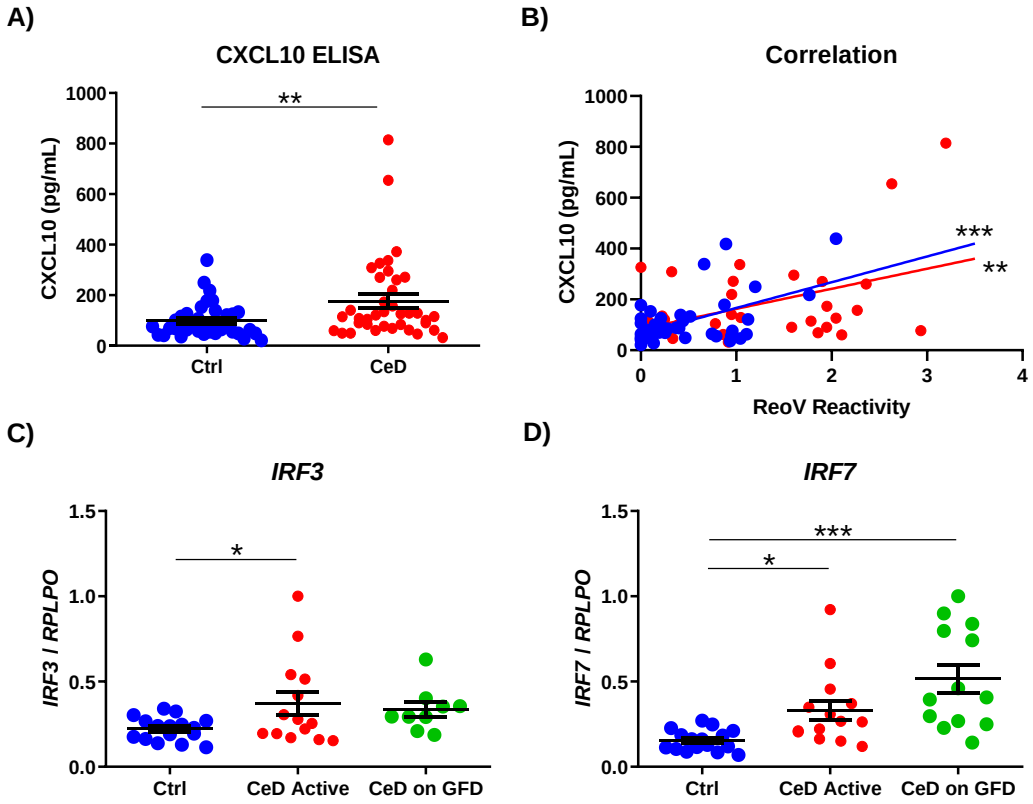

Figure 15. A) CXCL10 levels in sera samples from pediatric celiac (CeD) and non-celiac (Ctrl) patients, measured by ELISA. CXCL10 concentration was calculated using a standard curve. **B)** Pearson correlation between CXCL10 levels and reovirus serum reactivity in celiac (CeD, in red) and non-celiac (Ctrl, in blue) patients. R^2 (CeD) = 0.2001 and R^2 (Ctrl) = 0.2817. **C)** *IRF3* and **D)** *IRF7* expression in intestinal biopsy samples from celiac individuals with inflammation (CeD active), celiac individuals without inflammation after at least two years on a gluten-free diet (CeD on GFD) and non-celiac individuals (Ctrl). Relative expression was calculated with $2^{-\Delta\Delta Ct}$ method and *RPLPO* was used as housekeeping gene. ***p<0.001;**p<0.01;*p<0.05 based on t-student, Pearson correlation and ANOVA analyses.

3. m6A methylation in CeD

3.1. m6A methylation and m6A machinery in CeD

m6A RNA methylation has been found to take part in the regulation of the immune system and, among other processes, it is implicated in viral infections and autoimmunity (Bechara & Gaffen, 2021; Brocard et al., 2017; Dang et al., 2019; Maity & Das, 2016; Shulman & Stern-Ginossar, 2020; L. Tang et al., 2021). Thus, we wanted to evaluate m6A levels in the context of CeD. Using total RNA extracted from intestinal biopsies, we observed that CeD patients showed significantly higher m6A levels when compared to controls (Figure 16A).

Given that m6A levels are altered in CeD, we wondered whether this was due to the differential expression of some m6A machinery members. So, we quantified their expression in intestinal biopsy samples (Figure 16B-H). In concordance with the higher total m6A levels previously observed, both m6A writers presented elevated expression in active CeD patients. Lower expression of the writers was observed in CeD patients on GFD in comparison with the active disease status, what is similar to controls. *METTL3* showed significant difference between active CeD and non-celiac individuals (Figure 16B) and *METTL14* between active CeD patients and CeD patients on GFD (Figure 16C). Opposed to the expression pattern of *METTL14*, m6A eraser *ALKBH5* showed higher expression in the absence of gluten (Figure 16D). Regarding m6A readers, the expression of *YTHDC1*, *YTHDC2* and *YTHDF1* was found to be augmented in active CeD patients and restored to the levels observed in non-celiac individuals in patients on GFD (Figure 16E-G). *YTHDF2* also showed a reduced expression in CeD patients on GFD (Figure 16H). These results point to a general alteration of the m6A machinery in CeD, with an overall increase in the expression of its members in active CeD patients.

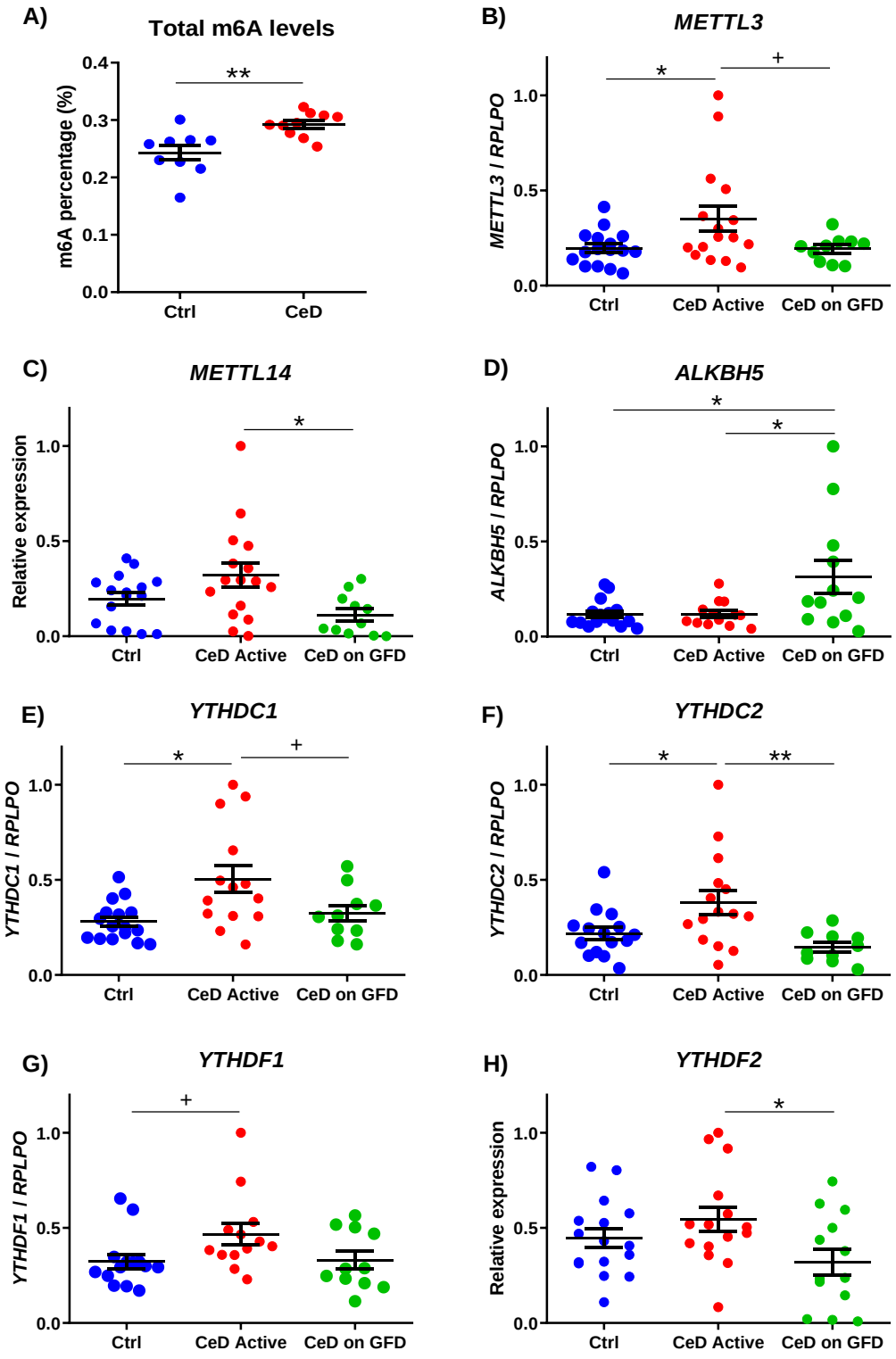

Figure 16. A) Total m6A percentage quantification by ELISA in RNA extracted from intestinal biopsies of celiac (CeD) and non-celiac (Ctrl) individuals. **B)** *METTL3*, **C)** *METTL14,* **D)** *ALKBH5*, **E)** *YTHDC1*, **E)** *YTHDC2,* **G)** *YTHDF1* and **H)** *YTHDF2* expression in intestinal biopsy samples from celiac individuals with inflammation (CeD active), celiac individuals without inflammation after at least two years on a gluten-free diet (CeD on GFD) and non-celiac individuals (Ctrl). Relative expression was calculated with $2^{-\Delta\Delta Ct}$ method and *RPLPO* was used as housekeeping gene. **p<0.01;*p<0.05;+p<0.1 based on t-student and ANOVA analyses.

Next, in order to assess the connections among m6A members, we calculated the correlation between those that presented altered expression and we confirmed that *METTL3* levels correlate with those of *YTHDC1* in CeD individuals (Figure 17A) and with *YTHDC2* levels in both groups (Figure 17B). No correlation was observed in any of the other combinations.

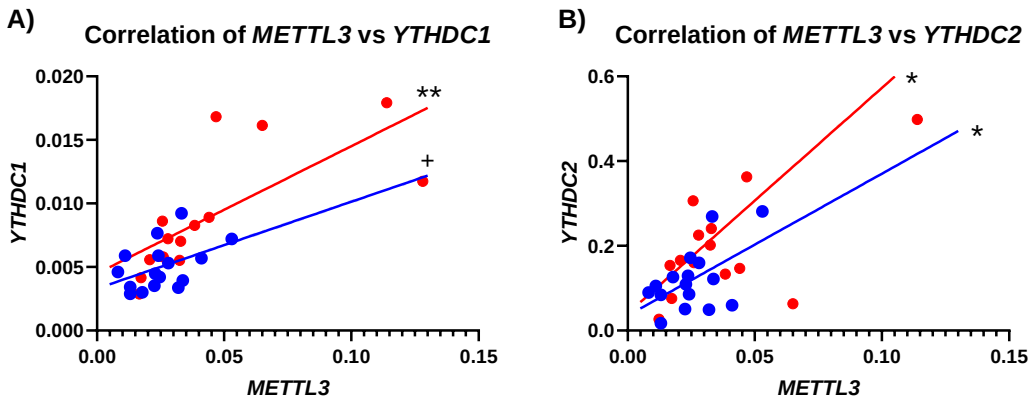

Figure 17. Pearson correlation analysis between expression of **A)** *METTL3* and *YTHDC1,* R^2 (CeD) = 0.5180; R^2 (Ctrl) = 0.1943; and **B)** *METTL3* and *YTHDC2,* R^2 (CeD) = 0.3541; R^2 (Ctrl) = 0.2895; in active CeD patients (in red) and non-celiac patients (in blue). **p<0.01;*p<0.05;+p<0.1.

3.2. Connection between the m6A machinery and antiviral response in CeD

As previously reported, the expression of several antiviral immune response genes and m6A machinery members was increased in CeD patients. To further investigate whether the observed upregulation might be somehow coordinated, we calculated the correlation between the expression of antiviral transcripts *IRF3* and *IRF7*, and the m6A machinery members *METTL3*, *YTHDC1* and *YTHDC2* (Figure 18A-C).

METTL3 expression was found to be correlated with *IRF3* only in active CeD patients (Figure 18A, left), whereas *METTL3* and *IRF7* expression were correlated in CeD and controls (Figure 18A, right). Regarding m6A readers, none of them correlated with antiviral transcripts in the control group (Figure 18B, C). Nevertheless, *YTHDC1* expression was correlated with both *IRF3* and *IRF7* (Figure 18B) in CeD patients. The same was observed in the case of *YTHDC2* with *IRF3* and *IRF7* (Figure 18C).

These results suggest a triple connection between m6A, antiviral response activation and CeD pathogenesis. Considering the correlation of the expression of several m6A machinery members with antiviral transcripts *IRF3* and *IRF7* in CeD, and taking into account the implication of m6A in the antiviral immune response and inflammation (J. Luo et al., 2021; Winkler et al., 2019), our data point to the involvement of alterations in the m6A machinery in the development of CeD, maybe through the modulation of the expression of *IRF3* or *IRF7*.

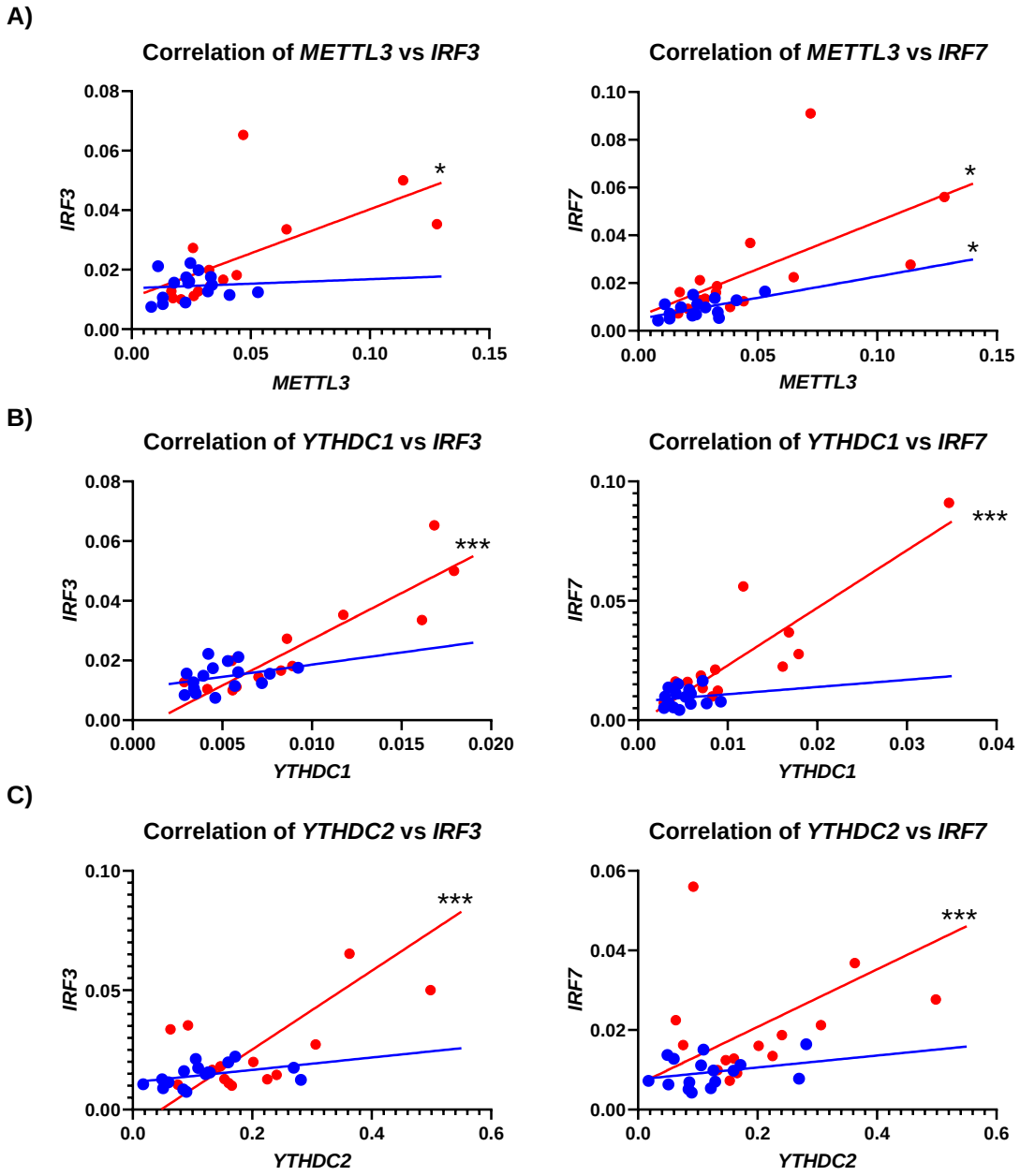

Figure 18. Pearson correlation analysis between expression of **A)** *METTL3* and *IRF3* (left), R^2 (CeD) = 0.3806; R^2 (Ctrl) = 0.0062; and *IRF7* (right), R^2 (CeD) = 0.3712; R^2 (Ctrl) = 0.3167; **B)** *YTHDC1* and *IRF3* (left), R^2 (CeD) = 0.8040 ; R^2 (Ctrl) = 0.1097; and *IRF7* (right), R^2 (CeD) = 0.7694; R^2 (Ctrl) = 0.218; and **C)** *YTHDC2* and *IRF3* (left), R^2 (CeD) = 0.8433; R^2 (Ctrl) = 0.1783; and *IRF7* (right), R^2 (CeD) = 0.5879; R^2 (Ctrl) = 0.0868; in active CeD patients (in red) and non-celiac patients (in blue). ***p<0.001;*p<0.05.

4. Evaluation of the combination of viral infections and gluten consumption in the intestine: The PIC+PTG *in vitro* model in HCT-15 intestinal cells

4.1. m6A machinery in PIC+PTG *in vitro* model

Taking into account that gluten consumption is the main known environmental factor contributing to CeD pathogenesis, and viral infections have been proposed as the additional environmental factor triggering disease development, we wondered how both these factors might influence the expression of m6A machinery members in the context of CeD. To investigate the combined effect of viral infections and gluten consumption, we generated an *in vitro* model of intestinal cells treated with a viral mimic and stimulated afterwards with pepsin- and trypsin-digested gliadin (PTG), the immunogenic fraction of gluten. Polyinosine-deoxycytidylic acid (Poly(I:C) or PIC) is a synthetic dsRNA molecule considered as a viral mimic because it activates the RIG-I-MAVS pathway when transfected into cells (Dauletbaev et al., 2015), in a manner similar to reovirus-derived RNA. As such, it is a suitable proxy for reovirus infections in *in vitro* experiments.

The mayor objective of this *in vitro* model was to recreate what might happen in the intestine of CeD patients. To do so, we treated the intestinal epithelial cell line HCT-15 with the viral mimic PIC for 24 hours. After replacing the media, cells were further incubated for 16h and were then stimulated with PTG. This model simulates *in vitro* a viral infection prior to gluten consumption.

Even though it is known that m6A levels are altered in host cells after viral infections (Dang et al., 2019) and the effect of PTG on intestinal cells has been described before (Olazagoitia-Garmendia et al., 2021), there is no information on how PIC affects m6A methylation in HCT-15 intestinal cells. Thus, we first assessed the effect of PIC on the overall m6A levels, and we observed that PIC treatment resulted in augmented m6A levels in intestinal cells (Figure 19A). As this increase in m6A levels mirrors the elevated levels observed in CeD patients, we next evaluated the expression of m6A machinery

members in our PIC+PTG model. These analyses revealed significant expression changes in some m6A machinery members in PIC and/or PIC+PTG stimulated cells (Table 7 and Figure 19B-H).

Table 7. Differential expression of m6A machinery members in PIC+PTG model ***p<0.001 and *p<0.05 based on ANOVA analyses.

m6A machinery member	PIC	PTG	PIC+PTG
METTL3	$\downarrow^{+}$	≈	$\uparrow^{*}$
METTL14	$\downarrow$	≈	$\uparrow^{*}$
ALKBH5	$\downarrow^{***}$	$\downarrow^{*}$	$\downarrow^{***}$
YTHDC1	$\downarrow$	≈	≈
YTHDC2	$\uparrow$	$\uparrow$	≈
YTHDF1	$\uparrow$	≈	$\uparrow$
YTHDF2	$\downarrow^{+}$	≈	$\downarrow$

PIC treatment alone provoked a downregulation tendency in the expression of most m6A machinery members. In the case of m6A writer *METTL3* (Figure 19B) and m6A reader *YTHDF2* (Figure 19H) the difference observed was almost significant. Only m6A eraser *ALKBH5* presented a significant reduction in its expression (Figure 19D). On the contrary, m6A readers *YTHDC2* (Figure 19F) and *YTHDF1* (Figure 19G) were slightly upregulated.

PTG stimulation alone resulted in alterations in *ALKBH5* and *YTHDC2*. The expression of *ALKBH5* was downregulated (Figure 19D), in concordance with the expression pattern observed in intestinal biopsies. *YTHDC2* expression was increased, albeit moderately (Figure 19F).

The combination of PIC and PTG caused the mayor changes observed in this model. Both m6A writers *METTL3* (Figure 19B) and *METTL14* (Figure 19C) showed significant overexpression when compared to PIC treatment alone. *ALKBH5* presented a very low expression, similar to when cells were under PIC treatment alone. Regarding m6A readers, the expression of *YTHDC1* and *YTHDC2* was similar to the non-treated (NT) condition, and *YTHDF1* and *YTHDF2* expression resembled the PIC treatment alone (Figure 19E-H).

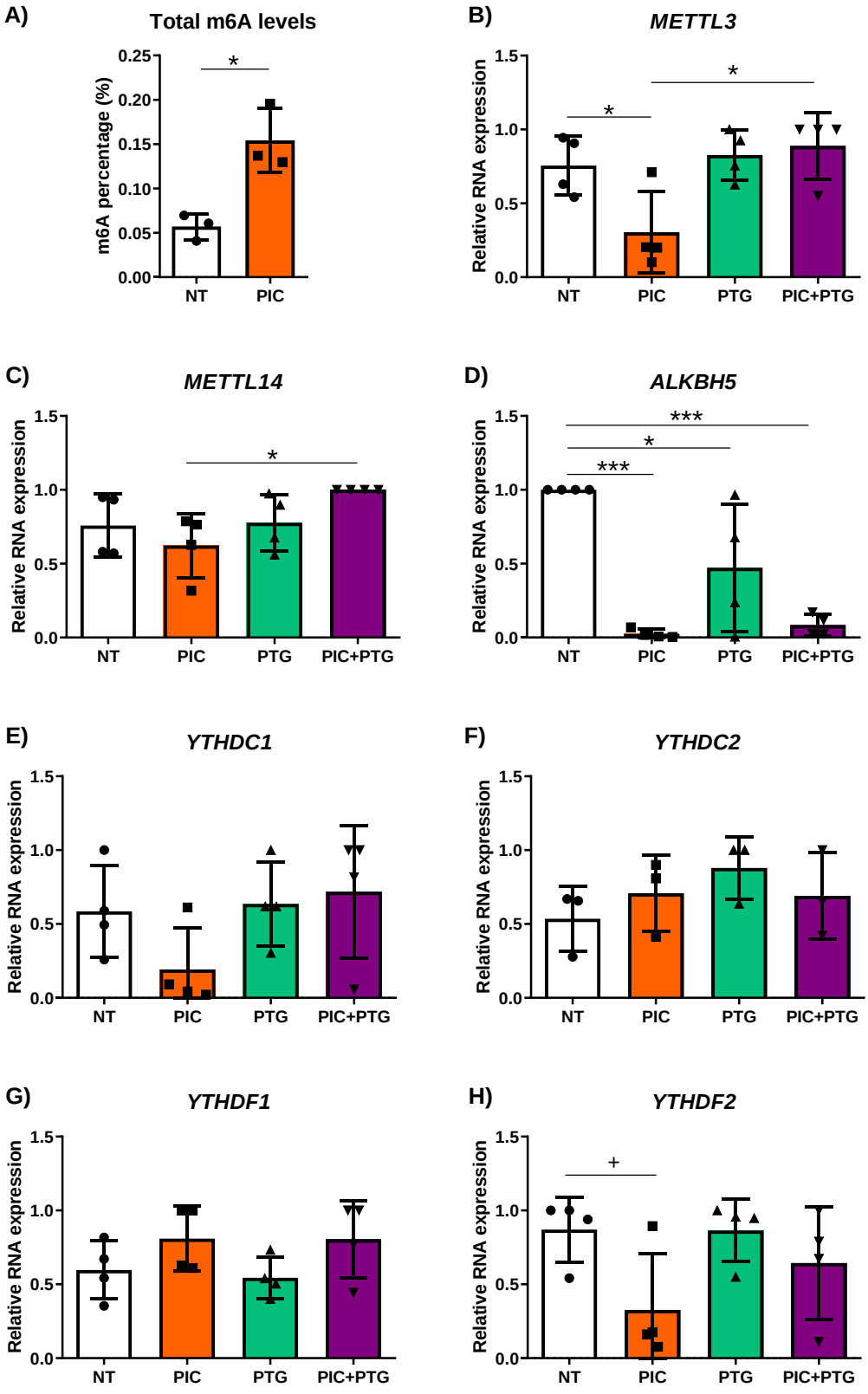

Figure 19. A) Total m6A percentage in RNAs extracted from HCT-15 cells treated with viral mimic PIC after 24h (PIC) and in non-treated cells (NT), measured by ELISA. **B)** *METTL3*, **C)** *METTL14*, **D)** *ALKBH5*, **E)** *YTHDC1*, **F)** *YTHDC2*, **G)** *YTHDF1* and **H)** *YTHDF2* expression levels in HCT-15 cells treated with PIC treatment (PIC), stimulated with gliadin (PTG), with both PIC treatment and PTG stimulation (PIC+PTG) and in non-treated cells (NT). Relative expression was calculated with $2^{-\Delta\Delta Ct}$ method and RPLPO was used as housekeeping gene. ***p<0.001; *p<0.05; +p<0.1 based on t-student and ANOVA analyses.

4.2. Proinflammatory and antiviral transcripts in PIC+PTG *in vitro* model

Apart from the m6A machinery members, we also analyzed the expression of several genes encoding proinflammatory cytokines that have been previously related to CeD pathogenesis (Abadie et al., 2020; Abadie & Jabri, 2014; León et al., 2006). We observed that the expression of *IL15* and *IL18* was increased when cells were treated with PIC and with PIC+PTG, but not with PTG alone (Figure 20A, B).

In addition, we quantified the expression of antiviral transcripts known to be implicated in the immune response to RNA virus infections (Ikushima et al., 2013; Schoggins & Rice, 2011; Uematsu & Akira, 2007). As expected, PIC treatment augmented the expression of the antiviral transcripts *IFNB1*, *IRF1*, *IRF3* and *IRF7* (Figure 20C-F). Interestingly, *IRF7* overexpression was even stronger when PIC treatment and PTG stimulation were combined (Figure 20F), suggesting that not only PIC but also PTG influences its upregulation. This synergistic induction of *IRF7* expression is also seen at the protein level (Figure 20G, H). No changes were observed in any of these genes when cells were stimulated with PTG alone.

4.2.1. IRF7 regulation in PIC+PTG in vitro model

We next wanted to evaluate whether the increase of IRF7 in the PIC+PTG model was due to alterations in the m6A machinery. For this purpose, we silenced the m6A writer METTL3 using specific siRNAs (Figure 21A, C) and afterwards the PIC treatment and PTG stimulation were carried out as previously described. In this scenario, we confirmed that the combination of PIC treatment and PTG stimulation also provoked an increase in IRF7 levels. However, this upregulation was not observed when METTL3 was silenced (Figure 21B, C).

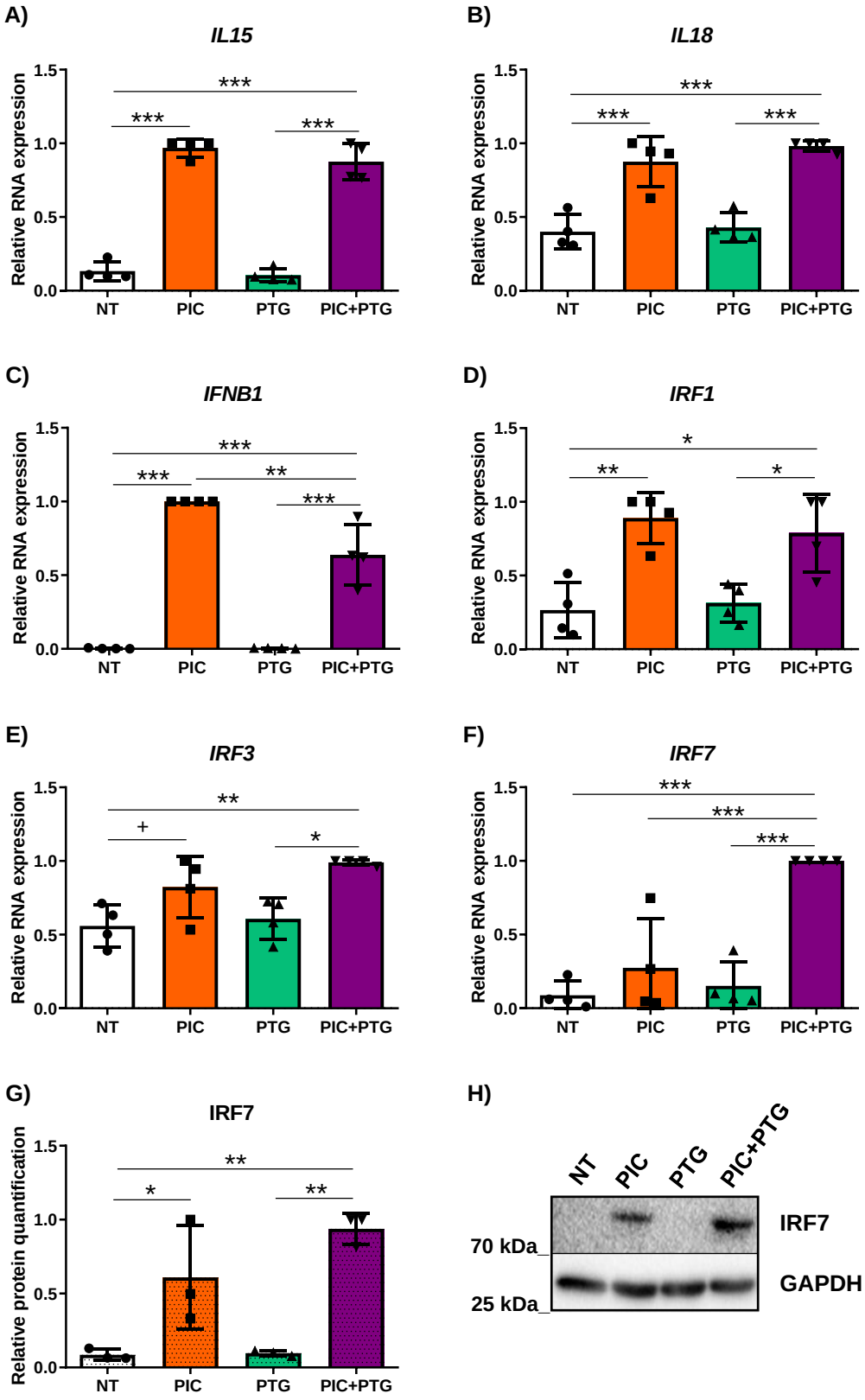

Figure 20. Expression analysis of **A)** *IL15* and **B)** *IL18* proinflammatory cytokines and **C)** *IFNB1*, **D)** *IRF1*, **E)** *IRF3* and **F)** *IRF7* antiviral transcripts; and **G-H)** IRF7 protein levels in HCT-15 cells treated HCT-15 cells treated with Poly(I;C) treatment (PIC), stimulated with gliadin (PTG), with both PIC treatment and PTG stimulation (PIC+PTG) and in non-treated cells (NT). Graphs regarding RNA or protein samples are shown with a solid background or a dot pattern, respectively. Relative expression was calculated with $2^{-\Delta\Delta Ct}$ method and *RPLPO* was used as housekeeping. Protein quantification was performed using ImageJ software. ***p<0.001; **p<0.01;*p<0.05,+p<0.1 based on ANOVA analysis.

In order to assess whether IRF7 regulation influences downstream antiviral and immune-related cytokines, we analyzed the expression of *CXCL10*, which we have already shown to be augmented in serum from pediatric CeD patients (Figure 15A). We observed the same effect as for IRF7, with PIC+PTG inducing an overall increase in *CXCL10* expression, that is reduced when METTL3 is silenced (Figure 21D).

Altogether, these results indicate that the m6A machinery is involved in IRF7 induction upon PIC treatment and PTG stimulation, and suggest that IRF7 might be regulated, at least in part, by m6A-dependent mechanisms. Furthermore, this effect of m6A-mediated regulation of IRF7 is also maintained in the downstream antiviral response, as represented by *CXCL10* expression.

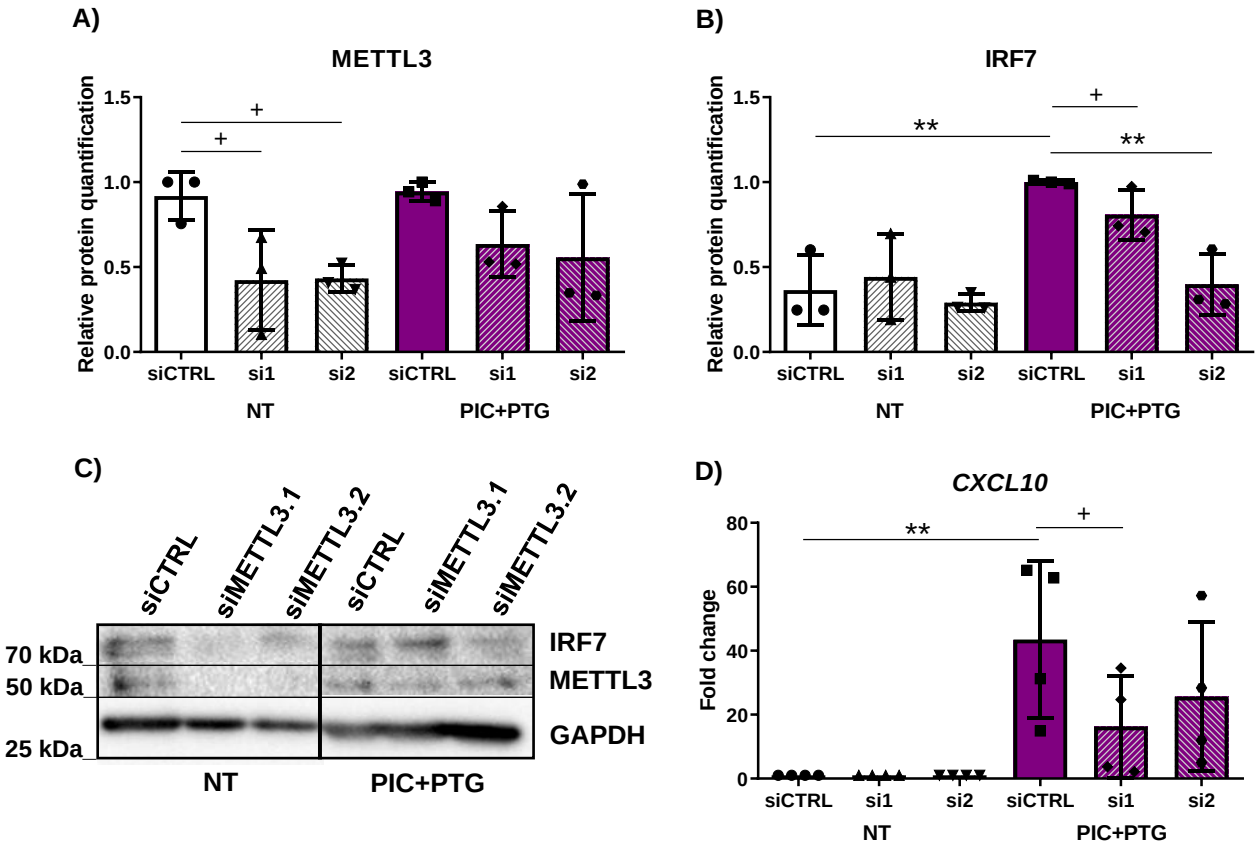

Figure 21. A-C) METTL3 and IRF7 protein levels and **D)** *CXCL10* expression in HCT-15 cells treated with PIC and stimulated with gliadin (PIC+PTG) or non-treated cells (NT) and transfected with specific siRNAs for METTL3 silencing (si1 or si2) or control siRNA (siCTRL). Relative expression was calculated with $2^{-\Delta\Delta Ct}$ method and *RPLPO* was used as housekeeping gene. Protein quantification was performed using ImageJ software. **p<0.01;*p<0.05;+p<0.1 based on ANOVA analysis.

5. m6A-mediated IRF7 regulation

5.1. Prediction of m6A motifs and confirmation of methylation of *IRF7* mRNA

The mRNA of *IRF7* has no m6A motifs annotated in the REPIC database (S. Liu et al., 2020), but this database lacks information about several tissues and cell lines, including the HCT-15 intestinal cell line. Hence, we used the SRAMP prediction server (Zhou et al., 2016) to evaluate possible m6A motifs within the *IRF7* mRNA sequence. We evaluated both the primary (Figure 22A) and mature RNA (Figure 22B) molecules of *IRF7*, and we selected as our study candidates for m6A methylation the two motifs with the highest scores matching the most frequent m6A consensus motif (Dominissini et al., 2012, 2013; Meyer et al., 2012) and present in both RNA forms. These two candidate m6A motifs are located on the sixth exon of *IRF7* (Figure 22C) and quite close to each other within the folded mature RNA molecule (Figure 22D, E).

Once we had selected the m6A motifs within the *IRF7* mRNA sequence, we next wanted to assess their methylation status *in vitro*. For this purpose, we designed specific primers flanking the region where these two predicted m6A motifs are located and performed m6A RNA immunoprecipitation followed by qPCR analysis (meRIP-qPCR). Using this approach, we were able to confirm that the two predicted m6A sites within *IRF7* CDS are indeed methylated in the HCT-15 intestinal cell line (Figure 22F), validating the prediction made by SRAMP.

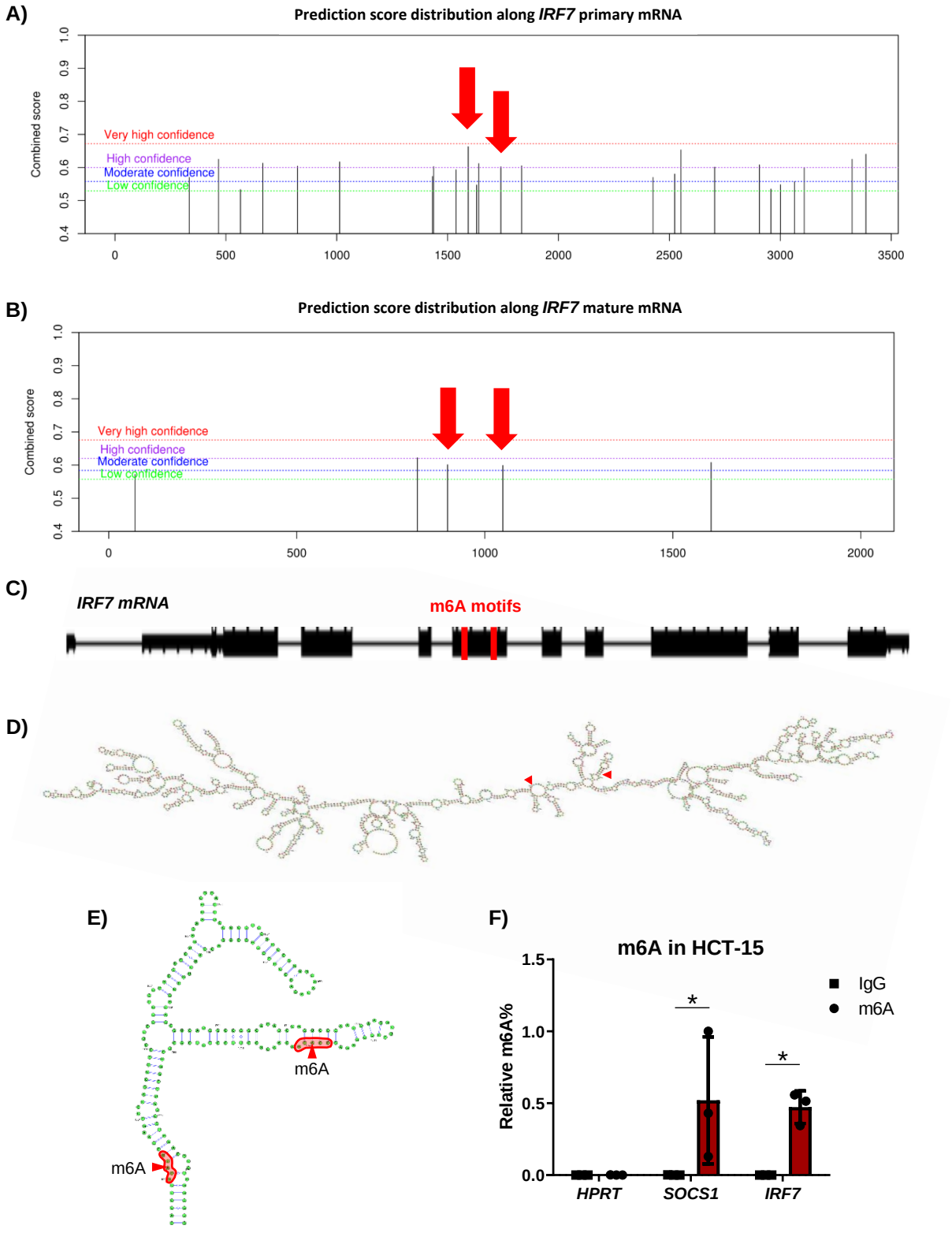

Figure 22. Prediction scores of m6A motifs using **A)** primary *IRF7* RNA and **B)** mature *IRF7* mRNA as input, obtained using SRAMP prediction server. Red arrows indicate the two m6A motifs selected as candidates. **C)** Schematic representation of the primary *IRF7* mRNA indicating the location of the candidate m6A motifs in red. **D)** Mature *IRF7* mRNA secondary structure by RNAfold software. The A nucleotides of each candidate m6A motifs are marked by small red triangles. **E)** Secondary structure of the zoomed region where candidate m6A sites are located, obtained by SRAMP prediction server, **F)** Comparison of relative m6A methylation on *IRF7* mRNA with *HPRT* and *SOCS1* mRNAs, negative and positive controls, respectively. *p<0.05 based on ANOVA analysis.

5.2. IRF7 regulation by m6A machinery members

5.2.1. IRF7 regulation by m6A writer METTL3

METTL3 is the catalytic component of the m6A writer complex (X. Wang et al., 2017; Y. Yang et al., 2018), and we had observed that it was altered after PIC treatment and PTG stimulation, and that its silencing affected IRF7 induction in the PIC+PTG model. Thus, we wanted to assess whether there is a direct relationship between this m6A writer and IRF7 levels.

We evaluated whether METTL3 protein interacts with *IRF7* mRNA using RIP-qPCR. For the qPCR step, we used the same primers flanking the region with the m6A motifs, and we confirmed the direct interaction between METTL3 and *IRF7* mRNA (Figure 23A). Specific METTL3 immunoprecipitation was verified by WB (Figure 23B). In order to analyze the direct effect of METTL3 on *IRF7* expression levels, we overexpressed that m6A writer using an overexpression plasmid (Figure 23C, D). We quantified the expression of primary and mature *IRF7* mRNA molecules, and we observed that while mature *IRF7* levels were elevated (Figure 23E), primary *IRF7* mRNA presented lower levels when METTL3 was overexpressed (Figure 23F). IRF7 protein amounts were also analyzed in both conditions. In concordance with the expression pattern of mature *IRF7* mRNA, IRF7 protein amounts were augmented upon METTL3 overexpression (Figure 23G, H).

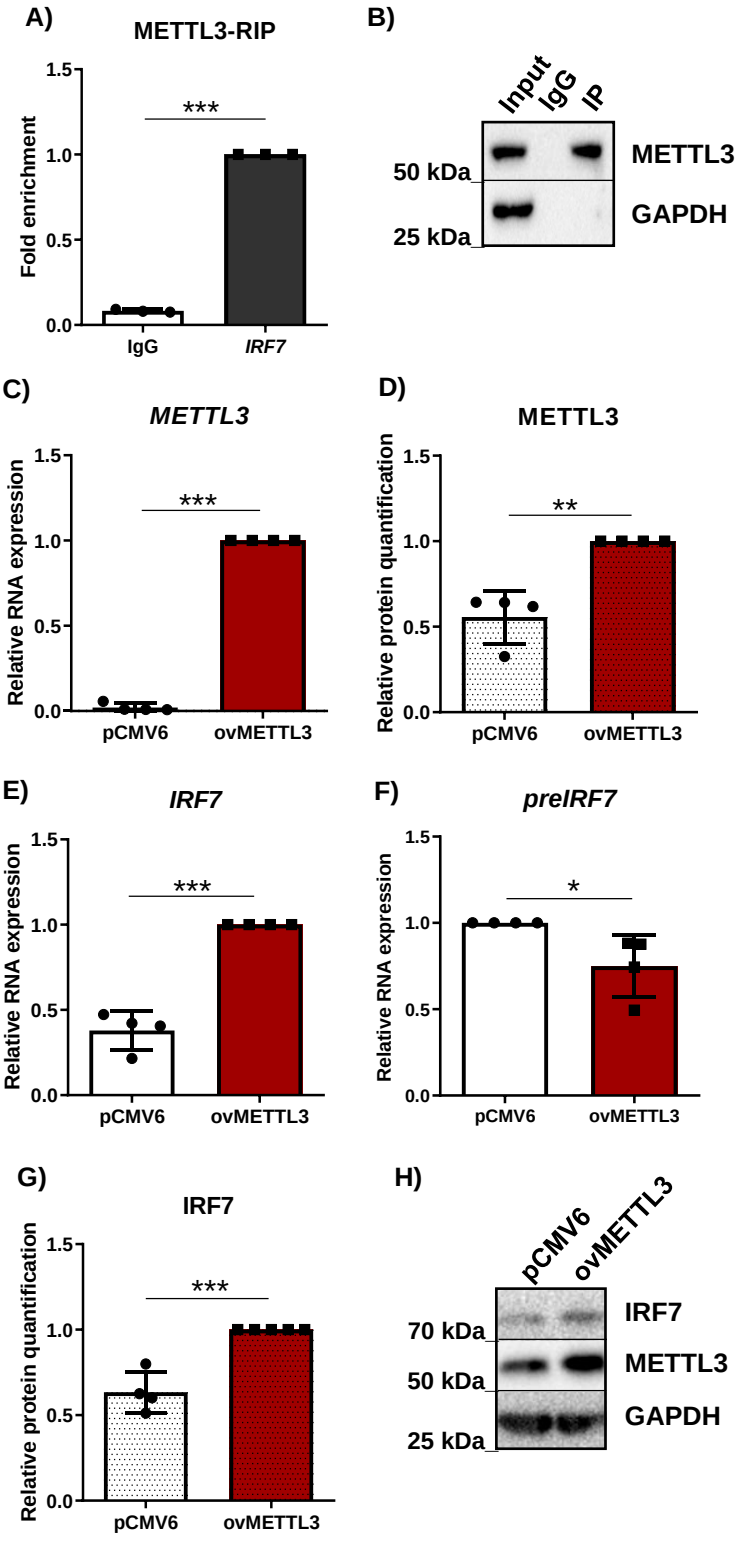

Figure 23. A) METTL3-*IRF7* mRNA interaction enrichment quantification by qPCR after METTL3 RNA immunoprecipitation (RIP-qPCR). Fold enrichment was calculated by the percent input method. **B)** Representative WB image of the METTL3 specific immunoprecipitation. **C)** *METTL3* expression, **D)** METTL3 protein quantification, **E)** mature *IRF7* and **F)** primary *IRF7* RNA expression, and **G)** IRF7 protein levels in METTL3 overexpressed (ovMETTL3) and non-overexpressed (pCMV6) cells. **H)** Representative WB image of the METTL3 overexpression and IRF7 induction. Graphs regarding RNA or protein samples are shown with a solid background or a dot pattern, respectively. Relative expression was calculated with $2^{-\Delta\Delta Ct}$ method and *RPLPO* was used as housekeeping gene. Protein quantification was performed using ImageJ software. ***p<0.001;**p<0.01;+p<0.1 based on t-student analysis.

5.2.2. IRF7 regulation by m6A eraser ALKBH5

ALKBH5 is one of the two known m6A erasers, together with FTO. However, in contrast to FTO, ALKBH5 showed substrate specificity and only binds m6A marks (Mauer et al., 2017; Zou et al., 2016). Moreover, it is known to be downregulated after viral infections (Y. Liu et al., 2019; A. Wang et al., 2022), as we observed in our PIC+PTG model.

As previously done with METTL3, we first analyzed ALKBH5 and *IRF7* mRNA interaction by RIP-qPCR. We were able to confirm that ALKBH5 binds to the *IRF7* CDS, where m6A sites are located (Figure 24A). ALKBH5 immunoprecipitation was verified by WB (Figure 24B). Afterwards, we silenced ALKBH5 with specific siRNAs (Figure 24C, D), generating a m6A-enriched scenario (Figure 24E). In line with the higher m6A levels and concordant with the results observed when METTL3 was overexpressed, mature *IRF7* mRNA presented elevated expression when ALKBH5 is silenced (Figure 24F). As we observed before, primary IRF7 mRNA showed the opposite expression pattern to mature mRNA (Figure 24G). Finally, reduction of ALKBH5 levels resulted in an increase of IRF7 protein amounts (Figure 24H, I).

Altogether, these results consolidate our previous observations in the PIC+PTG model, and confirm that IRF7 regulation, both at the RNA and protein levels, is influenced by m6A methylation and mediated by m6A writer METTL3 and m6A eraser ALKBH5. Moreover, m6A methylation seems to positively regulate the expression of IRF7.

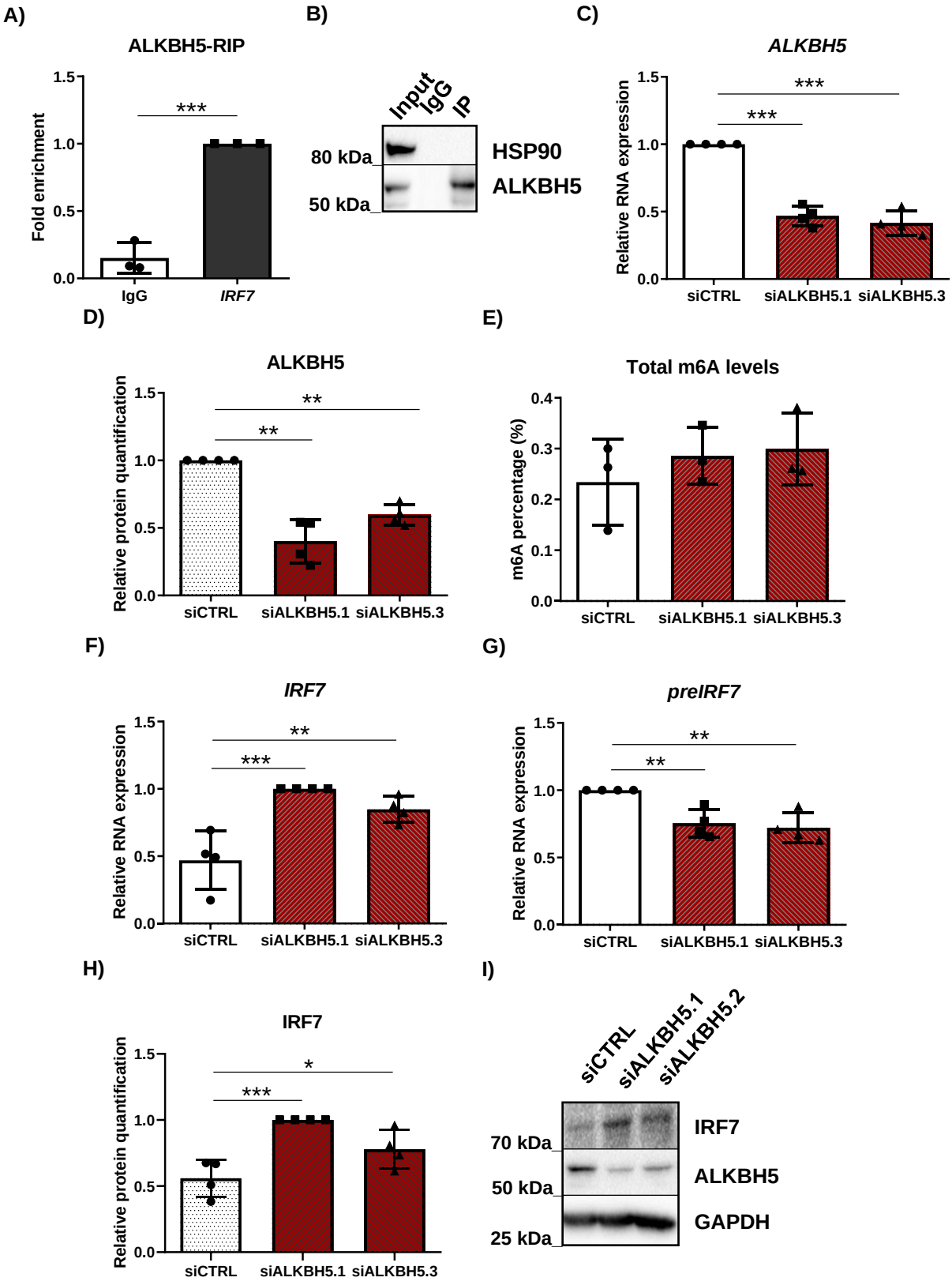

Figure 24. A) ALKBH5-*IRF7* mRNA interaction enrichment quantification by qPCR after ALKBH5 RNA immunoprecipitation (RIP-qPCR). Fold enrichment was calculated by the percent input method. **B)** Representative WB image of the ALKBH5 specific immunoprecipitation. **C)** Total m6A percentage, **D)** *ALKBH5* expression, **E)** ALKBH5 protein quantification, **F)** mature *IRF7* and **G)** primary *IRF7* RNA expression, and **H)** IRF7 protein levels in cells transfected with ALKBH5 specific siRNAs (si1 or si3) and control siRNA (siCTRL). **I)** Representative WB image of the ALKBH5 downregulation and IRF7 induction. Graphs regarding RNA or protein samples are shown with a solid background or a darker dot pattern, respectively. Relative expression was calculated with $2^{-\Delta\Delta Ct}$ method and *RPLPO* was used as housekeeping gene. Protein quantification was performed using ImageJ software. ***p<0.001;**p<0.01;*p<0.05 based on t-student and ANOVA analyses.

5.3. Effect of m6A on *IRF7* mRNA metabolism

5.3.1. Influence of m6A in IRF7 mRNA localization

m6A marks are considered an export signal for certain transcripts (Lesbirel & Wilson, 2019), and upon viral infection, some antiviral transcripts have been found to be demethylated by ALKBH5 in order to be retained in the nucleus and inhibit innate antiviral response (Q. Zheng et al., 2017). Taking this into account, we wondered whether the localization of *IRF7* mRNA was affected by viral infections and m6A methylation. Thus, intestinal cells were separated into nuclear and cytoplasmic fractions and *IRF7* mRNA was quantified in both. We first evaluated if the viral mimic PIC influenced *IRF7* mRNA localization, and we observed that in basal conditions the antiviral transcript is in the cytoplasm while after PIC treatment, it is also detected in the nucleus (Figure 25A). When m6A writer METTL3 was overexpressed the *IRF7* transcript was kept primarily in the nucleus (Figure 25B).

m6A reader YTHDC1 recognizes m6A marks and induces the translocation of m6A-containing mRNA molecules to the cytoplasm via nuclear export factors SRSF3 and NFX1 (Lesbirel & Wilson, 2019; Roundtree et al., 2017). To further investigate the implication of YTHDC1 in IRF7 regulation, we overexpressed YTHDC1 (Figure 25C, D) together with METTL3 overexpression, and we analyzed *IRF7* expression. If YTHDC1 affected *IRF7* transcript nuclear export, we would expect to observe higher IRF7 protein amounts. However, we saw no differences derived from YTHDC1 upregulation, neither at the RNA nor protein levels (Figure 25E-G), suggesting that YTHDC1 might not take part in this process.

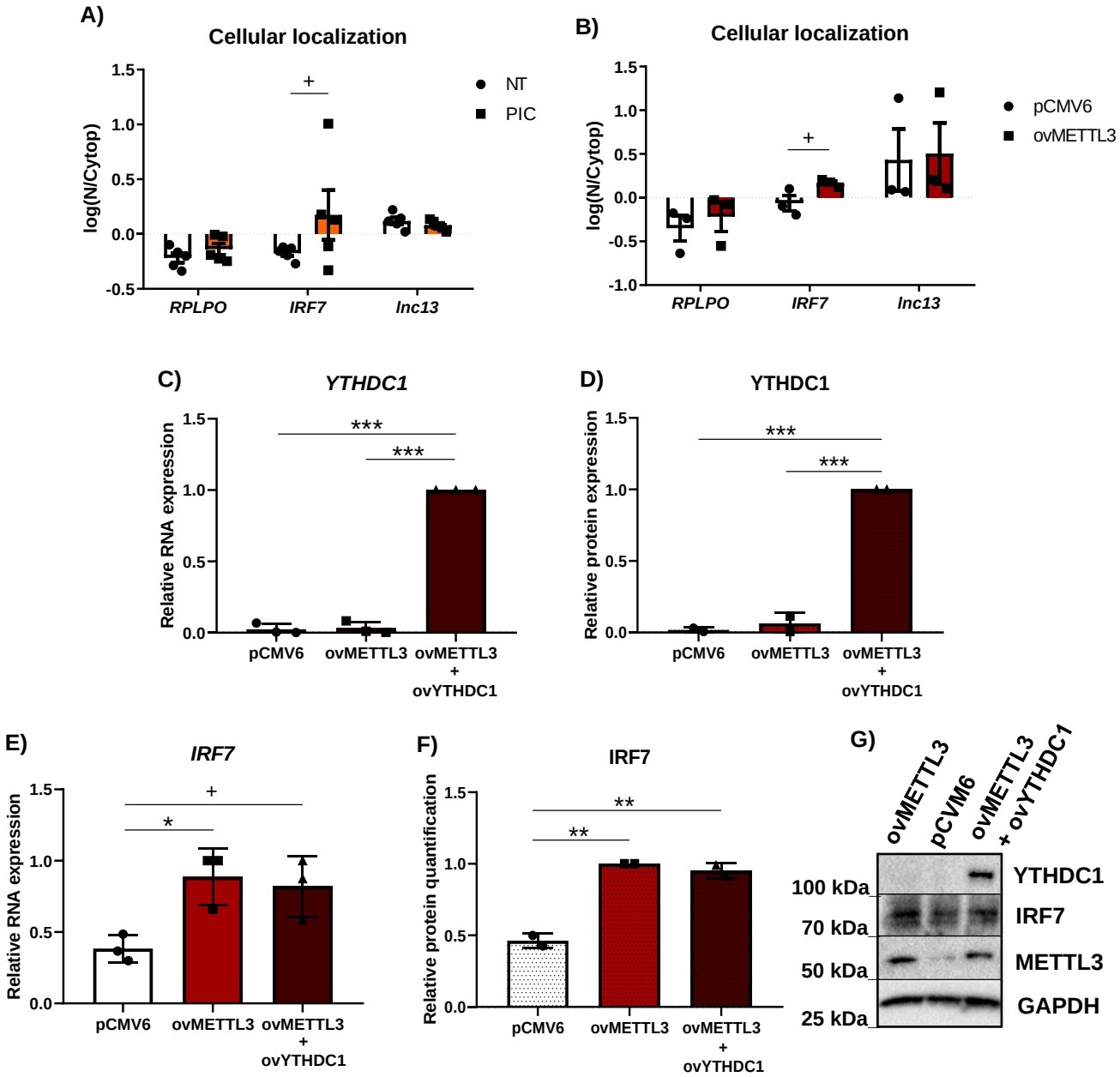

Figure 25. Cellular localization of *IRF7* mRNA in **A)** cells treated with PIC and non-treated (NT) cells and **B)** *METTL3* overexpressed (ovMETTL3) and non-overexpressed (pCMV6) cells. *RPLPO* and *lcn13* were used as cytoplasmic and nuclear controls, respectively. **C)** *YTHDC1* expression and **D)** YTHDC1 protein quantification, **E)** *IRF7* expression and **F)** IRF7 protein quantification in METTL3 overexpressed (ovMETTL3), METTL3 and YTHDC1 (ovMETTL3+ovYTHDC1) and non-overexpressed (pCMV6) cells. **G)** Representative WB image of the METTL3 and YTHDC1 overexpression and IRF7 protein levels. Graphs regarding RNA or protein samples are shown with a solid background or a dot pattern, respectively. Relative expression was calculated with $2^{-\Delta\Delta Ct}$ method and *RPLPO* was used as housekeeping gene. Protein quantification was performed using ImageJ software. ***p<0.001;**p<0.01;*p<0.05;+p<0.1 based on ANOVA analysis.

5.3.2. Influence of m6A in IRF7 mRNA stability

m6A marks have been described to influence mRNA molecule stability (Mauer et al., 2017; Shi et al., 2017; X. Wang et al., 2014). Thus, after discarding m6A implication in nuclear export, we postulated that the m6A deposition on *IRF7* mRNA may alter its stability. To test this hypothesis, we first overexpressed METTL3 and inhibited *de novo* transcription using actinomycin D. We saw no differences between these two conditions (Figure 26A). Next, we overexpressed METTL3 and inhibited *de novo* protein synthesis with cycloheximide. We analyzed *IRF7* expression, and we did not observe any significant changes (Figure 26B), These results advocate that m6A does not affect *IRF7* mRNA stability.

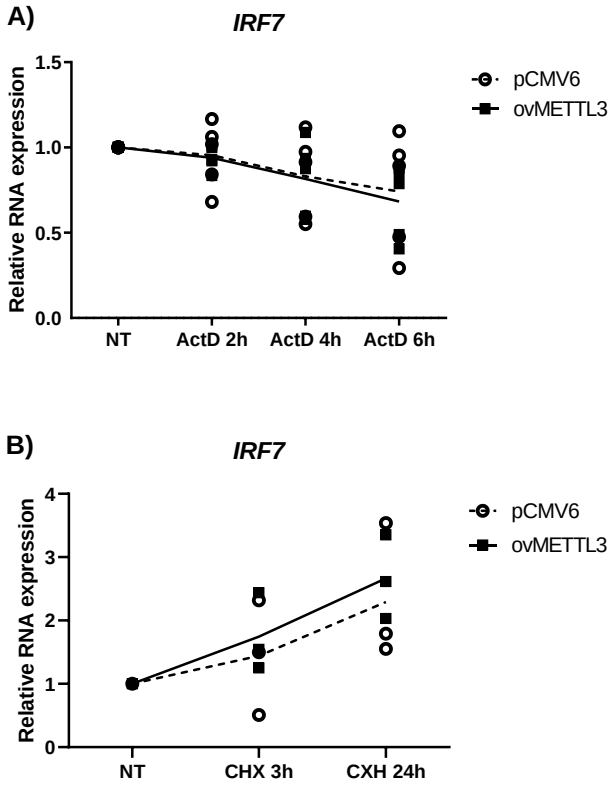

Figure 24. Relative expression of *IRF7* in *METTL3* overexpressed (ovMETTL3) and non-overexpressed (pCMV6) cells upon **A)** actinomycin D (ActD) treatment for 2h, 4h, and 6h and **B)** cycloheximide (CHX) treatment for 3h and 24h. Relative expression was calculated with $2^{-\Delta\Delta Ct}$ method.

5.3.3. Influence of m6A in IRF7 mRNA translation

m6A modifications are also involved in the regulation of mRNA translation (X. Wang et al., 2015; Y. Yang et al., 2017). Considering that YTHDC2 showed enriched binding to m6A sites within CDSs (Mao et al., 2019) and confirmed m6A motifs on *IRF7* mRNA are located within its CDS, we decided to focus on YTHDC2.

We postulated that it might interact with *IRF7* mRNA. To test this idea, we used the same approach that we had used for the confirmation of the interaction between METTL3 and ALKBH5. Thus, using RIP of YTHDC2 protein followed by *IRF7* RT-qPCR quantification, we were able to confirm YTHDC2 and *IRF7* mRNA binding (Figure 27A). Specific YTHDC2 immunoprecipitation was verified by WB (Figure 27B). Once the interaction between YTHDC2 and *IRF7* mRNA had been confirmed, and in order to evaluate its effect on IRF7 we perturbed YTHDC2 expression with an overexpression plasmid (Figure 27C, D). We analyzed IRF7 expression at both RNA and protein levels, and we observed that YTHDC2 overexpression led to the increase of both *IRF7* mRNA (Figure 27E) and protein (Figure 27F, G).

These results confirm that m6A reader YTHDC2 plays a key role on IRF7 regulation. Moreover, these data also support the involvement of m6A in *IRF7* mRNA translation process.

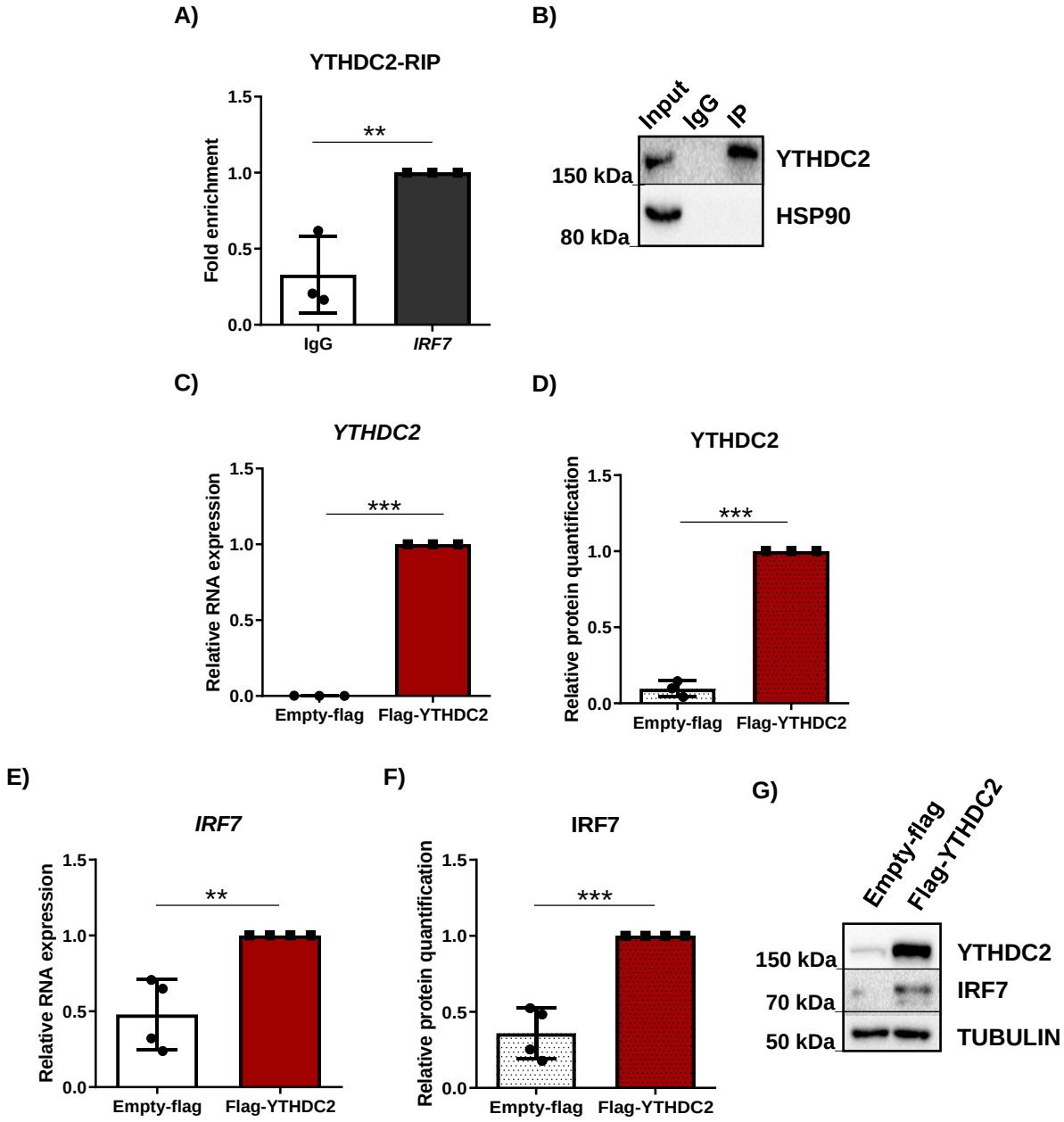

Figure 27. A) YTHDC2-*IRF7* mRNA interaction enrichment quantification by qPCR after YTHDC2 RNA immunoprecipitation (RIP-qPCR). Fold enrichment was calculated by the percent input method. **B)** Representative WB image of the YTHDC2 specific immunoprecipitation. **C)** *YTHDC2* expression, **D)** YTHDC2 protein quantification, and **E)** *IRF7* expression and **F)** IRF7 protein quantification in YTHDC2 overexpressed (Flag-YTHDC2) and non-overexpressed (Empty-flag) cells. **G)** Representative WB image of the YTHDC2 overexpression and IRF7 induction. Relative expression was calculated with $2^{-\Delta\Delta Ct}$ method and *RPLPO* was used as housekeeping gene. Protein quantification was performed using ImageJ software. ***p<0.001;**p<0.01 based on t-student analysis.

5.4. Contribution of m6A methylation on the regulation of IRF7 levels

To investigate the functional effects of m6A methylation on IRF7, we treated cells with cycloleucine, an inhibitor of m6A deposition, and analyzed *IRF7* mRNA and protein amounts. Even though the differences in *IRF7* expression upon cycloleucine treatment compared to the non-treated condition are very small, *IRF7* expression is reduced 10% when m6A is inhibited (Figure 28A). Protein amounts are also lower (Figure 28B).

Nevertheless, cycloleucine affects general m6A methylation levels, so to assess the specific role of the m6A methylation mark within the *IRF7* CDS, we generated a m6A-depleted (MUT) *IRF7* expression plasmid by replacing the adenine in the nucleotides within the confirmed m6A motifs with a cytosine (Figure 28C). The mutations were silent point mutations that did not alter the amino acid sequence. The same amount of both plasmids was transfected into HCT-15 intestinal cells in order to compare m6A-depleted (MUT) and wild-type (WT) *IRF7*, and RNA and protein levels were analyzed. The expression of *IRF7* at RNA level turned out to be similar in both WT and MUT conditions (Figure 28D). Interestingly, we observed significantly lower IRF7 protein amounts when m6A motifs had been depleted (Figure 28E, F), indicating that the lack of m6A motifs prevents IRF7 protein synthesis.

Taking these results into account and considering that YTHDC2 promotes translation in an m6A-dependent manner, and that it interacts with *IRF7* mRNA, we wondered whether the protein synthesis deficiency is due to the impairment of YTHDC2 binding to *IRF7* mRNA in the absence of m6A motifs. Hence, we carried out a YTHDC2-RIP followed by *IRF7* quantification by RT-qPCR comparing the conditions where WT or MUT *IRF7* were overexpressed. Using this approach, we confirmed that the interaction between YTHDC2 reader and *IRF7* mRNA was abolished in the absence m6A marks (Figure 28G). Altogether, these results showed that m6A methylation and YTHDC2 binding to *IRF7* mRNA are required for translation and for IRF7 protein synthesis.

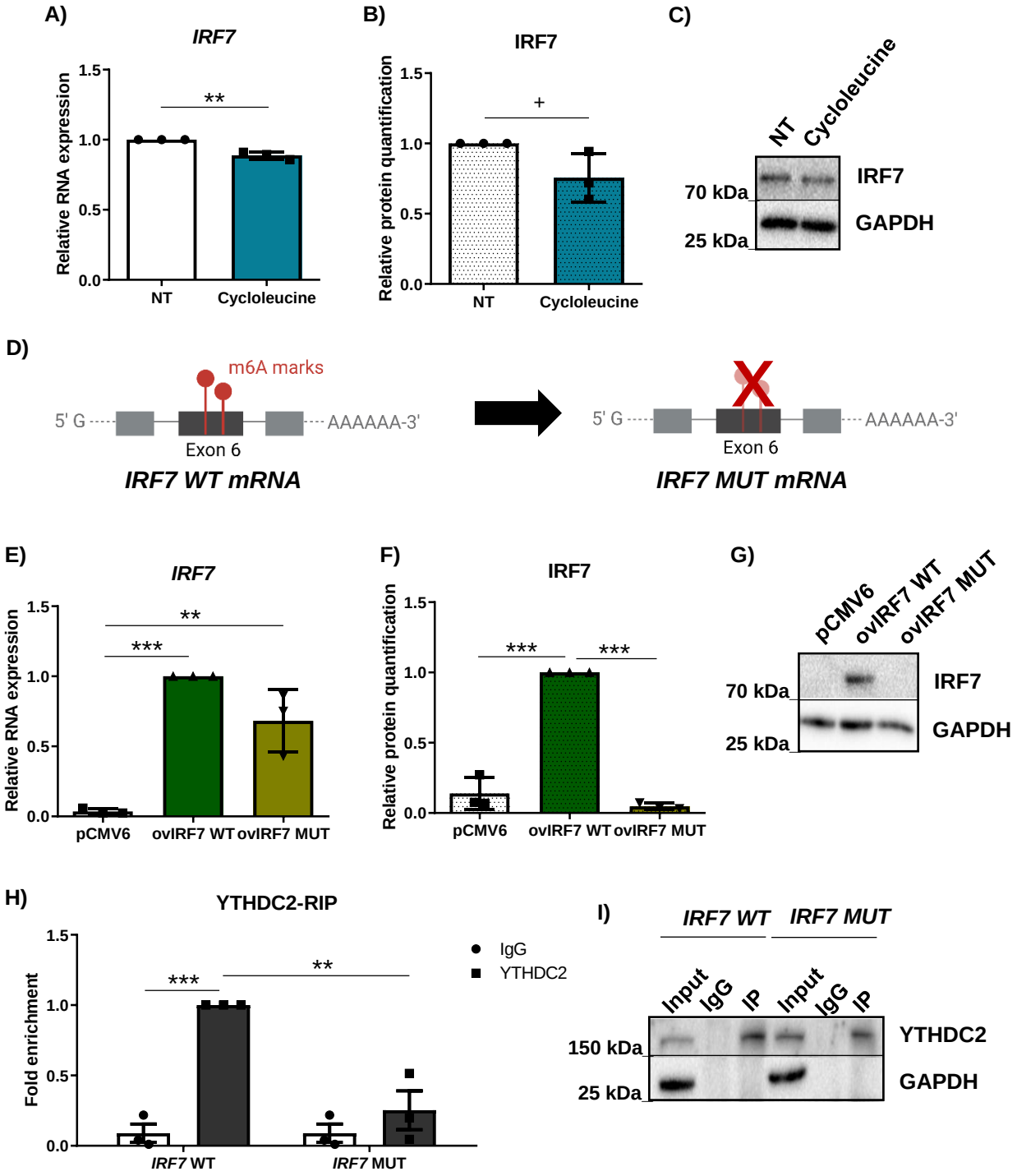

Figure 28. A) *IRF7* expression and **B)** IRF7 protein amount in cells treated with cycloleucine (Cycloleucine) and non-treated (NT) cells. **C)** Representative WB image of the IRF7 protein levels. **D)** A schematic image of the m6A motifs modification by A→C silent point mutations. Image created with BioRender. **E)** *IRF7* expression and **F)** IRF7 protein quantification in cells transfected with m6A motifs containing (WT) and m6A-truncated (MUT) *IRF7* overexpression plasmid and in non-overexpressed cells (pCMV6). **G)** Representative WB image of IRF7 protein levels. **H)** YTHDC2-*IRF7* mRNA interaction enrichment quantification by qPCR after ALKBH5 RNA immunoprecipitation (RIP-qPCR) when cells are transfected with WT or MUT *IRF7* overexpression plasmid. Fold enrichment was calculated by the percent input method. **I)** Representative WB image of the YTHDC2 specific immunoprecipitation. Graphs regarding RNA or protein samples are shown with a solid background or a dot pattern, respectively. Relative expression was calculated with $2^{-\Delta\Delta Ct}$ method and *RPLPO* was used as housekeeping gene. Protein quantification was performed using ImageJ software. ***p<0.001;**p<0.01;+p<0.1 based on t-student and ANOVA analyses.

6. Influence of m6A in IRF7 downstream activity

IRF7 plays a pivotal role in the of the IFN-I response and the maintenance of antiviral response (Honda K et al., 2005; Schmid et al., 2010). On this basis, we wondered whether the lack of m6A methylation on the *IRF7* CDS may also affect its downstream activity. Hence, we analyzed the expression of several downstream genes in the IFN-I and JAK-STAT pathways, comparing WT and MUT *IRF7* overexpression conditions. We observed that *IFBN1* (Figure 29A) and *STAT1* (Figure 29B) were increased when WT *IRF7* is overexpressed, but their expression levels when m6A motifs were depleted from *IRF7* CDS were similar to those in the non-overexpressed control condition, in concordance with the previously observed reduction of IRF7 (Figure 28E, F). These results confirm the need of the m6A methylation marks not only for IRF7 regulation, but also for its downstream functions.

IRF7 binds to promoters of ISGs and other genes in an ISRE-dependent manner to induce their expression (Schmid et al., 2010). Hence, we evaluated the expression of cytokines *CXCL10* and *CXCL16*, both contain an IRF7-binding motif according to Gene Set Enrichment Analysis and Molecular Signature Database (Liberzon et al., 2015; Subramanian et al., 2005). However, only *CXCL10* showed changes in expression that were dependent on the amount of IRF7 protein (Figure 29C), presenting an expression pattern resembling that of *IFNB1* and *STAT1*. No changes in *CXCL16* expression were observed between the WT and MUT conditions (Figure 29D).

To further investigate the effect of m6A apart from ISGs, we also quantified the expression of *LINC00173*, a lncRNA reported to be involved in the transcriptional regulation of cytokines upon viral infection (Postler et al., 2017), and that also has an ISRE for IRF7 on its promoter. None of the variants of *LINC00173* (Figure 29E, F) showed differential expression when either WT or MUT *IRF7* were overexpressed, although it is slightly upregulated in when *IRF7* lacks m6A motifs.

These results indicate that while *CXCL10* expression is IRF7-dependent, *CXCL16* and *LINC00173* do not seem to be regulated by IRF7, at least directly, suggesting that the ISRE on their promoters for IRF7 binding might not be functional and/or that other transcription factors apart from IRF7 may affect their expression and cover/compensate the effect of IRF7 reduction.

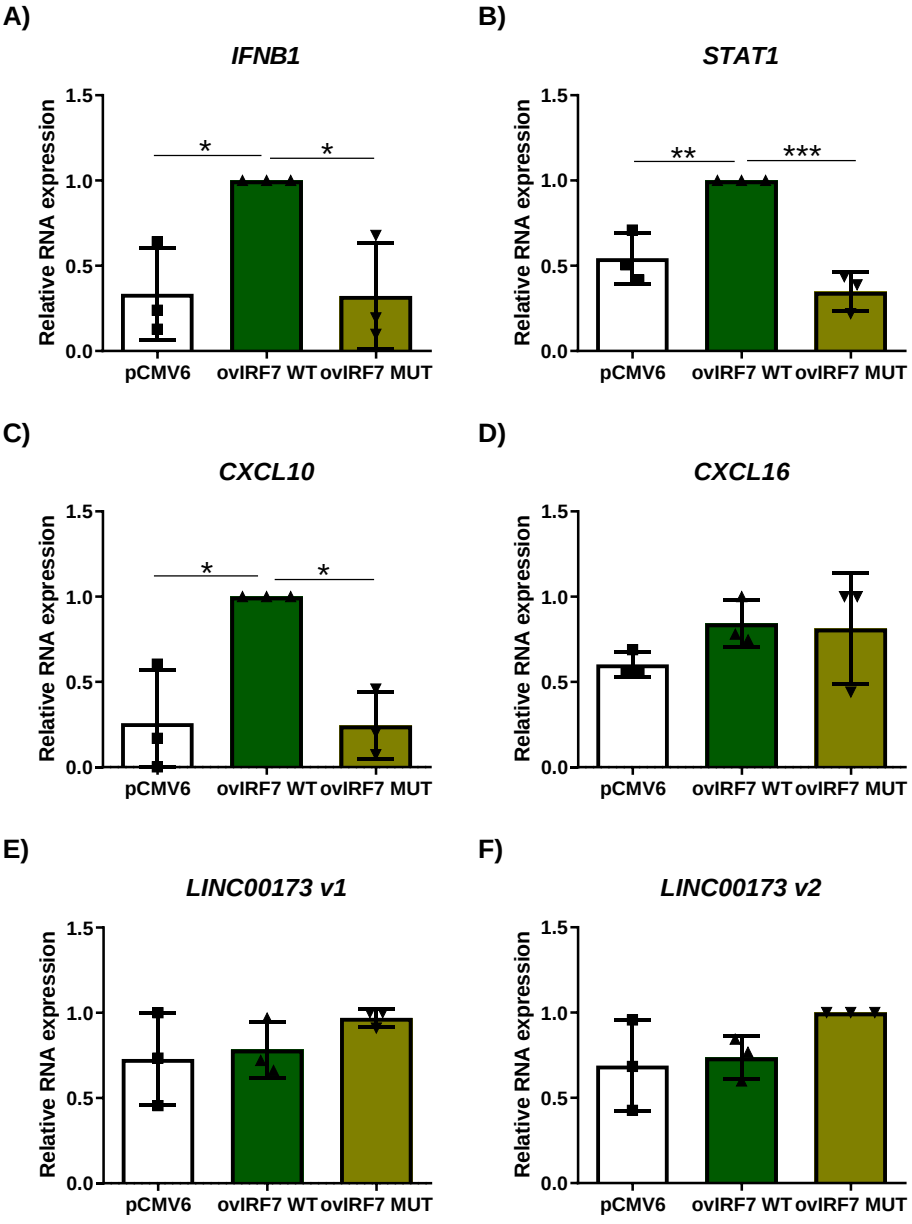

Figure 29. A) *INFB1,* **B)** *STAT1,* **C)** *CXCL10*, **D)** *CXCL16*, **E)** *LINC00173* variant 1 and **F)** *LINC00173* variant 2 expressions in cells transfected with m6A motifs containing (WT) and m6A-truncated (MUT) *IRF7* overexpression plasmid and in non-overexpressed cells (pCMV6). Relative expression was calculated with $2^{-\Delta\Delta Ct}$ method and *RPLPO* was used as housekeeping gene. ***p<0.001;**p<0.01;*p<0.05 based on ANOVA analysis.

DISCUSSION

Viral infections have been proposed as environmental triggering factors for several autoimmune disorders (Bjornevik et al., 2022; Hussein & Rahal, 2019; Oikarinen et al., 2021; Smatti et al., 2019). Specifically, an association between enteric dsRNA virus, such as reovirus and rotavirus and CeD development has been reported in several studies (Bouziat et al., 2017; Brigleb et al., 2022; Kemppainen et al., 2017; Lars C Stene et al., 2006). In fact, Bouziat *et al* first observed loss of tolerance to gluten in reovirus infected mice (Bouziat et al., 2017). This connection was later corroborated by Brigleb *et al* (Brigleb et al., 2022), proposing reovirus infections as the viral triggering agent involved in CeD development.

Specifically, Bouziat *et al* showed that CeD patients tend to have more anti-reovirus antibody titers than control individuals (Bouziat et al., 2017). In that study the approach used for the detection of anti-reovirus antibodies in human serum was the plaque-reduction neutralization assay. In the current study, an ELISA-based reovirus particle detection technique was developed for the detection of anti-reovirus antibodies. Using this approach, we were able to quantify the reactivity against reovirus in serum in a more efficient manner. Moreover, it provided a more direct measurement than the virus neutralization-based assay. Using this ELISA-based approach, we observed that pediatric CeD patients present significantly higher serum reactivity to reovirus, therefore confirming the previous observations by Bouziat et al and supporting the association of reovirus infection and CeD.

CXCL10 has been shown to be expressed in different tissues upon viral infection, suggesting an essential role for this chemokine in the antiviral response, by contributing to the activation, recruitment, and migration of certain subsets of immune cells, such as NK cells to the sites of infection (Trifilo et al., 2004). Moreover, several studies have reported that CXCL10 production is augmented after reovirus infection (Carew et al., 2017; Douville et al., 2008), and that this increase induces NK cell recruitment (Prestwich et al.,

2009). Hence, in the present study we also measured pro-inflammatory cytokine CXCL10 concentration in serum samples, and in accordance with the serum reactivity to reovirus, CeD patients also showed higher CXCL10 levels. Indeed, we were able to confirm the correlation between these two parameters, suggesting that reovirus infections may be, in part, responsible of the higher CXCL10 levels.

IRF3 and IRF7 are the master regulating factors of antiviral response after dsRNA virus infections and key components for IFN-I production and innate immune activation (Ning et al., 2011; Yanai et al., 2018). dsRNA molecules are recognized by TLR3, RIG-I and/or MDA5 receptors initiating a signaling cascade that leads to the phosphorylation of IRF3 and IRF7, and their consequent activation and translocation to the nucleus (Ikushima et al., 2013; Matsumoto & Seya, 2008; Ning et al., 2011; Yanai et al., 2018). IRF3 is constitutively present in the cell, and it mainly takes part in the early stages of the antiviral response (Yanai et al., 2018). Conversely, IRF7 is usually expressed at low levels in basal conditions and is activated at later stages of the antiviral response. IRF7 it is implicated in the maintenance of the IFN pathway by a positive regulation loop (Erickson & Gale, 2008; Litvak et al., 2012; W. Wu et al., 2020). In accordance with the higher reactivity against reovirus and increased CXCL10 levels observed in serum, we also found that the antiviral immune response is augmented in the intestine of CeD patients. Both, *IRF3* and *IRF7,* were overexpressed in intestinal biopsies of active CeD patients, and *IRF7* expression remained upregulated in CeD patients on GFD. In this group, *IRF3* expression is slightly higher than in controls, but lower than in active CeD patients. Taking into account the role of IRF7, these results suggest that the antiviral immune response remains activated even after the removal of gluten from the diet. The constitutive increase of *IRF7* observed in the intestine of CeD patients, may be due to previous and repeated viral infections such as those mediated by reovirus, leading to an augmented basal inflammatory status in CeD patients, that could precede the development of the disease.

Considering the relationship between viral infections and m6A alterations (Dang et al., 2019; Tsai & Cullen, 2020; Williams et al., 2019) and our recent report of m6A implication in CeD (Olazagoitia-Garmendia et al., 2021), we wondered whether the constitutively enhanced antiviral response could be related to the alteration of m6A in the intestine of CeD patients. We have recently reported that gliadin increases overall m6A levels, together with an augmented expression of several m6A machinery members in intestinal cells (Olazagoitia-Garmendia et al., 2021). Our results confirmed the increase of total m6A previously observed in CeD patients. In addition, we also wanted to analyze the expression of m6A machinery members in CeD patients, and we observed that the expression pattern of m6A machinery genes is broadly altered in celiac disease. On the one hand, writers *METTL3* and *METTL14* present higher expression levels in active CeD patients when compared to non-CeD patients and CeD patients on a GFD. Accordingly, the readers analyzed here, *YTHDC1*, *YTHCD2*, *YTHDF1* and *YTHDF2,* also displayed augmented expression in active CeD patients, but not in patients on GFD. On the other hand, eraser *ALKBH5* showed relatively low expression in non-CeD individuals and active CeD patients in comparison with CeD patients on GFD, suggesting that the presence of gluten on the diet might be the reason for such downregulation. Altogether, these results confirm the previously reported higher m6A levels in cells upon gliadin treatment (Olazagoitia-Garmendia et al., 2021) and corroborate the implication of m6A machinery in disease development. Besides, we found that the expression of several m6A machinery members correlates with the expression of *IRF3* and *IRF7* in CeD and non-CeD patients, suggesting a relationship between antiviral transcripts and m6A machinery members and their potential implication in CeD onset.

To recreate an *in vitro* CeD scenario in which both viral infection and gliadin are implicated , we generated a model in which we treated cells with PIC, the synthetic analog of dsRNA molecules, and afterwards stimulated them with PTG. Our aim was to mimic gluten exposure after a previous viral infection, a condition that may happen in the

intestine of prospective CeD patients. On the other hand, we also wanted to evaluate the expression of the m6A machinery members previously analyzed in the intestinal samples and assess the effects of these agents on the observed alterations.

When PIC is transfected to cells, it is recognized by RIG-I receptor, as it happens with its natural analog dsRNAs. This recognition initiates a signaling cascade that leads to the induction of IFN-I production (Dauletbaev et al., 2015). It has been shown that the stability of *IFNB1* transcript is affected by m6A methylation in a METTL3-dependent manner (Winkler et al., 2019), so *METTL3* reduction can be considered as an induction mechanism of the antiviral immune response. Accordingly, in our *in vitro* model, m6A writer *METTL3* was downregulated when cells were treated with PIC. *METTL3* has also been reported to be upregulated after long term gliadin exposure (Olazagoitia-Garmendia et al., 2021). We did not observe the same effect after 4h stimulation, probably due to the shorter exposure time. However, even if gliadin stimulation alone did not alter *METTL3* expression, it did provoke an increase in its expression when cells were also under PIC treatment. This increment is also observed in *METTL14*, the other m6A writer analyzed. The expression of m6A eraser *ALKBH5* was significantly different in our model, being downregulated in all the conditions when compared to the non-treated (NT) condition. ALKBH5 impairment after viral infections has been previously described (Y. Liu et al., 2019), and this was confirmed by our PIC treatment. *ALKBH5* also showed reduced expression after gliadin stimulation, resembling the results observed in intestinal biopsies. To our knowledge, this is the first time that alterations in the expression of m6A demethylase *ALKBH5* are related with gliadin exposure. Altogether, our results showed that the levels of m6A machinery is altered by a combination of a mimic viral infection and gliadin stimulation, which might lead to an overall increase on m6A levels. Nevertheless, the mechanisms underlying this regulation are not understood and further studies are needed in order to clarify this. Hence, regarding the relevance of m6A modifications in health and disease, deciphering how m6A machinery members are

regulated in response to different stimuli and conditions is of great interest and may open the door to the development of new therapeutic approaches.

IRF7 is a key transcription factor involved in the antiviral immune response. Many studies have described how IRF7 is regulated at the protein level (reviewed in (Ning et al., 2011). Using our *in vitro* model, we found that gliadin stimulation intensifies the induction of IRF7 expression upon PIC treatment, both at the RNA and protein levels. Furthermore, we confirmed that this induction was, at least in part, due to alterations in the m6A machinery, since METTL3 silencing resulted in a decrease on the PIC- and gliadin-mediated IRF7 induction. Thus, our results suggest that the m6A machinery is involved in the constitutive upregulation of IRF7 observed in celiac patients and that this can be a result of a combination of reovirus infection and gluten exposure.

To date, there were no reports about m6A motifs within the *IRF7* mRNA sequence. Using the online available tool SRAMP (Zhou et al., 2016), we predicted several m6A motifs within the IRF7 CDS. Furthermore, we verified that those motifs are methylated in HCT-15 intestinal cells. Additionally, we also confirmed that *IRF7* mRNA interacts with m6A writer METTL3 and eraser ALKBH5, and that its RNA and protein amounts are altered when METTL3 and ALKBH5 are manipulated. These data point to an m6A-dependent IRF7 regulation, where augmented m6A levels induce IRF7 protein synthesis. Noteworthily, primary *IRF7* mRNA was also altered, but it showed the opposite expression pattern to mature RNA, suggesting that m6A methylation might also affect RNA processing.

Based on this premise, we evaluated how m6A methylation influences *IRF7* RNA metabolism. It has been reported that upon a viral infection, ALKBH5 is recruited by DDX46 helicase inducing the demethylation of several antiviral transcripts. Subsequently, these transcripts are retained in the nucleus, and this inhibits their translation into effector proteins hindering the innate immune response against the virus (Q. Zheng et al., 2017). In the case of *IRF7* mRNA, localization changes were observed

after PIC treatment and in response to METTL3 overexpression, increasing the nuclear proportion of the transcript. m6A reader YTHDC1 is involved in nuclear export pf m6A-containing transcripts (Lesbirel & Wilson, 2019; Roundtree et al., 2017), provoking a probable increase in protein amounts. However, we did not observed the expected higher IRF7 protein levels, suggesting the localization of *IRF7* mRNA was not affected when YTHDC1 was overexpressed together with METTL3 and that YTHDC1 does not seem to take part in *IRF7* nuclear export/retention process. Hence, the *IRF7* mRNA localization shift observed after PIC treatment and METTL3 overexpression may be due to the increased transcription rather than nuclear retention of the transcript.

YTHDC1 also participates in RNA splicing via an m6A-dependent mechanism (C. Tang et al., 2017; Xiao et al., 2016). Although m6A methylation seemed to affect *IRF7* mRNA processing, we did not observe any changes in *IRF7* expression after YTHDC1 and METTL3 overexpression, so we could speculate that m6A and, more specifically YTHDC1, is not involved in the splicing process of *IRF7*. Nevertheless, other processes such as 5'capping and addition of poly-A tail are essential for the synthesis of mature RNA molecules, so m6A-mediated alterations of pre-*IRF7* need further investigation in order to clarify the real effect of m6A in *IRF7* mRNA processing.

m6A methylation has also been described to influence the stability of mRNA molecules, being the deposition of m6A marks within mRNA sequences a cause for a shorter life of mRNA molecules (Boo & Kim, 2020; Shi et al., 2017; Tang et al., 2017; Wang et al., 2014). However, we did not observe changes in *IRF7* mRNA stability when overexpressing METTL3 and after inhibiting transcription and/or translation processes by actinomycin D and cycloheximide, respectively. On the contrary, we did not evaluate *IRF7* mRNA stability in a condition with reduced m6A levels, hence the possible consequences of a lack of m6A on *IRF7* remain unknown and it could affect its stability.

m6A modifications are also involved in the regulation of mRNA translation (X. Wang et al., 2015; Y. Yang et al., 2017). Among others, YTHDF1, YTHDF3 and YTHDC2 have been reported to promote translation of m6A-containing transcripts (Hsu et al., 2017; A. Li et al., 2017; Zong et al., 2021). However, these m6A readers present different binding affinities, and unlike YTHDF1 and YTHDF3 that are preferentially bound to UTRs of of m6A-containing transcripts, YTHDC2 shows enriched binding to m6A sites within CDSs (Mao et al., 2019). Apart from recognizing and binding to m6A motifs, YTHDC2 also has the ability to unfold RNA molecules through its helicase activity (Hsu et al., 2017; Wojtas et al., 2017). Indeed, it is the only known m6A reader with this activity. m6A motifs are enriched in 3'UTRs of mRNA transcripts and in lesser extent in 5'UTRs (Meyer et al., 2012). However, m6A marks have also been identified within coding sequences, and although the translation of these transcripts has been reported to be less efficient than those of transcripts without m6A marks, abrogation of m6A marks from m6A-containing mRNA molecules can impair their translation (Mao et al., 2019). As such, m6A marks can play a double role in translation: on the one hand, m6A marks provoke ribosome pausing in methylated A nucleotides, slowing down translation and decreasing its efficiency; and on the other hand, m6A marks are recognized by YTHDC2, which unfolds mRNA secondary structure and enhances overall translation of the methylated mRNA transcripts to which it binds (Mao et al., 2019). Besides, YTHDC2 has also been reported to promote non-canonical, cap-independent, and IRES-mediated translation (Kim & Siddiqui, 2021). Here, we confirmed that IRF7 is regulated YTHDC2, since its expression is augmented when YTHDC2 is overexpressed.

As previously mentioned, we found that IRF7 production is regulated by METTL3 and ALKBH5, and thus we concluded it is m6A-dependent. This m6A-dependent regulation of IRF7 was also corroborated as its gene expression and protein production were lower when m6A deposition is inhibited by cycloleucine. To assess the functional effects of m6A methylation within the *IRF7* CDS, a mutated *IRF7* mRNA construct was generated

by removing the confirmed m6A motifs. The generated mutations were silent and did not affect the amino acid sequence of IRF7. We observed that overexpression of the WT plasmid resulted in elevated protein levels, but no IRF7 protein increase was observed when the mutated *IRF7* was overexpressed, even though RNA levels were similar in both scenarios. These results indicate that m6A modifications do not directly affect *IRF7* expression at the RNA level but are essential for IRF7 protein synthesis. Moreover, YTHDC2-*IRF7* mRNA interaction only occurs in an m6A-dependent and m6A-specific manner as it is abolished when m6A marks are removed. Altogether, these results reveal the implication of m6A in *IRF7* mRNA translation and identify YTHDC2 as a novel regulator of m6A-dependent IRF7 protein synthesis.

IRF7 is a master regulator of the IFN-I response (Honda K et al., 2005). It is regulated by a positive feedback loop that keeps innate immunity activated, and it is a key transcription factor for the maintenance of antiviral activity (Erickson & Gale, 2008; Litvak et al., 2012; Ning et al., 2005; Schmid et al., 2010). In response to viral infection IRF7 is activated by phosphorylation and translocated to the nucleus, where it binds to ISRE sequences present in the promoters of some genes. Consequently, the expression of IFN-I and other ISG are increased after IRF7 activation. IFN-β, STAT1 and CXCL10 are implicated in different stages of the immune response, have been described to participate in the CeD characteristic intestinal inflammation (Bondar et al., 2014; Mazzarella et al., 2003; Monteleone et al., 2004), and are all induced by IRF7 (Samarajiwa et al., 2009). Here we showed that the expression of IRF7 downstream genes *IFNB1*, *STAT1* and *CXCL10* can be indirectly influenced by m6A modifications via the regulation of IRF7 protein amount.

IFN-I family members play a pivotal role during viral infections, and CXCL10 is known for its role in chemotaxis of immune cells, such as NK cells (Bondar et al., 2014; Elemam et al., 2022; Trifilo et al., 2004). Brigleb *et al* demonstrated the implication of NK cells in the reovirus-induced loss of tolerance to dietary antigens (Brigleb et al., 2022). Furthermore, they also described that NK cell activation and recruitment are mediated by an IFN-I

dependent pathway and enhance IFN-II production. Taking these previous results and the results obtained in our study into account, we postulate that in the context of CeD, m6A machinery-mediated induction of IRF7 levels may be responsible, at least in part, of the proinflammatory immune response upon reovirus infection induced by activation of NK cells. This presumption is based on four facts: 1) CeD patients showed augmented CXCL10 levels in serum that correlate with serum reactivity to reovirus; 2) IRF7 is implicated in the IFN-I pathway, and its expression is upregulated in CeD patients, regardless of disease status; 3) m6a levels and the expression of m6A machinery members are augmented in CeD patients, and *METTL3* and *YTHDC2* expression correlate with *IRF7* expression, implying a linear connection between them in the intestine; and 4) m6A methylation is essential for IRF7 protein synthesis via m6A reader YTHDC2 and indirectly influences *CXCL10* expression. Although this hypothesis needs to be fully proven, it opens the door to novel research lines that could further explain the implication of reovirus infections in CeD development. Besides, it would display m6A as a new potential target to control the immune response cascade from the early beginning.

In summary, this study presents a new connection between viral infections and CeD through epitranscriptomic modifications. We have proven the relation between reovirus infection and CeD, confirming reovirus as a new viral triggering agent for CeD development. In addition, we present a new m6A-dependent mechanism of *IRF7* regulation, in which m6A writer METTL3, eraser ALKBH5 and reader YTHDC2 are implicated (Figure 30).

Furthermore, although further studies are still needed, our results provide helpful information to fill the gap on our understanding of the way NK cells might be activated upon viral infection in the context of CeD. Finally, our data manifest the importance of innate immunity and antiviral immune response in CeD and propose IRF7 as an interesting candidate for follow-up studies. Altogether, these results shed light on the complexity of CeD onset and open the door for future prevention approaches such as

vaccines against reovirus, or development of new therapeutic targets focused on m6A-dependent gene regulation.

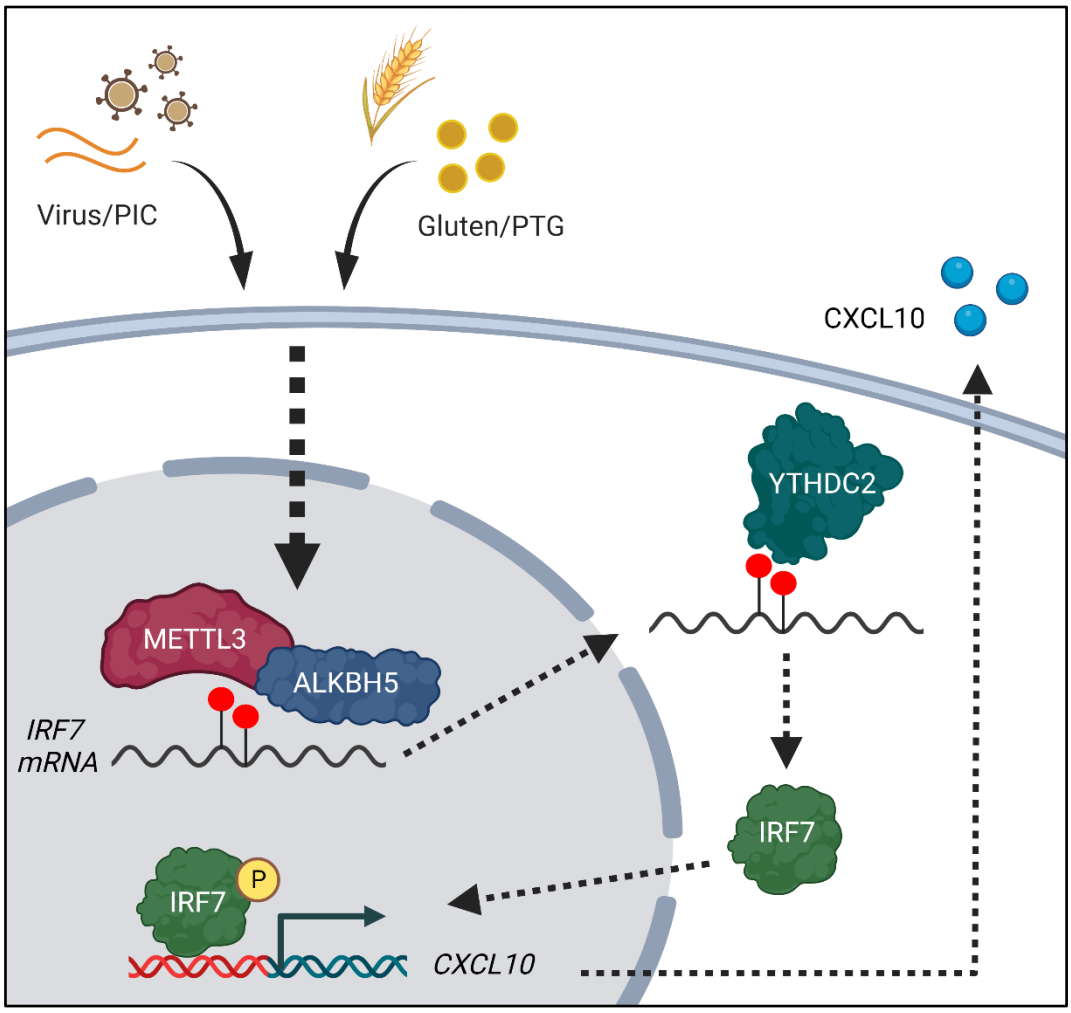

Figure 30. m6A-mediated regulation of IRF7. Viral infection (PIC treatment) and gluten consumption (gliadin stimulation) alter the expression of m6A writer *METTL3* and eraser *ALKBH5*, what lead to an m6A-dependant IRF7 increase. m6A reader YTHDC2 binds to methylated *IRF7* mRNA and enhances its translation and IRF7 protein synthesis, affecting to the expression of IRF7 downstream genes such as proinflammatory *CXCL10*. Image created with BioRender.

CONCLUSIONS

1. This work confirms reovirus as a viral triggering agent in CeD.
    a. We have optimized a straightforward, ELISA-based technique for detection and quantification of anti-reovirus antibodies in serum.
    b. There is a relation between reovirus infection and CeD, and pediatric CeD individuals present an augmented immune response against reovirus, as a significantly higher serum reactivity to reovirus particles.

2. The antiviral immune response is involved in CeD pathogenesis.
    a. CeD patients present increased serum CXCL10 levels, that are correlated with anti-reovirus serum reactivity.
    b. Two master transcription factors of the innate immune response to viral infections, IRF3 and IRF7, are upregulated in active CeD individuals.

3. There is an alteration of the m6A machinery in CeD.
    a. Total m6A levels are augmented in CeD.
    b. In active CeD, the expression of m6A writer *METTL3* and m6A readers *YTHDC1* and *YTHDC2* is higher, and correlates with the expression of antiviral transcripts IRF3 and IRF7. Moreover, m6A eraser ALKBH5 appears to be influenced by gluten consumption, and is upregulated when gluten is removed from the diet.

4. We have generated an *in vitro* intestinal-cell model resembling a possible scenario in CeD individuals before disease onset.
    a. In this combined model, the m6A machinery is altered and a strong, METTL3-dependant increase in the expression of IRF7 is also observed.
    b. IRF7 is regulated by a m6A-dependant mechanism involving m6A writer METTL3, eraser ALKBH5 and reader YTHDC2, and m6A methylation within its CDS is essential for IRF7 protein synthesis and correct downstream signaling, including the expression of proinflammatory cytokine *CXCL10*.

BIBLIOGRAPHY

Abadie, V., & Jabri, B. (2014). IL-15: A central regulator of celiac disease immunopathology. *Immunological Reviews*, *260*(1), 221–234. https://doi.org/10.1111/imr.12191

Abadie, V., Kim, S. M., Lejeune, T., Palanski, B. A., Ernest, J. D., Tastet, O., Voisine, J., Discepolo, V., Marietta, E. V., Hawash, M. B. F., Ciszewski, C., Bouziat, R., Panigrahi, K., Horwath, I., Zurenski, M. A., Lawrence, I., Dumaine, A., Yotova, V., Grenier, J. C., … Jabri, B. (2020). IL-15, gluten and HLA-DQ8 drive tissue destruction in coeliac disease. *Nature*, *578*(7796), 600–604. https://doi.org/10.1038/s41586-020-2003-8

Alexopoulou, L., Holt, A. C., Medzhitov, R., & Flavell, R. A. (2001). Recognition of double-stranded RNA and activation of NF-kB by Toll-like receptor 3. *Nature*, *413*(6857), 732–738. https://doi.org/ 10.1038/35099560

Allegretti, Y. L., Bondar, C., Guzman, L., Cueto Rua, E., Chopita, N., Fuertes, M., Zwirner, N. W., & Chirdo, F. G. (2013). Broad MICA/B Expression in the Small Bowel Mucosa: A Link between Cellular Stress and Celiac Disease. *PLoS ONE*, *8*(9), e73658. https://doi.org/10.1371/journal.pone.0073658

Arango, D., Sturgill, D., Alhusaini, N., Dillman, A. A., Sweet, T. J., Hanson, G., Hosogane, M., Sinclair, W. R., Nanan, K. K., Mandler, M. D., Fox, S. D., Zengeya, T. T., Andresson, T., Meier, J. L., Coller, J., & Oberdoerffer, S. (2018). Acetylation of Cytidine in mRNA Promotes Translation Efficiency. *Cell*, *175*(7), 1872–1886. https://doi.org/10.1016/j.cell.2018.10.030

Balkhi, M. Y., Fitzgerald, K. A., & Pitha, P. M. (2010). IKKα negatively regulates IRF-5 function in a MyD88–TRAF6 pathway. *Cellular Signalling*, *22*(1), 117–127. https://doi.org/10.1016/j.cellsig.2009.09.021

Banchereau, J., & Pascual, V. (2006). Type I Interferon in Systemic Lupus Erythematosus and Other Autoimmune Diseases. *Immunity*, *25*(3), 383–392. https://doi.org/10.1016/J.IMMUNI.2006.08.010

Barone, M. V., Troncone, R., & Auricchio, S. (2014). Gliadin peptides as triggers of the proliferative and stress/innate immune response of the celiac small intestinal mucosa. *International Journal of Molecular Sciences*, *15*(11), 20518–20537. https://doi.org/10.3390/ijms151120518

Bartosovic, M., Molares, H. C., Gregorova, P., Hrossova, D., Kudla, G., & Vanacova, S. (2017). N6-methyladenosine demethylase FTO targets pre-mRNAs and regulates alternative splicing and 3′-end processing. *Nucleic Acids Research*, *45*(19), 11356–11370. https://doi.org/10.1093/nar/gkx778

Bechara, R., & Gaffen, S. L. (2021). '(m6)A' stands for 'autoimmunity': reading, writing, and erasing RNA modifications during inflammation. *Trends in Immunology*, *42*(12), 1073–1076. https://doi.org/10.1016/j.it.2021.10.002

Bergstrøm, B., Aune, M. H., Awuh, J. A., Kojen, J. F., Blix, K. J., Ryan, L., Flo, T. H., Mollnes, T. E., Espevik, T., & Stenvik, J. (2015). TLR8 Senses Staphylococcus aureus RNA in Human Primary Monocytes and Macrophages and Induces IFN-β Production via a TAK1-IKKβ-IRF5 Signaling Pathway. *The Journal of Immunology*, *195*(3), 1100–1111. https://doi.org/10.4049/jimmunol.1403176

Bjornevik, K., Cortese, M., Healy, B. C., Kuhle, J., Mina, M. J., Leng, Y., Elledge, S. J., Niebuhr, D. W., Scher, A. I., Munger, K. L., & Ascherio, A. (2022). Longitudinal analysis reveals high prevalence of Epstein-Barr virus associated with multiple sclerosis. *Science*, *375*(6578), 296–301. https://doi.org/10.1126/SCIENCE.ABJ8222

Bondar, C., Araya, R. E., Guzman, L., Rua, E. C., & Chopita, N. (2014). Role of CXCR3/CXCL10 Axis in Immune Cell Recruitment into the Small Intestine in Celiac Disease. *PLoS ONE*, *9*(2), 89068. https://doi.org/10.1371/journal.pone.0089068

Boo, S. H., & Kim, Y. K. (2020). The emerging role of RNA modifications in the regulation of mRNA stability. *Experimental and Molecular Medicine*, *52*(3), 400–408. https://doi.org/10.1038/s12276-020-0407-z

Bouziat, R., Hinterleitner, R., Brown, J. J., Stencel-Baerenwald, J. E., Ikizler, M., Mayassi, T., Meisel, M., Kim, S. M., Discepolo, V., Pruijssers, A. J., Ernest, J. D., Iskarpatyoti, J. A., Costes, L. M. M., Lawrence, I., Palanski, B. A., Varma, M., Zurenski, M. A., Khomandiak, S., McAllister, N., … Jabri, B. (2017). Reovirus infection triggers inflammatory responses to dietary antigens and development of celiac disease. *Science*, *356*(6333), 44–50. https://doi.org/10.1126/science.aah5298

Briani, C., Samaroo, D., & Alaedini, A. (2008). Celiac disease: From gluten to autoimmunity. *Autoimmunity Reviews*, *7*(8), 644–650. https://doi.org/10.1016/j.autrev.2008.05.006

Brigleb, P. H., Kouame, E., Fiske, K. L., Taylor, G. M., Urbanek, K., Medina Sanchez, L., Hinterleitner, R., Jabri, B., & Dermody, T. S. (2022). NK cells contribute to reovirus-induced IFN responses and loss of tolerance to dietary antigen. *JCI Insight*, *7*(16), e159823. https://doi.org/10.1172/jci

Brocard, M., Ruggieri, A., & Locker, N. (2017). m6A RNA methylation, a new hallmark in virus-host interactions. *Journal of General Virology*, *98*(9), 2207–2214. https://doi.org/10.1099/jgv.0.000910

Cai, X., Chiu, Y.-H., & Chen, Z. J. (2014). The cGAS-cGAMP-STING Pathway of Cytosolic DNA Sensing and Signaling. *Molecular Cell*, *54*(2), 289–296. https://doi.org/10.1016/j.molcel.2014.03.040

Caillaud, A., Prakash, A., Smith, E., Masumi, A., Hovanessian, A. G., Levy, D. E., & Marié, I. (2002). Acetylation of Interferon Regulatory Factor-7 by p300/CREB-binding Protein (CBP)-associated Factor (PCAF) Impairs its DNA Binding. *Journal of Biological Chemistry*, *277*(51), 49417–49421. https://doi.org/10.1074/jbc.M207484200

Caio, G., Volta, U., Sapone, A., Leffler, D. A., de Giorgio, R., Catassi, C., & Fasano, A. (2019). Celiac disease: a comprehensive current review. *BMC Medicine*, *17*(1), 1–20. https://doi.org/10.1186/s12916-019-1380-z

Cao, Z., Sugimura, N., Burgermeister, E., Ebert, M. P., Zuo, T., & Lan, P. (2022). The gut virome: A new microbiome component in health and disease. *EBioMedicine*, *81*, 104113. https://doi.org/10.1016/j

Carew, J. S., Espitia, C. M., Zhao, W., Mita, M. M., Mita, A. C., & Nawrocki, S. T. (2017). Oncolytic reovirus inhibits angiogenesis through induction of CXCL10/IP-10 and abrogation of HIF activity in soft tissue sarcomas. *Oncotarget*, *8*(49), 86769. https://doi.org/10.18632/ONCOTARGET.21423

Castellanos-Rubio, A., Fernandez-Jimenez, N., Kratchmarov, R., Luo, X., Bhagat, G., Green, P. H. R., Schneider, R., Kiledjian, M., Bilbao, J. R., & Ghosh, S. (2016). A long noncoding RNA associated with susceptibility to celiac disease. *Science*, *352*(6281), 91–95. https://doi.org/10.1126/science.aad0467

Castellanos-Rubio, A., Santin, I., Irastorza, I., Castaño, L., Carlos Vitoria, J., & Bilbao, J. R. (2009). TH17 (and TH1) signatures of intestinal biopsies of CD patients in response to gliadin. *Autoimmunity*, *42*(1), 69–73. https://doi.org/10.1080/08916930802350789

Cecilio, L. A., & Bonatto, M. W. (2015). THE PREVALENCE OF HLA DQ2 AND DQ8 IN PATIENTS WITH CELIAC DISEASE, IN FAMILY AND IN GENERAL POPULATION. *Arquivos Brasileiros de Cirurgia Digestiva : ABCD = Brazilian Archives of Digestive Surgery*, *28*(3), 183. https://doi.org/10.1590/S0102-67202015000300009

Chan, M. P., Onji, M., Fukui, R., Kawane, K., Shibata, T., Saitoh, S., Ohto, U., Shimizu, T., Barber, G. N., & Miyake, K. (2015). DNase II-dependent DNA digestion is required for DNA sensing by TLR9. *Nature Communications*, *6*(1), 5853. https://doi.org/10.1038/ncomms6853

Chen, T., Hao, Y.-J., Zhang, Y., Li, M.-M., Wang, M., Han, W., Wu, Y., Lv, Y., Hao, J., Wang, L., Li, A., Yang, Y., Jin, K.-X., Zhao, X., Li, Y., Ping, X.-L., Lai, W.-Y., Wu, L.-G., Jiang, G., Wang, H.-L., Sang, L., Wang, X.-J., Yang, Y.-G., & Zhou, Q. (2015). m6A RNA Methylation Is Regulated by MicroRNAs and Promotes Reprogramming to Pluripotency. *Cell Stem Cell*, *16*(3), 289–301. https://doi.org/10.1016/j.stem.2015.01.016

Chen, W., & Royer, W. E. (2010). Structural insights into interferon regulatory factor activation. *Cellular Signalling*, *22*(6), 883–887. https://doi.org/10.1016/j.cellsig.2009.12.005

Chiang, H. Sen, & Liu, H. M. (2019). The molecular basis of viral inhibition of IRF- and STAT-dependent immune responses. *Frontiers in Immunology*, 9, 3086. https://doi.org/10.3389/fimmu.2018.03086

Choi, J., Ieong, K.-W., Demirci, H., Chen, J., Petrov, A., Prabhakar, A., O'Leary, S. E., Dominissini, D., Rechavi, G., Soltis, S. M., Ehrenberg, M., & Puglisi, J. D. (2016). N(6)-methyladenosine in mRNA disrupts tRNA selection and translation-elongation dynamics. *Nature Structural & Molecular Biology*, *23*(2), 110–115. https://doi.org/10.1038/nsmb.3148

Cicarelli, G., della Rocca, G., Amboni, M., Ciacci, C., Mazzacca, G., Filla, A., & Barone, P. (2003). Clinical and neurological abnormalities in adult celiac disease. *Neurological Sciences*, *24*(5), 311–317. https://doi.org/10.1007/s10072-003-0181-4

Ciccocioppo, R., di Sabatino, A., & Corazza, G. R. (2005). The immune recognition of gluten in coeliac disease. *Clinical and Experimental Immunology*, *140*(3), 408–416. https://doi.org/10.1111/j.1365-2249.2005.02783.x

Colina, R., Costa-Mattioli, M., Dowling, R. J. O., Jaramillo, M., Tai, L.-H., Breitbach, C. J., Martineau, Y., Larsson, O., Rong, L., Svitkin, Y. V, Makrigiannis, A. P., Bell, J. C., & Sonenberg, N. (2008). Translational control of the innate immune response through IRF-7. *Nature*, *452*(7185), 323–329. https://doi.org/10.1038/nature06730

Csumita, M., Csermely, A., Horvath, A., Nagy, G., Monori, F., Göczi, L., Orbea, H.-A., Reith, W., & Széles, L. (2019). Specific enhancer selection by IRF3, IRF5 and IRF9 is determined by ISRE half-sites, 5 and 3 flanking bases, collaborating transcription factors and the chromatin

environment in a combinatorial fashion. *Nucleic Acids Research*, *48*(2), 589–604. https://doi.org/10.1093/nar/gkz1112

Daffis, S., Samuel, M. A., Suthar, M. S., Keller, B. C., Gale, M., & Diamond, M. S. (2008). Interferon Regulatory Factor IRF-7 Induces the Antiviral Alpha Interferon Response and Protects against Lethal West Nile Virus Infection. *Journal of Virology*, *82*(17), 8465–8475. https://doi.org/10.1128/JVI.00918-08

Dang, W., Xie, Y., Cao, P., Xin, S., Wang, J., Li, S., Li, Y., & Lu, J. (2019). N6-methyladenosine and viral infection. *Frontiers in Microbiology*, *10*, 417. https://doi.org/10.3389/fmicb.2019.00417

Dauletbaev, N., Cammisano, M., Herscovitch, K., & Lands, L. C. (2015). Stimulation of the RIG-I/MAVS Pathway by Polyinosinic:Polycytidylic Acid Upregulates IFN-β in Airway Epithelial Cells with Minimal Costimulation of IL-8. *The Journal of Immunology*, *195*(6), 2829–2841. https://doi.org/10.4049/jimmunol.1400840

de Oliveira Mann, C. C., & Hornung, V. (2021). Molecular mechanisms of nonself nucleic acid recognition by the innate immune system. *European Journal of Immunology*, *51*(8), 1897–1910. https://doi.org/10.1002/eji.202049116

Desrosiers, R., Friderici, K., & Rottman, F. (1974). Identification of Methylated Nucleosides in Messenger RNA from Novikoff Hepatoma Cells. *Proceedings of the National Academy of Sciences of the United States of America*, *71*(10), 3971. https://doi.org/10.1073/PNAS.71.10.3971

Dieli-Crimi, R., Cénit, M. C., & Núñez, C. (2015). The genetics of celiac disease: A comprehensive review of clinical implications. *Journal of Autoimmunity*, *64*, 26–41. https://doi.org/10.1016/J.JAUT.2015.07.003

Dominissini, D., Moshitch-Moshkovitz, S., Salmon-Divon, M., Amariglio, N., & Rechavi, G. (2013). Transcriptome-wide mapping of N6-methyladenosine by m 6A-seq based on immunocapturing and massively parallel sequencing. *Nature Protocols*, *8*(1), 176–189. https://doi.org/10.1038/nprot.2012.148

Dominissini, D., Moshitch-Moshkovitz, S., Schwartz, S., Salmon-Divon, M., Ungar, L., Osenberg, S., Cesarkas, K., Jacob-Hirsch, J., Amariglio, N., Kupiec, M., Sorek, R., & Rechavi, G. (2012). Topology of the human and mouse m6A RNA methylomes revealed by m6A-seq. *Nature*, *485*(7397), 201–206. https://doi.org/10.1038/nature11112

Dominissini, D., Nachtergaele, S., Moshitch-Moshkovitz, S., Peer, E., Kol, N., Shay Ben-Haim, M., Dai, Q., Di Segni, A., Salmon-Divon, M., Clark, W. C., Zheng, G., Pan, T., Solomon, O., Eyal, E., Hershkovitz, V., Han, D., Doré, L. C., Amariglio, N., Rechavi, G., & He, C. (2016). The dynamic N 1-methyladenosine methylome in eukaryotic messenger RNA. *Nature*, *530*(7591), 441–446. https://doi.org/10.1038/nature16998

Douville, R. N., Su, R.-C., Coombs, K. M., Simons, F. E. R., & HayGlass, K. T. (2008). Reovirus Serotypes Elicit Distinctive Patterns of Recall Immunity in Humans. *Journal of Virology*, *82*(15), 7515–7523. https://doi.org/10.1128/JVI.00464-08/ASSET/80B43AC5-19B2-4C8F-8808-BCB195807935/ASSETS/GRAPHIC/ZJV0150808420006.JPEG

Du, H., Zhao, Y., He, J., Zhang, Y., Xi, H., Liu, M., Ma, J., & Wu, L. (2016). YTHDF2 destabilizes m6A-containing RNA through direct recruitment of the CCR4–NOT deadenylase complex. *Nature Communications*, *7*(1), 12626. https://doi.org/10.1038/ncomms12626

Dubois, P. C. A., Trynka, G., Franke, L., Hunt, K. A., Romanos, J., Curtotti, A., Zhernakova, A., Heap, G. A. R., Ádány, R., Aromaa, A., Bardella, M. T., van den Berg, L. H., Bockett, N. A., de La Concha, E. G., Dema, B., Fehrmann, R. S. N., Fernández-Arquero, M., Fiatal, S., Grandone, E., … van Heel, D. A. (2010). Multiple common variants for celiac disease influencing immune gene expression. *Nature Genetics*, *42*(4), 295. https://doi.org/10.1038/NG.543

Durbin, A. F., Wang, C., Marcotrigiano, J., & Gehrke, L. (2016). RNAs Containing Modified Nucleotides Fail To Trigger RIG-I Conformational Changes for Innate Immune Signaling. *MBio*, *7*(5), e00833-16. https://doi.org/10.1128/MBIO.00833-16

Elemam, N. M., Talaat, I. M., & Maghazachi, A. A. (2022). CXCL10 Chemokine: A Critical Player in RNA and DNA Viral Infections. *Viruses*, *14*(11), 2445. https://doi.org/10.3390/v14112445

Erickson, A. K., & Gale, M. (2008). Regulation of interferon production and innate antiviral immunity through translational control of IRF-7. *Cell Research*, *18*(4), 433–435. https://doi.org/10.1038/cr.2008.46

Feighery, C. (1999). Fortnightly review: Coeliac disease. *BMJ*, *319*(7204), 236–239. https://doi.org/10.1136/bmj.319.7204.236

Filippi, C. M., & Von Herrath, M. G. (2008). Viral trigger for type 1 diabetes: pros and cons. *Diabetes*, *57*(11), 2863–2871. https://doi.org/10.2337/DB07-1023

Finkbeiner, S. R., Allred, A. F., Tarr, P. I., Klein, E. J., & Kirkwood, C. D. (2008). Metagenomic Analysis of Human Diarrhea: Viral Detection and Discovery. *PLoS Pathog*, *4*(2), 1000011. https://doi.org/10.1371/journal.ppat.1000011

Fitzgerald, K. A., McWhirter, S. M., Faia, K. L., Rowe, D. C., Latz, E., Golenbock, D. T., Coyle, A. J., Liao, S.-M., & Maniatis, T. (2003). IKKε and TBK1 are essential components of the IRF3 signaling pathway. *Nature Immunology*, *4*(5), 491–496. https://doi.org/10.1038/ni921

Fulci, V., Stronati, L., Cucchiara, S., Laudadio, I., & Carissimi, C. (2021). Molecular Sciences Emerging Roles of Gut Virome in Pediatric Diseases. *International Journal of Molecular Sciences*, *22*(8), 4127. https://doi.org/10.3390/ijms22084127

Furuichi, Y., & Sekiya, T. (2015). Review Discovery of m 7 G-cap in eukaryotic mRNAs. *Proceedings of the Japan Academy, Series B*, *91*(8), 394–409. https://doi.org/10.2183/pjab.91.394

Fustin, J.-M., Doi, M., Yamaguchi, Y., Hida, H., Nishimura, S., Yoshida, M., Isagawa, T., Morioka, M. S., Kakeya, H., Manabe, I., & Okamura, H. (2013). RNA-Methylation-Dependent RNA Processing Controls the Speed of the Circadian Clock. *Cell*, *155*(4), 793–806. https://doi.org/10.1016/j.cell.2013.10.026

Geula, S., Moshitch-Moshkovitz, S., Dominissini, D., Mansour, A. A., Kol, N., Salmon-Divon, M., Hershkovitz, V., Peer, E., Mor, N., Manor, Y. S., Ben-Haim, M. S., Eyal, E., Yunger, S., Pinto, Y., Jaitin, D. A., Viukov, S., Rais, Y., Krupalnik, V., Chomsky, E., Zerbib, M., Maza, I., Rechavi, Y., Massarwa,R., Hanna, S., Amit, I., Levanon, E. Y., Amariglio, N., Stern-Ginossar,

N., Novershtern, N., Rechavi, G., & Hanna, J. H. (2015). m6A mRNA methylation facilitates resolution of naïve pluripotency toward differentiation. *Science*, *347*(6225), 1002–1006. https://doi.org/10.1126/science.1261417

Goel, G., Tye-Din, J. A., Qiao, S.-W., Russell, A. K., Mayassi, T., Ciszewski, C., Sarna, V. K., Wang, S., Goldstein, K. E., Dzuris, J. L., Williams, L. J., Xavier, R. J., A Lundin, K. E., Jabri, B., Sollid, L. M., & Anderson, R. P. (2019). Cytokine release and gastrointestinal symptoms after gluten challenge in celiac disease. *Science Advances*, *5*(8), eaaw7756. https://doi.org/10.1126/sciadv.aaw7756

Gokhale, N. S., McIntyre, A. B. R., McFadden, M. J., Roder, A. E., Kennedy, E. M., Gandara, J. A., Hopcraft, S. E., Quicke, K. M., Vazquez, C., Willer, J., Ilkayeva, O. R., Law, B. A., Holley, C. L., Garcia-Blanco, M. A., Evans, M. J., Suthar, M. S., Bradrick, S. S., Mason, C. E., & Horner, S. M. (2016). N6-Methyladenosine in Flaviviridae Viral RNA Genomes Regulates Infection. *Cell Host & Microbe*, *20*(5), 654–665. https://doi.org/10.1016/J.CHOM.2016.09.015

Graindorge, A., Pinheiro, I., Nawrocka, A., Mallory, A. C., Tsvetkov, P., Gil, N., Carolis, C., Buchholz, F., Ulitsky, I., Heard, E., Taipale, M., & Shkumatava, A. (2019). In-cell identification and measurement of RNA-protein interactions. *Nature Communications*, *10*(1), 5317. https://doi.org/10.1038/s41467-019-13235-w

Green, P. H. R. (2005). The many faces of celiac disease: Clinical presentation of celiac disease in the adult population. *Gastroenterology*, *128*, S74–S78. https://doi.org/10.1053/j.gastro.2005.02.016

Green, P. H. R., Stavropoulos, S. N., Panagi, S. G., Goldstein, S. L., Mcmahon, D. J., Absan, H., & Neugut, A. I. (2001). Characteristics of Adult Celiac Disease in the USA: Results of a National Survey. *The American Journal of Gastroenterology*, *96*(1), 126–131.

Gregory, A. C., Zablocki, O., Zayed, A. A., Howell, A., Bolduc, B., & Sullivan, M. B. (2020). The Gut Virome Database Reveals Age-Dependent Patterns of Virome Diversity in the Human Gut. *Cell Host and Microbe*, *28*(5), 724–740. https://doi.org/10.1016/j.chom.2020.08.003

Gruber, A. R., Lorenz, R., Bernhart, S. H., Ck, R. N., & Hofacker, I. L. (2008). The Vienna RNA Websuite. *Nucleic Acids Research*, *36*, W70–W74. https://doi.org/10.1093/nar/gkn188

Haghbin, M., Rostami-Nejad, M., Forouzesh, F., Sadeghi, A., Rostami, K., Aghamohammadi, E., Asadzadeh-Aghdaei, H., Masotti, A., & Zali, M. R. (2019). The role of CXCR3 and its ligands CXCL10 and CXCL11 in the pathogenesis of celiac disease. *Medicine*, *98*(25), e15949. https://doi.org/10.1097/MD.0000000000015949

Hao, H., Hao, S., Chen, H., Chen, Z., Zhang, Y., Wang, J., Wang, H., Zhang, B., Qiu, J., Deng, F., & Guan, W. (2019). N 6-methyladenosine modification and METTL3 modulate enterovirus 71 replication. *Nucleic Acids Research*, *47*(1), 362–374. https://doi.org/10.1093/nar/gky1007

Harper, J. E., Miceli, S. M., Roberts, R. J., & Manley, J. L. (1990). Sequence specificity of the human mRNA N6-adenosine methylase *in vitro*. *Nucleic Acids Research*, *18*(19), 5735–5741. https://doi.org/10.1093/nar/18.19.5735

Hemmi, H., Takeuchi, O., Sato, S., Yamamoto, M., Kaisho, T., Sanjo, H., Kawai, T., Hoshino, K., Takeda, K., & Akira, S. (2004). The Roles of Two IκB Kinase-related Kinases in Lipopolysaccharide and Double Stranded RNA Signaling and Viral Infection. *Journal of Experimental Medicine*, *199*(12), 1641–1650. https://doi.org/10.1084/jem.20040520

Higgs, R., Lazzari, E., Wynne, C., Ní Gabhann, J., Espinosa, A., Wahren-Herlenius, M., & Jefferies, C. A. (2010). Self Protection from Anti-Viral Responses – Ro52 Promotes Degradation of the Transcription Factor IRF7 Downstream of the Viral Toll-Like Receptors. *PLoS ONE*, *5*(7), e11776. https://doi.org/10.1371/journal.pone.0011776

Hiscott, J. (2007). Convergence of the NF-κB and IRF pathways in the regulation of the innate antiviral response. *Cytokine & Growth Factor Reviews*, *18*(5–6), 483–490. https://doi.org/10.1016/j.cytogfr.2007.06.002

Honda, K., & Taniguchi, T. (2006). IRFs: master regulators of signalling by Toll-like receptors and cytosolic pattern-recognition receptors. *Nature Reviews. Immunology*, *6*(9), 644–658. https://doi.org/10.1038/NRI1900

Honda K, Yanai H, Negishi H, Asagiri M, Sato M, Mizutani T, Ohba Y, Takaoka A, Yoshida N, & Taniguchi T. (2005). IRF-7 is the master regulator of type-I interferon-dependent immune responses. *Nature*, *434*(7034), 772–777. https://doi.org/10.1038/nature03419

Hsu, P. J., Zhu, Y., Ma, H., Guo, Y., Shi, X., Liu, Y., Qi, M., Lu, Z., Shi, H., Wang, J., Cheng, Y., Luo, G., Dai, Q., Liu, M., Guo, X., Sha, J., Shen, B., & He, C. (2017). Ythdc2 is an N6 - methyladenosine binding protein that regulates mammalian spermatogenesis. *Cell Research*, *27*(9), 1115–1127. https://doi.org/10.1038/cr.2017.99

Hü, S., Mention, J.-J., Monteiro, R. C., Zhang, S., Cellier, C., Schmitz, J., Bahram, S., & Cerf-Bensussan, N. (2004). A Direct Role for NKG2D/MICA Interaction in Villous Atrophy during Celiac Disease intestine by a T cell “cocktail” composed mainly of acti-Virginie Verkarre, 2 Nassima Fodil, 6 vated CD4 T cells in the lamina propria and CD8 T cells contains a consensus YxxM tyrosine-based motif in its. *Immunity*, *21*, 367–377.

Huang, H., Weng, H., Sun, W., Qin, X., Shi, H., Wu, H., Zhao, B. S., Mesquita, A., Liu, C., Yuan, C. L., Hu, Y. C., Hüttelmaier, S., Skibbe, J. R., Su, R., Deng, X., Dong, L., Sun, M., Li, C., Nachtergaele, S., … Chen, J. (2018). Recognition of RNA N 6 -methyladenosine by IGF2BP proteins enhances mRNA stability and translation. *Nature Cell Biology*, *20*(3), 285–295. https://doi.org/10.1038/s41556-018-0045-z

Husby, S., Koletzko, S., Korponay-Szabó, I. R., Mearin, M. L., Phillips, A., Shamir, R., Troncone, R., Giersiepen, K., Branski, D., Catassi, C., Lelgeman, M., Mäki, M., Ribes-Koninckx, C., Ventura, A., & Zimmer, K. P. (2012). European society for pediatric gastroenterology, hepatology, and nutrition guidelines for the diagnosis of coeliac disease. *Journal of Pediatric Gastroenterology and Nutrition*, *54*(1),136–160. https://doi.org/10.1097/MPG.0b013e31821a23d0

Hussain, S., Aleksic, J., Blanco, S., Dietmann, S., & Frye, M. (2013). Characterizing 5-methylcytosine in the mammalian epitranscriptome. *Genome Biology*, *14*(11), 1–10. http://genomebiology.com/2013/14/11/215

Hussein, H. M., & Rahal, E. A. (2019). The role of viral infections in the development of autoimmune diseases. *Critical Reviews in Microbiology*, 45(4), 394–412. https://doi.org/10.1080/1040841X.2019.1614904

Hyöty, H., & Taylor, K. (2002). The role of viruses in human diabetes. *Diabetologia*, *45*(10), 1353–1361. https://doi.org/10.1007/s00125-002-0852-3

Ikushima, H., Negishi, H., & Taniguchi, T. (2013). The IRF family transcription factors at the interface of innate and adaptive immune responses. *Cold Spring Harbor Symposia on Quantitative Biology*, *78*(1), 105–116. https://doi.org/10.1101/sqb.2013.78.020321

Ishikawa, H., Ma, Z., & Barber, G. N. (2009). STING regulates intracellular DNA-mediated, type I interferon-dependent innate immunity. *Nature*, *461*(7265), 788–793. https://doi.org/10.1038/nature08476

Ivashkiv, L. B., & Donlin, L. T. (2014). Regulation of type I interferon responses. *Nature Reviews Immunology*, *14*(1), 36–49. https://doi.org/10.1038/nri3581

Iwamura, T., Yoneyama, M., Yamaguchi, K., Suhara, W., Mori, W., Shiota, K., Okabe, Y., Namiki, H., & Fujita, T. (2001). Induction of IRF-3/-7 kinase and NF-κB in response to double-stranded RNA and virus infection: common and unique pathways. *Genes to Cells*, *6*(4), 375–388. https://doi.org/10.1046/j.1365-2443.2001.00426.x

Iwanaszko, M., & Kimmel, M. (2015). NF-κB and IRF pathways: cross-regulation on target genes promoter level. *BMC Genomics*, *16*(1), 307. https://doi.org/10.1186/s12864-015-1511-7

Jauregi-Miguel, A., Santin, I., Garcia-Etxebarria, K., Olazagoitia-Garmendia, A., Romero-Garmendia, I., Sebastian-delaCruz, M., Irastorza, I., Castellanos-Rubio, A., & Bilbao, J. R. (2019). MAGI2 Gene Region and Celiac Disease. *Frontiers in Nutrition*, *6*. https://doi.org/10.3389/fnut.2019.00187

Jelínková, L., Tučková, L., Cinová, J., Flegelová, Z., & Tlaskalová-Hogenová, H. (2004). Gliadin stimulates human monocytes to production of IL-8 and TNF-α through a mechanism involving NF-κB. *FEBS Letters*, *571*(1–3), 81–85. https://doi.org/10.1016/j.febslet.2004.06.057

Jia, G., Fu, Y., Zhao, X., Dai, Q., Zheng, G., Yang, Y., Yi, C., Lindahl, T., Pan, T., Yang, Y.-G., & He, C. (2011). N6-Methyladenosine in nuclear RNA is a major substrate of the obesity-associated FTO. *Nature Chemical Biology*, *7*(12), 885–887. https://doi.org/10.1038/nchembio.687

Julio-Pieper, M., López-Aguilera, A., Eyzaguirre-Velásquez, J., Olavarría-Ramírez, L., Ibacache-Quiroga, C., Bravo, J. A., & Cruz, G. (2021). Molecular Sciences Gut Susceptibility to Viral Invasion: Contributing Roles of Diet, Microbiota and Enteric Nervous System to Mucosal Barrier Preservation. *International Journal of Molecular Sciences*, *22*(9), 4734. https://doi.org/10.3390/ijms22094734

Kaján, G. L., Doszpoly, A., Tarján, Z. L., Vidovszky, M. Z., & Papp, T. (2020). Virus–Host Coevolution with a Focus on Animal and Human DNA Viruses. *Journal of Molecular Evolution*, *88*(1), 41–56. https://doi.org/10.1007/S00239-019-09913-4/FIGURES/1

Karikó, K., Buckstein, M., Ni, H., & Weissman, D. (2005). Suppression of RNA recognition by Toll-like receptors: The impact of nucleoside modification and the evolutionary origin of RNA. *Immunity*, *23*(2), 165–175. https://doi.org/10.1016/j.immuni.2005.06.008

Kato, H., Takeuchi, O., Sato, S., Yoneyama, M., Yamamoto, M., Matsui, K., Uematsu, S., Jung, A., Kawai, T., Ishii, K. J., Yamaguchi, O., Otsu, K., Tsujimura, T., Koh, C.-S., Reis e Sousa, C., Matsuura, Y., Fujita, T., & Akira, S. (2006). Differential roles of MDA5 and RIG-I helicases in the recognition of RNA viruses. *Nature*, *441*(7089), 101–105. https://doi.org/10.1038/nature04734

Kawai, T., & Akira, S. (2005). Toll-like receptor downstream signaling. *Arthritis Research & Therapy*, *7*(1), 12. https://doi.org/10.1186/ar1469

Kawai, T., & Akira, S. (2006a). Innate immune recognition of viral infection. *Nature Immunology*, *7*(2), 131–137. https://doi.org/10.1038/ni1303

Kawai, T., & Akira, S. (2006b). TLR signaling. *Cell Death and Differentiation*, *13*(5), 816–825. https://doi.org/10.1038/sj.cdd.4401850

Kawai, T., Sato, S., Ishii, K. J., Coban, C., Hemmi, H., Yamamoto, M., Terai, K., Matsuda, M., Inoue, J. I., Uematsu, S., Takeuchi, O., & Akira, S. (2004). Interferon-α induction through Toll-like receptors involves a direct interaction of IRF7 with MyD88 and TRAF6. *Nature Immunology*, *5*(10), 1061–1068. https://doi.org/10.1038/ni1118

Kemppainen, K. M., Lynch, K. F., Liu, E., Lönnrot, M., Simell, V., Briese, T., Koletzko, S., Hagopian, W., Rewers, M., She, J. X., Simell, O., Toppari, J., Ziegler, A. G., Akolkar, B., Krischer, J. P., Lernmark, Å., Hyöty, H., Triplett, E. W., & Agardh, D. (2017). Factors That Increase Risk of Celiac Disease Autoimmunity After a Gastrointestinal Infection in Early Life. *Clinical Gastroenterology and Hepatology*, *15*(5), 694–702. https://doi.org/10.1016/j.cgh.2016.10.033

Kennedy, E. M., Courtney, D. G., Tsai, K., & Cullen, B. R. (2017). Viral Epitranscriptomics. *Journal of Virology*, *91*(9), e02263-16. https://doi.org/10.1128/jvi.02263-16

Kim, G.-W., & Siddiqui, A. (2021). N6-methyladenosine modification of HCV RNA genome regulates cap-independent IRES-mediated translation via YTHDC2 recognition. *Procedings of the National Academy of Sciences of USA*, *118*(10), e2022024118. https://doi.org/10.1073/pnas.2022024118/-/DCSupplemental

Kim, S. M., & Jabri, B. (2015). Innate immunity: Actuating the gears of celiac disease pathogenesis HHS Public Access. *Best Pract Res Clin Gastroenterol*, *29*(3), 425–435. https://doi.org/10.1016/j.bpg.2015.05.001

Klein, S. L., & Flanagan, K. L. (2016). Sex differences in immune responses. *Nature Reviews Immunology*, *16*(10), 626–638. https://doi.org/10.1038/nri.2016.90

Knuckles, P., Lence, T., Haussmann, I. U., Jacob, D., Kreim, N., Carl, S. H., Masiello, I., Hares, T., Villaseñor, R., Hess, D., Andrade-Navarro, M. A., Biggiogera, M., Helm, M., Soller, M., Bühler, M., & Roignant, J.-Y. (2018). Zc3h13/Flacc is required for adenosine methylation by bridging the mRNA-binding factor Rbm15/Spenito to the m6A machinery component Wtap/Fl(2)d. *Genes & Development*, *32*(5–6), 415–429. https://doi.org/10.1101/gad.309146.117

Kobayashi, M., Ohsugi, M., Sasako, T., Awazawa, M., Umehara, T., Iwane, A., Kobayashi, N., Okazaki, Y., Kubota, N., Suzuki, R., Waki, H., Horiuchi, K., Hamakubo, T., Kodama, T., Aoe, S., Tobe, K., Kadowaki, T., & Ueki, K. (2018). The RNA Methyltransferase Complex of WTAP, METTL3, and METTL14 Regulates Mitotic Clonal Expansion in Adipogenesis. *Molecular and Cellular Biology*, *38*(16), e00116-18. https://doi.org/10.1128/mcb.00116-18

Krishnamurthy, S. R., Janowski, A. B., Zhao, G., Barouch, D., & Wang, D. (2016). Hyperexpansion of RNA Bacteriophage Diversity. *PLoS Biol*, *14*(3), 1002409. https://doi.org/10.1371/journal.pbio.1002409

Kubota, T., Matsuoka, M., Chang, T.-H., Tailor, P., Sasaki, T., Tashiro, M., Kato, A., & Ozato, K. (2008). Virus Infection Triggers SUMOylation of IRF3 and IRF7, Leading to the Negative Regulation of Type I Interferon Gene Expression. *Journal of Biological Chemistry*, *283*(37), 25660–25670. https://doi.org/10.1074/jbc.M804479200

Kumar, H., Kawai, T., Kato, H., Sato, S., Takahashi, K., Coban, C., Yamamoto, M., Uematsu, S., Ishii, K. J., Takeuchi, O., & Akira, S. (2006). Essential role of IPS-1 in innate immune responses against RNA viruses. *Journal of Experimental Medicine*, *203*(7), 1795–1803. https://doi.org/10.1084/jem.20060792

Kumar, S., & Mohapatra, T. (2021). Deciphering Epitranscriptome: Modification of mRNA Bases Provides a New Perspective for Post-transcriptional Regulation of Gene Expression. *Frontiers in Cell and Developmental Biology*, *9*, 628415. https://doi.org/10.3389/fcell.2021.628415

Lars C Stene, Margo C Honeyman, Edward J Hoffenberg, Joel E Haas, Ronald J Sokol, Lisa Emery, Iman Taki, Jill M Norris, Henry A Erlich, George S Eisenbarth, & Marian Rewers. (2006). Rotavirus infection frequency and risk of celiac disease autoimmunity in early childhood: a longitudinal study. *American Journal of Gastroenterology*, *101*(10), 2333–2340. https://doi.org/10.1111/j.1572-0241.2006.00741.x

Lee, E. Y., Lee, Z. H., & Song, Y. W. (2009). CXCL10 and autoimmune diseases. *Autoimmunity Reviews*, *8*(5), 379–383. https://doi.org/10.1016/j.autrev.2008.12.002

Lee, M. S., Kim, B., Oh, G. T., & Kim, Y. J. (2013). OASL1 inhibits translation of the type i interferon-regulating transcription factor IRF7. *Nature Immunology*, *14*(4), 346–355. https://doi.org/10.1038/ni.2535

Lejeune, T., Meyer, C., & Abadie, V. (2021). B Lymphocytes Contribute to Celiac Disease Pathogenesis. *Gastroenterology*, *160*(7), 2608–2610. https://doi.org/10.1053/j.gastro.2021.02.063

León, A. J., Garrote, J. A., Blanco-Quirós, A., Calvo, C., Fernández-Salazar, L., del Villar, A., Barrera, A., & Arranz, E. (2006). Interleukin 18 maintains a long-standing inflammation in coeliac disease patients. *Clinical and Experimental Immunology*, *146*(3), 479–485. https://doi.org/10.1111/j.1365-2249.2006.03239.x

Leonard, M. M., Valitutti, F., Karathia, H., Pujolassos, M., Kenyon, V., Fanelli, B., Troisi, J., Subramanian, P., Camhi, S., Colucci, A., Serena, G., Cucchiara, S., Maria Trovato, C., Malamisura, B., Francavilla, R., Elli, L., Hasan, N. A., Zomorrodi, A. R., Colwell, R., Fasano, A., The CD-GEMM Team, Sherman, P. M., Tarr, P. I., & Verdu, E. F. (2021). Microbiome signatures of progression toward celiac disease onset in at-risk children in a longitudinal prospective cohort study. *Procedings of the National Academy of Sciences of USA*, *118*(29), e2020322118. https://doi.org/10.1073/pnas.2020322118/-/DCSupplemental

Lerner, A. (2014). Serological diagnosis of celiac disease -moving beyond the tip of the iceberg. *International Journal of Celiac Disease*, *2*(2), 64–66. https://doi.org/10.12691/ijcd-2-2-8

Lerner, A., Arleevskaya, M., Schmiedl, A., & Matthias, T. (2017). Microbes and viruses are bugging the gut in celiac disease. Are they friends or foes? *Frontiers in Microbiology*, *8*, 1392. https://doi.org/10.3389/fmicb.2017.01392

Lerner, A., & Matthias, T. (2015). Rheumatoid arthritis–celiac disease relationship: Joints get that gut feeling. *Autoimmunity Reviews*, *14*(11), 1038–1047. https://doi.org/10.1016/J.AUTREV.2015.07.007

Lesbirel, S., & Wilson, S. A. (2019). The m 6 A-methylase complex and mRNA export. *Biochimica et Biophysica Acta - Gene Regulatory Mechanisms*, *1862*(3), 319–328. https://doi.org/10.1016/j.bbagrm.2018.09.008

Li, A., Chen, Y. S., Ping, X. L., Yang, X., Xiao, W., Yang, Y., Sun, H. Y., Zhu, Q., Baidya, P., Wang, X., Bhattarai, D. P., Zhao, Y. L., Sun, B. F., & Yang, Y. G. (2017). Cytoplasmic m 6 A reader YTHDF3 promotes mRNA translation. *Cell Research*, *27*(3), 444–447. https://doi.org/10.1038/cr.2017.10

Li, H. B., Tong, J., Zhu, S., Batista, P. J., Duffy, E. E., Zhao, J., Bailis, W., Cao, G., Kroehling, L., Chen, Y., Wang, G., Broughton, J. P., Chen, Y. G., Kluger, Y., Simon, M. D., Chang, H. Y., Yin, Z., & Flavell, R. A. (2017). M 6 A mRNA methylation controls T cell homeostasis by targeting the IL-7/STAT5/SOCS pathways. *Nature*, *548*(7667), 338–342. https://doi.org/10.1038/nature23450

Liang, G., & Bushman, F. D. (2021). The human virome: assembly, composition and host interactions. *Nature Reviews Microbiology*, *19*(8), 514–527. https://doi.org/10.1038/s41579-021-00536-5

Liberzon, A., Birger, C., Thorvaldsdóttir, H., Ghandi, M., Mesirov, J. P., & Tamayo, P. (2015). The Molecular Signatures Database Hallmark Gene Set Collection. *Cell Systems*, *1*(6), 417–425. https://doi.org/10.1016/j.cels.2015.12.004

Lin, S., Choe, J., Du, P., Triboulet, R., & Gregory, R. I. (2016). The m 6 A Methyltransferase METTL3 Promotes Translation in Human Cancer Cells. *Molecular Cell*, *62*(3), 335–345. https://doi.org/10.1016/j.molcel.2016.03.021

Linder, B., Grozhik, A. v, Olarerin-George, A. O., Meydan, C., Mason, C. E., & Jaffrey, S. R. (2015). Single-nucleotide resolution mapping of m6A and m6Am throughout the transcriptome. *Nature Methods*, *12*(8), 767–772. https://doi.org/10.1038/nmeth.3453

Lindfors, K., Lin, J., Lee, H. S., Hyöty, H., Nykter, M., Kurppa, K., Liu, E., Koletzko, S., Rewers, M., Hagopian, W., Toppari, J., Ziegler, A. G., Akolkar, B., Krischer, J. P., Petrosino, J. F., Lloyd, R. E., & Agardh, D. (2020). Metagenomics of the faecal virome indicate a cumulative effect of enterovirus and gluten amount on the risk of coeliac disease autoimmunity in genetically at risk children: The TEDDY study. *Gut*, *69*(8), 1416–1422. https://doi.org/10.1136/gutjnl-2019-319809

Ling, T., Weng, G. X., Lia, J., Li, C., Wang, W., Cao, L., Rao, H., Ju, C., & Xu, L. G. (2019). TARBP2 inhibits IRF7 activation by suppressing TRAF6-mediated K63-linked ubiquitination of IRF7. *Molecular Immunology*, *109*, 116–125. https://doi.org/10.1016/j.molimm.2019.02.019

Lionetti, E., Gatti, S., Pulvirenti, A., & Catassi, C. (2015). Celiac disease from a global perspective. *Best Practice and Research: Clinical Gastroenterology*, *29*(3), 365–379. https://doi.org/10.1016/j.bpg.2015.05.004

Litvak, V., Ratushny, A. v., Lampano, A. E., Schmitz, F., Huang, A. C., Raman, A., Rust, A. G., Bergthaler, A., Aitchison, J. D., & Aderem, A. (2012). A FOXO3-IRF7 gene regulatory circuit

limits inflammatory sequelae of antiviral responses. *Nature*, *490*(7420), 421–425. https://doi.org/10.1038/nature11428

Liu, N., Zhou, K. I., Parisien, M., Dai, Q., Diatchenko, L., & Pan, T. (2017). N6-methyladenosine alters RNA structure to regulate binding of a low-complexity protein. *Nucleic Acids Research*, *45*(10), 6051–6063. https://doi.org/10.1093/nar/gkx141

Liu, S., Zhu, A., He, C., & Chen, M. (2020). REPIC: A database for exploring the N 6-methyladenosine methylome. *Genome Biology*, *21*(1), 100. https://doi.org/10.1186/s13059-020-02012-4

Liu, Y., You, Y., Lu, Z., Yang, J., Li, P., Liu, L., Xu, H., Niu, Y., & Cao, X. (2019). N6-methyladenosine RNA modification–mediated cellular metabolism rewiring inhibits viral replication. *Science*, *365*(6458), 1171–1176. https://doi.org/10.1126/science.aax4468

Lou, X., Wang, J. J., Wei, Y. Q., & Sun, J. J. (2021). Emerging role of RNA modification N6-methyladenosine in immune evasion. *Cell Death and Disease*, 12(4), 300. https://doi.org/10.1038/s41419-021-03585-z

Lu, M., Zhang, Z., Xue, M., Zhao, B. S., Harder, O., Li, A., Liang, X., Gao, T. Z., Xu, Y., Zhou, J., Feng, Z., Niewiesk, S., Peeples, M. E., He, C., & Li, J. (2020). N 6-methyladenosine modification enables viral RNA to escape recognition by RNA sensor RIG-I. *Nature Microbiology*, *5*(4), 584–598. https://doi.org/10.1038/s41564-019-0653-9

Lu, R., Au, W.-C., Yeow, W.-S., Hageman, N., & Pitha, P. M. (2000). Regulation of the Promoter Activity of Interferon Regulatory Factor-7 Gene. *Journal of Biological Chemistry*, *275*(41), 31805–31812. https://doi.org/10.1074/jbc.M005288200

Lu, Y.-C., Yeh, W.-C., & Ohashi, P. S. (2008). LPS/TLR4 signal transduction pathway. *Cytokine*, *42*(2), 145–151. https://doi.org/10.1016/j.cyto.2008.01.006

Luang Xu, X., Liu, X., Sheng, N., Soe Oo, K., Liang, J., Hian Chionh, Y., Xu, J., Ye, F., Gao, Y.-G., Dedon, P. C., & Fu, X.-Y. (2017). Three distinct 3-methylcytidine (m 3 C) methyltransferases modify tRNA and mRNA in mice and humans. *Journal of Biological Chemistry*, *292*(35), 14695–14703. https://doi.org/10.1074/jbc.M117.798298

Luo, H., Liu, W., Zhang, Y., Yang, Y., Jiang, X., Wu, S., & Shao, L. (2021). METTL3-mediated m6A modification regulates cell cycle progression of dental pulp stem cells. *Stem Cell Research & Therapy*, *12*(1), 159. https://doi.org/10.1186/s13287-021-02223-x

Luo, J., Xu, T., & Sun, K. (2021). N6-Methyladenosine RNA Modification in Inflammation: Roles, Mechanisms, and Applications. *Frontiers in Cell and Developmental Biology*, *9*, 670711. Frontiers Media S.A. https://doi.org/10.3389/fcell.2021.670711

Machnicka, M. A., Milanowska, K., Oglou, O. O., Purta, E., Kurkowska, M., Olchowik, A., Januszewski, W., Kalinowski, S., Dunin-Horkawicz, S., Rother, K. M., Helm, M., Bujnicki, J. M., & Grosjean, H. (2013). MODOMICS: A database of RNA modification pathways - 2013 update. *Nucleic Acids Research*, *41*, D262-7. https://doi.org/10.1093/nar/gks1007

Maelfait, J., Bridgeman, A., Benlahrech, A., Cursi, C., & Rehwinkel, J. (2016). Restriction by SAMHD1 Limits cGAS/STING-Dependent Innate and Adaptive Immune Responses to HIV-1. *Cell Reports*, *16*(6), 1492–1501. https://doi.org/10.1016/j.celrep.2016.07.002

Maity, A., & Das, B. (2016). N6-methyladenosine modification in mRNA: Machinery, function and implications for health and diseases. *FEBS Journal*, *283*(9), 1607–1630. https://doi.org/10.1111/febs.13614

Mancino, A., & Natoli, G. (2016). Specificity and Function of IRF Family Transcription Factors: Insights from Genomics. *Journal of Interferon & Cytokine Research*, *36*(7), 462–469. https://doi.org/10.1089/JIR.2016.0004

Mao, Y., Dong, L., Liu, X. M., Guo, J., Ma, H., Shen, B., & Qian, S. B. (2019). m6A in mRNA coding regions promotes translation via the RNA helicase-containing YTHDC2. *Nature Communications*, *10*(1), 5332. https://doi.org/10.1038/s41467-019-13317-9

Marie, I., Durbin, JE., & Levy, DE. (1998). Differential viral induction of distinct interferon-alpha genes by positive feedback through interferon regulatory factor-7. *The EMBO Journal*, *17*(22), 6660–6669. https://doi.org/10.1093/emboj/17.22.6660

Mathlin, J., le Pera, L., & Colombo, T. (2020). A Census and Categorization Method of Epitranscriptomic Marks. *International Journal of Molecular Sciences*, *21*(13), 4684. https://doi.org/10.3390/ijms21134684

Matsumoto, M., & Seya, T. (2008). TLR3: Interferon induction by double-stranded RNA including poly(I:C). *Advanced Drug Delivery Reviews*, 60(7), 805–812. https://doi.org/10.1016/j.addr.2007.11.005

Mauer, J., Luo, X., Blanjoie, A., Jiao, X., Grozhik, A. v., Patil, D. P., Linder, B., Pickering, B. F., Vasseur, J. J., Chen, Q., Gross, S. S., Elemento, O., Debart, F., Kiledjian, M., & Jaffrey, S. R. (2017). Reversible methylation of m6 Am in the 5′ cap controls mRNA stability. *Nature*, *541*(7637), 371–375. https://doi.org/10.1038/nature21022

Mazzarella, G., MacDonald, T. T., Salvati, V. M., Mulligan, P., Pasquale, L., Stefanile, R., Lionetti, P., Auricchio, S., Pallone, F., Troncone, R., Monteleone, G., ed Endoscopia Digestiva, G., Ospedaliera, A., & Giuseppe Moscati, S. (2003). Constitutive Activation of the Signal Transducer and Activator of Transcription Pathway in Celiac Disease Lesions. *The American Journal of Pathology 162*(6), 1845-55. https://doi.org/ 0.1016/S0002-9440(10)64319-2

McFadden, M. J., McIntyre, A. B. R., Mourelatos, H., Abell, N. S., Gokhale, N. S., Ipas, H., Xhemalçe, B., Mason, C. E., & Horner, S. M. (2021). Post-transcriptional regulation of antiviral gene expression by N6-methyladenosine. *Cell Reports*, *34*(9), 108798 https://doi.org/10.1016/j.celrep.2021.108798

Medzhitov, R. (2001). Toll-like receptors and innate immunity. *Nature Reviews Immunology*, *1*(2), 135–145. https://doi.org/10.1038/35100529

Medzhitov, R., & Janeway, C. (2000). Innate immune recognition: mechanisms and pathways. *Immunological Reviews*, *173*(1), 89–97. https://doi.org/10.1034/J.1600-065X.2000.917309.X

Megiorni, F., & Pizzuti, A. (2012). HLA-DQA1 and HLA-DQB1 in Celiac disease predisposition: Practical implications of the HLA molecular typing. *Journal of Biomedical Science*, 19(1), 88. https://doi.org/10.1186/1423-0127-19-88

Mendoza-Gomez, L. M., Sebastian-delaCruz, M., Olazagoitia-Garmendia, A., González-Moro, I., Rojas-Márquez, H., Mentxaka, J., Santin, I., & Castellanos-Rubio, A. (2022). Preparation of pepsin trypsin digested gliadin for stimulation experiments. *Methods in Cell Biology*. https://doi.org/10.1016/BS.MCB.2022.11.005

Meresse, B., Ripoche, J., Heyman, H., & Cerf-Bensussan, N. (2009). Celiac disease: from oral tolerance to intestinal inflammation, autoimmunity and lymphomagenesis. *Mucosal Immunology*, *2*(1), 8–23. https://doi.org/10.1038/mi.2008.75

Meyer, K. D., Patil, D. P., Zhou, J., Zinoviev, A., Skabkin, M. A., Elemento, O., Pestova, T. V., Qian, S. B., & Jaffrey, S. R. (2015). 5′ UTR m6A Promotes Cap-Independent Translation. *Cell*, *163*(4), 999–1010. https://doi.org/10.1016/j.cell.2015.10.012

Meyer, K. D., Saletore, Y., Zumbo, P., Elemento, O., Mason, C. E., & Jaffrey, S. R. (2012). Comprehensive analysis of mRNA methylation reveals enrichment in 3′ UTRs and near stop codons. *Cell*, *149*(7), 1635–1646. https://doi.org/10.1016/j.cell.2012.05.003

Molberg O, Mcadam SN, Körner R, Quarsten H, Kristiansen C, Madsen L, Fugger L, Scott H, Norén O, Roepstorff P, Lundin KE, Sjöström H, & Sollid LM. (1998). Tissue transglutaminase selectively modifies gliadin peptides that are recognized by gut-derived T cells in celiac disease. *Nature Medicine*, *4*(6), 713–717. https://doi.org/10.1038/nm0698-713

Monteleone, I., Monteleone, G., del Vecchio Blanco, G., Vavassori, P., Cucchiara, S., MacDonald, T. T., & Pallone, F. (2004). Regulation of the T helper cell type 1 transcription factor T-bet in coeliac disease mucosa. *Gut*, *53*(8), 1090–1095. https://doi.org/10.1136/gut.2003.030551

Morales, D. J., & Lenschow, D. J. (2013). The Antiviral Activities of ISG15. *Journal of Molecular Biology*, *425*(24), 4995–5008. https://doi.org/10.1016/j.jmb.2013.09.041

Müller, U., Steinhoff, U., Reis, L. F. L., Hemmi, S., Pavlovic, J., Zinkernagel, R. M., & Aguet, M. (1994). Functional Role of Type I and Type II Interferons in Antiviral Defense. *Science*, *264*(5167), 1918–1921. https://doi.org/10.1126/science.8009221

Murray, J. A., Watson, T., Clearman, B., & Mitros, F. (2004). Effect of a gluten-free diet on gastrointestinal symptoms in celiac disease 1-3. *The American Journal of Clinical Nutrition*, *79*(4), 669–673. https://doi.org/ 10.1093/ajcn/79.4.669

Negishi, H., Fujita, Y., Yanai, H., Sakaguchi, S., Ouyang, X., Shinohara, M., Takayanagi, H., Ohba, Y., Taniguchi, T., & Honda, K. (2006). Evidence for licensing of IFN-induced IFN regulatory factor 1 transcription factor by MyD88 in Toll-like receptor-dependent gene induction program. *Procedings of the National Academy of Sciences of USA*, *103*(41), 15136–15141. https://doi.org/10.1073pnas.0607181103

Negishi, H., Taniguchi, T., & Yanai, H. (2018). The Interferon (IFN) Class of Cytokines and the IFN Regulatory Factor (IRF) Transcription Factor Family. *Cold Spring Harbor Perspectives in Biology*, *10*(11), a028423. https://doi.org/10.1101/cshperspect.a028423

Negishi, H., Yanai, H., Nakajima, A., Koshiba, R., Atarashi, K., Matsuda, A., Matsuki, K., Miki, S., Doi, T., Aderem, A., Nishio, J., Smale, S. T., Honda, K., & Taniguchi, T. (2012). Cross-interference of RLR and TLR signaling pathways modulates antibacterial T cell responses. *Nature Immunology*, *13*(7), 659–666. https://doi.org/10.1038/ni.2307

Nehyba, J., Hrdličková, R., & Bose, H. R. (2009). Dynamic Evolution of Immune System Regulators: The History of the Interferon Regulatory Factor Family. *Molecular Biology and Evolution*, *26*(11), 2539–2550. https://doi.org/10.1093/molbev/msp167

Nica, A. C., & Dermitzakis, E. T. (2013). Expression quantitative trait loci: Present and future. *Philosophical Transactions of the Royal Society B: Biological Sciences*, 368(1620), 20120362. https://doi.org/10.1098/rstb.2012.0362

Ning, S., Campos, A. D., Darnay, B. G., Bentz, G. L., & Pagano, J. S. (2008). TRAF6 and the Three C-Terminal Lysine Sites on IRF7 Are Required for Its Ubiquitination-Mediated Activation by the Tumor Necrosis Factor Receptor Family Member Latent Membrane Protein 1. *Molecular and Cellular Biology*, *28*(20), 6536–6546. https://doi.org/10.1128/MCB.00785-08

Ning, S., Huye, L. E., & Pagano, J. S. (2005). Regulation of the transcriptional activity of the IRF7 promoter by a pathway independent of interferon signaling. *Journal of Biological Chemistry*, *280*(13), 12262–12270. https://doi.org/10.1074/jbc.M404260200

Ning, S., Pagano, J. S., & Barber, G. N. (2011). IRF7: Activation, regulation, modification and function. *Genes and Immunity*, *12*(6), 399–414. https://doi.org/10.1038/gene.2011.21

Oertelt-Prigione, S. (2012). The influence of sex and gender on the immune response. In *Autoimmunity Reviews*, *11*(2012), A479–A485. https://doi.org/10.1016/j.autrev.2011.11.022

Oikarinen, M., Puustinen, L., Lehtonen, J., Hakola, L., Simell, S., Toppari, J., Ilonen, J., Veijola, R., Virtanen, S. M., Knip, M., & Hyöty, H. (2021). Enterovirus Infections Are Associated With the Development of Celiac Disease in a Birth Cohort Study. *Frontiers in Immunology*, *11*, 604529. https://doi.org/10.3389/fimmu.2020.604529

Olazagoitia-Garmendia, A., Zhang, L., Mera, P., Godbout, J. K., Sebastian-Delacruz, M., Garcia, I., Mendoza, L. M., Huerta, A., Irastorza, I., Bhagat, G., Green, P. H., Herrero, L., Serra, D., Rodriguez, J. A., Verdu, E. F., He, C., Bilbao, J. R., & Castellanos-Rubio, A. (2021). Gluten-induced RNA methylation changes regulate intestinal inflammation via allele-specific XPO1 translation in epithelial cells. *Gut*, *71*(1), 68–77. https://doi.org/10.1136/gutjnl-2020-322566

Palová-Jelínková, L., Dáňová, K., Drašarová, H., Dvořá, M., Funda, D. P., Fundová, P., Kotrbová - Kozak, A., Černá, M., Kamanová, J., Martin, S. F., Freudenberg, M., & Tučková, L. (2013). Pepsin Digest of Wheat Gliadin Fraction Increases Production of IL-1b via TLR4/MyD88/TRIF/MAPK/NF-kB Signaling Pathway and an NLRP3 Inflammasome Activation. *Plos One*, *8*(4), e62426. https://doi.org/10.1371/journal.pone.0062426

Patil, D. P., Chen, C.-K., Pickering, B. F., Chow, A., Jackson, C., Guttman, M., & Jaffrey, S. R. (2016). m6A RNA methylation promotes XIST-mediated transcriptional repression. *Nature*, *537*(7620), 369–373. https://doi.org/10.1038/nature19342

Paun, A., & Pitha, P. M. (2007). The IRF family, revisited. *Biochimie*, *89*(6–7), 744–753. https://doi.org/10.1016/J.BIOCHI.2007.01.014

Pecora, F., Persico, F., Gismondi, P., Fornaroli, F., Iuliano, S., de'Angelis, G. L., & Esposito, S. (2020). Gut Microbiota in Celiac Disease: Is There Any Role for Probiotics? *Frontiers in Immunology*, *11*, 957. https://doi.org/10.3389/fimmu.2020.00957

Perry, A. K., Chow, E. K., Goodnough, J. B., Yeh, W.-C., & Cheng, G. (2004). Differential Requirement for TANK-binding Kinase-1 in Type I Interferon Responses to Toll-like Receptor Activation and Viral Infection. *Journal of Experimental Medicine*, *199*(12), 1651–1658. https://doi.org/10.1084/jem.20040528

Pestka, S., Krause, C. D., & Walter, M. R. (2004). Interferons, interferon-like cytokines, and their receptors. *Immunological Reviews*, *202*(1), 8–32. https://doi.org/10.1111/j.0105-2896.2004.00204.x

Ping, X. L., Sun, B. F., Wang, L., Xiao, W., Yang, X., Wang, W. J., Adhikari, S., Shi, Y., Lv, Y., Chen, Y. S., Zhao, X., Li, A., Yang, Y., Dahal, U., Lou, X. M., Liu, X., Huang, J., Yuan, W. P., Zhu, X. F., … Yang, Y. G. (2014). Mammalian WTAP is a regulatory subunit of the RNA N6-methyladenosine methyltransferase. *Cell Research*, *24*(2), 177–189. https://doi.org/10.1038/cr.2014.3

Platanias, L. C. (2005). Mechanisms of type-I- and type-II-interferon-mediated signalling. *Nature Reviews Immunology*, *5*(5), 375–386. https://doi.org/10.1038/nri1604

Postler, T. S., Pantry, S. N., Desrosiers, R. C., & Ghosh, S. (2017). Identification and characterization of a long non-coding RNA up-regulated during HIV-1 infection. *Virology*, *511*, 30–39. https://doi.org/10.1016/j.virol.2017.08.006

Prestwich, R. J., Errington, F., Steele, L. P., Ilett, E. J., Morgan, R. S. M., Harrington, K. J., Pandha, H. S., Selby, P. J., Vile, R. G., & Melcher, A. A. (2009). Reciprocal Human Dendritic Cell–Natural Killer Cell Interactions Induce Antitumor Activity Following Tumor Cell Infection by Oncolytic Reovirus. *The Journal of Immunology*, *183*(7), 4312–4321. https://doi.org/10.4049/JIMMUNOL.0901074

Qin, B. Y., Liu, C., Lam, S. S., Srinath, H., Delston, R., Correia, J. J., Derynck, R., & Lin, K. (2003). Crystal structure of IRF-3 reveals mechanism of autoinhibition and virus-induced phosphoactivation. *Nature Structural & Molecular Biology*, *10*(11), 913–921. https://doi.org/10.1038/nsb1002

Rodrigo, L. (2016). Neurogluten. *Gastroenterology & Hepatology International Journal*, *1*(2), 1–2. https://doi.org/10.23880/ghij-16000110

Rosenfeld, A. B., Qian, E., Shen, L., Melendez, M., Mishra, N., Lipkin, W. I., & Racaniello, V. R. (2022). Cross-Reactive Antibody Responses against Nonpoliovirus Enteroviruses. *MBio*, *13*(1), e03660-21. https://journals.asm.org/journal/mbio

Roundtree, I. A., Luo, G.-Z., Zhang, Z., Wang, X., Zhou, T., Cui, Y., Sha, J., Huang, X., Guerrero, L., Xie, P., He, E., Shen, B., & He, C. (2017). YTHDC1 mediates nuclear export of N 6-methyladenosine methylated mRNAs. *ELife*, *6*, e31311. https://doi.org/10.7554/eLife.31311.001

Rubio-Tapia, A., & Murray, J. A. (2010). Classification and management of refractory coeliac disease. *Gut*, *59*(4), 547–557. https://doi.org/10.1136/GUT.2009.195131

Samarajiwa, S. A., Forster, S., Auchettl, K., & Hertzog, P. J. (2009). INTERFEROME: The database of interferon regulated genes. *Nucleic Acids Research*, *37*, D852–D547. https://doi.org/10.1093/nar/gkn732

Samasca, G., Sur, G., Lupan, I., & Deleanu, D. (2014). Gluten-free diet and quality of life in celiac disease. *Gastroenterology and Hepatology From Bed to Bench*, *7*(3), 139–143.

Santana-de Anda, K., Gómez-Martín, D., Díaz-Zamudio, M., & Alcocer-Varela, J. (2011). Interferon regulatory factors: Beyond the antiviral response and their link to the development of autoimmune pathology. *Autoimmunity Reviews*, *11*(2), 98–103. https://doi.org/10.1016/j.autrev.2011.08.006

Sato, M., Hata, N., Asagiri, M., Nakaya, T., Taniguchi, T., & Tanaka, N. (1998). Positive feedback regulation of type I *IFN* genes by the IFN-inducible transcription factor IRF-7. *FEBS Letters*, *441*(1), 106–110. https://doi.org/10.1016/S0014-5793(98)01514-2

Schmid, S., Mordstein, M., Kochs, G., García-Sastre, A., & TenOever, B. R. (2010). Transcription factor redundancy ensures induction of the antiviral state. *Journal of Biological Chemistry*, *285*(53), 42013–42022. https://doi.org/10.1074/jbc.M110.165936

Schneider, W. M., Chevillotte, M. D., & Rice, C. M. (2014). Interferon-Stimulated Genes: A Complex Web of Host Defenses. *Annual Review of Immunology*, *32*(1), 513–545. https://doi.org/10.1146/annurev-immunol-032713-120231

Schoggins, J. W., & Rice, C. M. (2011). Interferon-stimulated genes and their antiviral effector functions. *Current Opinion in Virology*, *1*(6), 519–525. https://doi.org/10.1016/j.coviro.2011.10.008

Schulzke, J. D., Bentzel, C. J., Schulzke, I., Riecken, E. O., & Fromm, M. (1998). Epithelial tight junction structure in the jejunum of children with acute and treated celiac sprue. *Pediatric Research*, *43*(4 I), 435–441. https://doi.org/10.1203/00006450-199804000-00001

Schwartz, S. (2016). Cracking the epitranscriptome. *RNA*, *22*(2), 169–174. http://www.rnajournal.org/cgi/doi/10.

Schwartz, S., Mumbach, M. R., Jovanovic, M., Wang, T., Maciag, K., Bushkin, G. G., Mertins, P., Ter-Ovanesyan, D., Habib, N., Cacchiarelli, D., Sanjana, N. E., Freinkman, E., Pacold, M. E., Satija, R., Mikkelsen, T. S., Hacohen, N., Zhang, F., Carr, S. A., Lander, E. S., & Regev, A. (2014). Perturbation of m6A Writers Reveals Two Distinct Classes of mRNA Methylation at Internal and 5′ Sites. *Cell Reports*, *8*(1), 284–296. https://doi.org/10.1016/j.celrep.2014.05.048

Sciurti, M., Fornaroli, F., Gaiani, F., Bonaguri, C., Leandro, G., di Mario, F., & De'angelis, G. L. (2018). Genetic susceptibilty and celiac disease: What role do HLA haplotypes play? *Acta Biomedica*, *89*(9), 17–21. https://doi.org/10.23750/abm.v89i9-S.7953

Sharma, S., tenOever, B. R., Grandvaux, N., Zhou, G.-P., Lin, R., & Hiscott, J. (2003). Triggering the Interferon Antiviral Response Through an IKK-Related Pathway. *Science*, *300*(5622), 1148–1151. https://doi.org/10.1126/science.1081315

Sherry, B. (2009). Rotavirus and reovirus modulation of the interferon Response. *Journal of Interferon and Cytokine Research*, 29(9), 559–567. https://doi.org/10.1089/jir.2009.0072

Shi, H., Wang, X., Lu, Z., Zhao, B. S., Ma, H., Hsu, P. J., Liu, C., & He, C. (2017). YTHDF3 facilitates translation and decay of N 6-methyladenosine-modified RNA. *Cell Research*, *27*(3), 315–328. https://doi.org/10.1038/cr.2017.15

Shulman, Z., & Stern-Ginossar, N. (2020). The RNA modification N 6-methyladenosine as a novel regulator of the immune system. *Nature Immunology*, *21*(5), 501–512. https://doi.org/10.1038/s41590-020-0650-4

Silano, M., Vincentini, O., & De Vincenzi, M. (2009). Toxic, Immunostimulatory and Antagonist Gluten Peptides in Celiac Disease. *Current Medicinal Chemistry*, *16*(12), 1489–1498. https://doi.org/ 10.2174/092986709787909613

Simen Zhao, B., & He, C. (2015). Pseudouridine in a new era of RNA modifications. *Cell Research*, *25*(2), 153–154. https://doi.org/10.1038/cr.2014.143

Sin, W. X., Yeong, J. P. S., Lim, T. J. F., Su, I. H., Connolly, J. E., & Chin, K. C. (2020). IRF-7 Mediates Type I IFN Responses in Endotoxin-Challenged Mice. *Frontiers in Immunology*, *11*, 640. https://doi.org/10.3389/fimmu.2020.00640

Slotkin, W., & Nishikura, K. (2013). Adenosine-to-inosine RNA editing and human disease. *Genome Medicine*, *5*(11), 1–13. http://genomemedicine.com/content/5/11/105

Smatti, M. K., Cyprian, F. S., Nasrallah, G. K., al Thani, A. A., Almishal, R. O., & Yassine, H. M. (2019). Viruses and autoimmunity: A review on the potential interaction and molecular mechanisms. *Viruses*, 11(8), 762. https://doi.org/10.3390/v11080762

Soleimanjahi, H., & Heydarabadi, F. H. (2022). Reovirus and Rotaviruses. *Encyclopedia of Infection and Immunity*, 131–145. https://doi.org/10.1016/B978-0-12-818731-9.00050-1

Spencer, L., Olawuni, B., & Singh, P. (2022). Gut Virome: Role and Distribution in Health and Gastrointestinal Diseases. *Frontiers in Cellular and Infection Microbiology*, *12*, 836706. Frontiers Media S.A. https://doi.org/10.3389/fcimb.2022.836706

Steele, L., Errington, F., Prestwich, R., Ilett, E., Harrington, K., Pandha, H., Coffey, M., Selby, P., Vile, R., & Melcher, A. (2011). Pro-inflammatory cytokine/chemokine production by reovirus treated melanoma cells is PKR/NF-κB mediated and supports innate and adaptive anti-tumour immune priming. *Molecular Cancer*, *10*, 20. https://doi.org/10.1186/1476-4598-10-20

Su, R., Dong, L., Li, C., Nachtergaele, S., Wunderlich, M., Qing, Y., Deng, X., Wang, Y., Weng, X., Hu, C., Yu, M., Skibbe, J., Dai, Q., Zou, D., Wu, T., Yu, K., Weng, H., Huang, H., Ferchen, K., … Chen, J. (2018). R-2HG Exhibits Anti-tumor Activity by Targeting FTO/m6A/MYC/CEBPA Signaling. *Cell*, *172*(1–2), 90-105. https://doi.org/10.1016/j.cell.2017.11.031

Subramanian, A., Tamayo, P., Mootha, V. K., Mukherjee, S., Ebert, B. L., Gillette, M. A., Paulovich, A., Pomeroy, S. L., Golub, T. R., Lander, E. S., & Mesirov, J. P. (2005). Gene set enrichment analysis: A knowledge-based approach for interpreting genome-wide expression profiles. *Procedings of the National Academy of Sciences of USA*, *102*(43), 15545–15550. www.pnas.orgcgidoi10.1073pnas.0506580102

Sun, L., Wu, J., Du, F., Chen, X., & Chen, Z. J. (2013). Cyclic GMP-AMP Synthase Is a Cytosolic DNA Sensor That Activates the Type I Interferon Pathway. *Science*, *339*(6121), 786–791. https://doi.org/10.1126/science.1232458

Sun, Q., Sun, L., Liu, H.-H., Chen, X., Seth, R. B., Forman, J., & Chen, Z. J. (2006). The Specific and Essential Role of MAVS in Antiviral Innate Immune Responses. *Immunity*, *24*(5), 633–642. https://doi.org/10.1016/j.immuni.2006.04.004

Takaoka, A., Yanai, H., Kondo, S., Duncan, G., Negishi, H., Mizutani, T., Kano, S., Honda, K., Ohba, Y., Mak, T. W., & Taniguchi, T. (2005). Integral role of IRF-5 in the gene induction programme activated by Toll-like receptors. *Nature*, *434*(7030), 243–249. https://doi.org/10.1038/nature03308

Tamura, T., Yanai, H., Savitsky, D., & Taniguchi, T. (2008). The IRF Family Transcription Factors in Immunity and Oncogenesis. *Annual Review of Immunology*, *26*(1), 535–584. https://doi.org/10.1146/annurev.immunol.26.021607.090400

Tanabe, A., Tanikawa, K., Tsunetomi, M., Takai, K., Ikeda, H., Konno, J., Torigoe, T., Maeda, H., Kutomi, G., Okita, K., Mori, M., & Sahara, H. (2016). RNA helicase YTHDC2 promotes cancer metastasis via the enhancement of the efficiency by which HIF-1α mRNA is translated. *Cancer Letters*, *376*(1), 34–42. https://doi.org/10.1016/j.canlet.2016.02.022

Tanaka, N., Kawakami, T., & Taniguchi, T. (1993). Recognition DNA Sequences of Interferon Regulatory Factor 1 (IRF-1) and IRF-2, Regulators of Cell Growth and the Interferon System. *Molecular and Cellular Biology*, *13*(8), 4531–4538. https://doi.org/10.1128/mcb.13.8.4531-4538.1993

Tang, C., Klukovich, R., Peng, H., Wang, Z., Yu, T., Zhang, Y., Zheng, H., Klungland, A., & Yan, W. (2017). ALKBH5-dependent m6A demethylation controls splicing and stability of long 3'-UTR mRNAs in male germ cells. *Proceedings of the National Academy of Sciences of the United States of America*, *115*(2), E325–E333. https://doi.org/10.1073/pnas.1717794115

Tang, L., Wei, X., Li, T., Chen, Y., Dai, Z., Lu, C., & Zheng, G. (2021). Emerging Perspectives of RNA N6-methyladenosine (m6A) Modification on Immunity and Autoimmune Diseases. *Frontiers in Immunology*, 12, 630358. https://doi.org/10.3389/fimmu.2021.630358

Taniguchi, T., & Takaoka, A. (2001). A weak signal for strong responses: interferon-alpha/beta revisited. *Nature Reviews Molecular Cell Biology*, *2*(5), 378–386. https://doi.org/10.1038/35073080

Trifilo, M. J., Montalto-Morrison, C., Stiles, L. N., Hurst, K. R., Hardison, J. L., Manning, J. E., Masters, P. S., & Lane, T. E. (2004). CXC Chemokine Ligand 10 Controls Viral Infection in the Central Nervous System: Evidence for a Role in Innate Immune Response through Recruitment and Activation of Natural Killer Cells. *Journal of Virology*, *78*(2), 585–594. https://doi.org/10.1128/JVI.78.2.585-594.2004/FORMAT/EPUB

Trynka, G., Hunt, K. A., Bockett, N. A., Romanos, J., Mistry, V., Szperl, A., Bakker, S. F., Bardella, M. T., Bhaw-Rosun, L., Castillejo, G., de La Concha, E. G., de Almeida, R. C., Dias, K. R. M., van Diemen, C. C., Dubois, P. C. A., Duerr, R. H., Edkins, S., Franke, L., Fransen, K., … van Heel, D. A. (2011). Dense genotyping identifies and localizes multiple common and rare variant association signals in celiac disease. *Nature Genetics*, *43*(12), 1193–1201. https://doi.org/10.1038/ng.998

Tsai, K., & Cullen, B. R. (2020). Epigenetic and epitranscriptomic regulation of viral replication. *Nature Reviews Microbiology*, *18*(10), 559–570. https://doi.org/10.1038/s41579-020-0382-3

Uematsu, S., & Akira, S. (2007). Toll-like receptors and type I Interferons. *Journal of Biological Chemistry*, *282*(21), 15319–15324. https://doi.org/10.1074/jbc.R700009200

van Heel, D. A., Franke, L., Hunt, K. A., Gwilliam, R., Zhernakova, A., Inouye, M., Wapenaar, M. C., Barnardo, M. C. N. M., Bethel, G., Holmes, G. K. T., Feighery, C., Jewell, D., Kelleher, D., Kumar, P., Travis, S., Walters, J. R. F., Sanders, D. S., Howdle, P., Swift, J., … Wijmenga, C. (2007). A genome-wide association study for celiac disease identifies risk variants in the region harboring IL2 and IL21. *Nature Genetics*, *39*(7), 827. https://doi.org/10.1038/NG2058

Veals, S. A., Schindler, C., Leonard, D., Fu, X. Y., Aebersold, R., Darnell, J. E., & Levy, D. E. (1992). Subunit of an alpha-interferon-responsive transcription factor is related to interferon regulatory factor and Myb families of DNA-binding proteins. *Molecular and Cellular Biology*, *12*(8), 3315–3324. https://doi.org/10.1128/mcb.12.8.3315-3324.1992

Visscher, P. M., Brown, M. A., McCarthy, M. I., & Yang, J. (2012). Five years of GWAS discovery. *American Journal of Human Genetics*, *90*(1),7–24. https://doi.org/10.1016/j.ajhg.2011.11.029

Wang, A., Tao, W., Tong, J., Gao, J., Wang, J., Hou, G., Qian, C., Zhang, G., Li, R., Wang, D., Ren, X., Zhang, K., Ding, S., Flavell, R., Li, H. B., Pan, W., & Zhu, S. (2022). m6A modifications regulate intestinal immunity and rotavirus infection. *ELife*, *11*, e73628. https://doi.org/10.7554/eLife.73628

Wang, P., Doxtader, K. A., & Nam, Y. (2016). Structural Basis for Cooperative Function of Mettl3 and Mettl14 Methyltransferases. *Molecular Cell*, *63*(2), 306–317. https://doi.org/10.1016/j.molcel.2016.05.041

Wang, X., Huang, J., Zou, T., & Yin, P. (2017). Human m6A writers: Two subunits, 2 roles. *RNA Biology*, 14(3), 300–304. https://doi.org/10.1080/15476286.2017.1282025

Wang, X., Lu, Z., Gomez, A., Hon, G. C., Yue, Y., Han, D., Fu, Y., Parisien, M., Dai, Q., Jia, G., Ren, B., Pan, T., & He, C. (2014). N 6-methyladenosine-dependent regulation of messenger RNA stability. *Nature*, *505*(7481), 117–120. https://doi.org/10.1038/nature12730

Wang, X., Zhao, B. S., Roundtree, I. A., Lu, Z., Han, D., Ma, H., Weng, X., Chen, K., Shi, H., & He, C. (2015). N6-methyladenosine modulates messenger RNA translation efficiency. *Cell*, *161*(6), 1388–1399. https://doi.org/10.1016/j.cell.2015.05.014

Wang, Y., Li, Y., Toth, J. I., Petroski, M. D., Zhang, Z., & Zhao, J. C. (2014). N6-methyladenosine modification destabilizes developmental regulators in embryonic stem cells. *Nature Cell Biology*, *16*(2), 191–198. https://doi.org/10.1038/ncb2902

Wardowska, A. (2021). m6A RNA Methylation in Systemic Autoimmune Diseases-A New Target for Epigenetic-Based Therapy? *Pharmaceuticals*, *14*(3), 218. https://doi.org/10.3390/ph14030218

Wathelet, M. G., Lin, C. H., Parekh, B. S., Ronco, L. V., Howley, P. M., & Maniatis, T. (1998). Virus infection induces the assembly of coordinately activated transcription factors on the IFN-β enhancer in vivo. *Molecular Cell*, *1*(4), 507–518. https://doi.org/10.1016/S1097-2765(00)80051-9

Wilhelmi, I., Roman, E., & Sánchez-Fauquier, A. (2003). Viruses causing gastroenteritis. *Clinical Microbiology and Infection*, *9*(4), 247–262. https://doi.org/10.1046/J.1469-0691.2003.00560.X

Williams, G. D., Gokhale, N. S., & Horner, S. M. (2019). Regulation of Viral Infection by the RNA Modification N6-methyladenosine. *Annual Review of Virology*, *6*(1), 235–253. https://doi.org/10.1146/annurev-virology-092818

Winkler, R., Gillis, E., Lasman, L., Safra, M., Geula, S., Soyris, C., Nachshon, A., Tai-Schmiedel, J., Friedman, N., Le-Trilling, V. T. K., Trilling, M., Mandelboim, M., Hanna, J. H., Schwartz, S., & Stern-Ginossar, N. (2019). m 6 A modification controls the innate immune response to infection by targeting type I interferons. *Nature Immunology*, *20*(2), 173–182. https://doi.org/10.1038/s41590-018-0275-z

Wojtas, M. N., Pandey, R. R., Mendel, M., Homolka, D., Sachidanandam, R., & Pillai, R. S. (2017). Regulation of m6A Transcripts by the 3'→5' RNA Helicase YTHDC2 Is Essential for a Successful Meiotic Program in the Mammalian Germline. *Molecular Cell*, *68*(2), 374–387. https://doi.org/10.1016/j.molcel.2017.09.021

Wu, J., & Chen, Z. J. (2014). Innate Immune Sensing and Signaling of Cytosolic Nucleic Acids. *Annual Review of Immunology*, *32*(1), 461–488. https://doi.org/10.1146/annurev-immunol-032713-120156

Wu, J., Sun, L., Chen, X., Du, F., Shi, H., Chen, C., & Chen, Z. J. (2013). Cyclic GMP-AMP Is an Endogenous Second Messenger in Innate Immune Signaling by Cytosolic DNA. *Science*, *339*(6121), 826–830. https://doi.org/10.1126/science.1229963

Wu, W., Zhang, W., Tian, L., Brown, B. R., Walters, M. S., & Metcalf, J. P. (2020). IRF7 is required for the second phase interferon induction during influenza virus infection in human lung epithelia. *Viruses*, *12*(4), 377. https://doi.org/10.3390/v12040377

Xiao, W., Adhikari, S., Dahal, U., Chen, Y. S., Hao, Y. J., Sun, B. F., Sun, H. Y., Li, A., Ping, X. L., Lai, W. Y., Wang, X., Ma, H. L., Huang, C. M., Yang, Y., Huang, N., Jiang, G. Bin, Wang, H. L., Zhou, Q., Wang, X. J., … Yang, Y. G. (2016). Nuclear m6A Reader YTHDC1 Regulates mRNA Splicing. *Molecular Cell*, *61*(4), 507–519. https://doi.org/10.1016/j.molcel.2016.01.012

Xu, K., Yang, Y., Feng, G.-H., Sun, B.-F., Chen, J.-Q., Li, Y.-F., Chen, Y.-S., Zhang, X.-X., Wang, C.-X., Jiang, L.-Y., Liu, C., Zhang, Z.-Y., Wang, X.-J., Zhou, Q., Yang, Y.-G., & Li, W. (2017). Mettl3-mediated m 6 A regulates spermatogonial differentiation and meiosis initiation. *Cell Research*, *27*(9), 1100–1114. https://doi.org/10.1038/cr.2017.100

Yanai, H., Chiba, S., Hangai, S., Kometani, K., Inoue, A., Kimura, Y., Abe, T., Kiyonari, H., Nishio, J., Taguchi-Atarashi, N., Mizushima, Y., Negishi, H., Grosschedl, R., & Taniguchi, T. (2018). Revisiting the role of IRF3 in inflammation and immunity by conditional and specifically targeted gene ablation in mice. *Proceedings of the National Academy of Sciences of the United States of America*, *115*(20), 5253–5258. https://doi.org/10.1073/PNAS.1803936115/-/DCSUPPLEMENTAL

Yang, J., Wang, H., & Zhang, W. (2019). Regulation of Virus Replication and T Cell Homeostasis by N 6 -Methyladenosine. *Virologica Sinica*, *34*(1), 22–29. https://doi.org/10.1007/s12250-018-0075-5

Yang, Y., Fan, X., Mao, M., Song, X., Wu, P., Zhang, Y., Jin, Y., Yang, Y., Chen, L. L., Wang, Y., Wong, C. C. L., Xiao, X., & Wang, Z. (2017). Extensive translation of circular RNAs driven by N 6 -methyladenosine. *Cell Research*, *27*(5), 626–641. https://doi.org/10.1038/cr.2017.31

Yang, Y., Hsu, P. J., Chen, Y. S., & Yang, Y. G. (2018). Dynamic transcriptomic m6A decoration: Writers, erasers, readers and functions in RNA metabolism. *Cell Research*, 28(6), 616–624. https://doi.org/10.1038/s41422-018-0040-8

Yoneyama, M., Kikuchi, M., Matsumoto, K., Imaizumi, T., Miyagishi, M., Taira, K., Foy, E., Loo, Y.-M., Gale, M., Akira, S., Yonehara, S., Kato, A., & Fujita, T. (2005). Shared and Unique Functions of the DExD/H-Box Helicases RIG-I, MDA5, and LGP2 in Antiviral Innate Immunity. *The Journal of Immunology*, *175*(5), 2851–2858. https://doi.org/10.4049/jimmunol.175.5.2851

Yoneyama, M., Suhara W, Fukuhara Y, Fukuda M, Nishida E, & Fujita T. (1998). Direct triggering of the type I interferon system by virus infection: activation of a transcription factor complex containing IRF-3 and CBP/p300. *The EMBO Journal*, *17*(4), 1087–1095. https://doi.org/10.1093/emboj/17.4.1087

Yue, Y., Liu, J., Cui, X., Cao, J., Luo, G., Zhang, Z., Cheng, T., Gao, M., Shu, X., Ma, H., Wang, F., Wang, X., Shen, B., Wang, Y., Feng, X., He, C., & Liu, J. (2018). VIRMA mediates preferential m6A mRNA methylation in 3'UTR and near stop codon and associates with alternative polyadenylation. *Cell Discovery*, *4*(10), 1–17. https://doi.org/10.1038/s41421-018-0019-0

Yue, Y., Liu, J., & He, C. (2015). RNA N 6-methyladenosine methylation in post-transcriptional gene expression regulation. *Genes & Development*, *29*, 1343–1355. https://doi.org/10.1101/gad.262766

Zhang, B., zur Hausen, A., Orlowska-Volk, M., Jäger, M., Bettendorf, H., Stamm, S., Hirschfeld, M., Yiqin, O., Tong, X., Gitsch, G., & Stickeler, E. (2010). Alternative Splicing-Related Factor YT521. *International Journal of Gynecological Cancer*, *20*(4), 492–499. https://doi.org/10.1111/IGC.0b013e3181d66ffe

Zhang, C., Chen, Y., Sun, B., Wang, L., Yang, Y., Ma, D., Lv, J., Heng, J., Ding, Y., Xue, Y., Lu, X., Xiao, W., Yang, Y.-G., & Liu, F. (2017). m6A modulates haematopoietic stem and progenitor cell specification. *Nature*, *549*(7671), 273–276. https://doi.org/10.1038/nature23883

Zhang, L., & Pagano, J. S. (2002). Review: Structure and Function of IRF-7. *Journal of Interferon & Cytokine Research*, *22*(1), 95–101. https://doi.org/10.1089/107999002753452700

Zhang, X., Chen, B. di, Zhao, L. dan, & Li, H. (2020). The Gut Microbiota: Emerging Evidence in Autoimmune Diseases. *Trends in Molecular Medicine*, 26(9) 862–873. https://doi.org/10.1016/j.molmed.2020.04.001

Zhang, Y., Wang, X., Zhang, X., Wang, J., Ma, Y., Zhang, L., & Cao, X. (2019). RNA-binding protein YTHDF3 suppresses interferon-dependent antiviral responses by promoting FOXO3 translation. *Proceedings of the National Academy of Sciences of the United States of America*, *116*(3), 976–981. https://doi.org/10.1073/pnas.1812536116

Zhao, X., Yang, Y., Sun, B.-F., Shi, Y., Yang, X., Xiao, W., Hao, Y.-J., Ping, X.-L., Chen, Y.-S., Wang, W.-J., Jin, K.-X., Wang, X., Huang, C.-M., Fu, Y., Ge, X.-M., Song, S.-H., Jeong, H. S., Yanagisawa, H., Niu, Y., … Yang, Y.-G. (2014). FTO-dependent demethylation of N6-methyladenosine regulates mRNA splicing and is required for adipogenesis. *Cell Research*, *24*(12), 1403–1419. https://doi.org/10.1038/cr.2014.151

Zhen, D., Wu, Y., Zhang, Y., Chen, K., Song, B., Xu, H., Tang, Y., Wei, Z., & Meng, J. (2020). m6A Reader: Epitranscriptome Target Prediction and Functional Characterization of N6-Methyladenosine (m6A) Readers. *Frontiers in Cell and Developmental Biology*, *8*, 741. https://doi.org/10.3389/fcell.2020.00741

Zheng, G., Dahl, J. A., Niu, Y., Fedorcsak, P., Huang, C.-M., Li, C. J., Vågbø, C. B., Shi, Y., Wang, W.-L., Song, S.-H., Lu, Z., Bosmans, R. P. G., Dai, Q., Hao, Y.-J., Yang, X., Zhao, W.-M., Tong, W.-M., Wang, X.-J., Bogdan, F., … He, C. (2013). ALKBH5 Is a Mammalian RNA Demethylase that Impacts RNA Metabolism and Mouse Fertility. *Molecular Cell*, *49*(1), 18–29. https://doi.org/10.1016/j.molcel.2012.10.015

Zheng, Q., Hou, J., Zhou, Y., Li, Z., & Cao, X. (2017). The RNA helicase DDX46 inhibits innate immunity by entrapping m 6 A-demethylated antiviral transcripts in the nucleus. *Nature Immunology*, *18*(10), 1094–1103. https://doi.org/10.1038/ni.3830

Zhong, B., Yang, Y., Li, S., Wang, Y.-Y., Li, Y., Diao, F., Lei, C., He, X., Zhang, L., Tien, P., & Shu, H.-B. (2008). The Adaptor Protein MITA Links Virus-Sensing Receptors to IRF3 Transcription Factor Activation. *Immunity*, *29*(4), 538–550. https://doi.org/10.1016/j.immuni.2008.09.003

Zhou, Y., Zeng, P., Li, Y. H., Zhang, Z., & Cui, Q. (2016). SRAMP: Prediction of mammalian N6-methyladenosine (m6A) sites based on sequence-derived features. *Nucleic Acids Research*, *44*(10), e91. https://doi.org/10.1093/nar/gkw104

Zong, X., Xiao, X., Shen, B., Jiang, Q., Wang, H., Lu, Z., Wang, F., Jin, M., Min, J., Wang, F., & Wang, Y. (2021). The N 6-methyladenosine RNA-binding protein YTHDF1 modulates the translation of TRAF6 to mediate the intestinal immune response. *Nucleic Acids Research*, *49*(10), 5537–5552. https://doi.org/10.1093/nar/gkab343

Zou, S., Toh, J. D. W., Wong, K. H. Q., Gao, Y. G., Hong, W., & Woon, E. C. Y. (2016). N 6 - Methyladenosine: A conformational marker that regulates the substrate specificity of human demethylases FTO and ALKBH5. *Scientific Reports*, *6*, 25677. https://doi.org/10.1038/srep25677